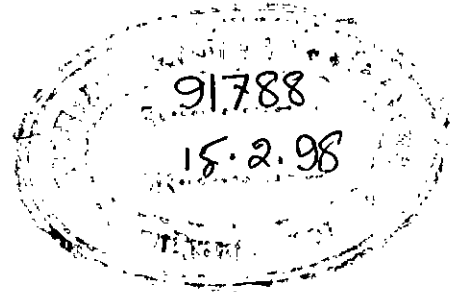


**EFFICIENT OPERATION OF A VARIABLE LOAD THREE  
PHASE INDUCTION MOTOR BY PULSE WIDTH  
MODULATED VOLTAGE CONTROLLER**

By

**SHAIKH NOORA ALAM**



A Thesis

submitted to the Department of Electrical and Electronic Engineering,  
Bangladesh University of Engineering and Technology, Dhaka, Bangladesh.

in partial fulfilment of the requirements for the degree

of

**Master of Science in Electrical and Electronic Engineering**

Department of Electrical and Electronic Engineering  
Bangladesh University of Engineering and Technology  
Dhaka, Bangladesh.



January 22, 1998.

**Dedicated**

**to**

**my parents**

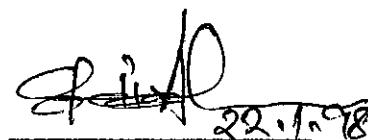
## DECLARATION

I hereby declare that this research work has been carried out by me and it has not been submitted elsewhere for the award of any other degree or diploma.

Countersigned

  
22.1.98

(Dr. Mohammad Ali Choudhury)  
Suopervisor

  
22.1.98


(Shaikh Noora Alam)  
Student

## APPROVAL

The thesis "EFFICIENT OPERATION OF A VARIABLE LOAD THREE PHASE INDUCTION MOTOR BY PULSE WIDTH MODULATED VOLTAGE CONTROLLER" submitted by Shaikh Noora Alam, Roll no. 921318F, Session 1990-91-92 to the Department of Electrical and Electronic Engineering, Bangladesh University of Engineering and Technology, Dhaka, Bangladesh has been accepted as satisfactory for partial fulfillment of the requirements for the degree of Master of science in Electrical and Electronic Engineering. The Thesis Title was approved by CASR in meeting 123, dated June 17, 1996, Resolution 13 and the board of Examiners was approved by CASR in meeting 125, dated December 05, 1996, Resolution 31.

### BOARD OF EXAMINERS

1. Dr. Mohammad Ali Choudhury  
Professor  
Department of Electrical & Electronic Engg.  
BUET, Dhaka-1000  
Bangladesh.

  
Chairman 22.1.98  
(Supervisor)

2. Head  
Department of Electrical & Electronic Engg.  
BUET, Dhaka-1000  
Bangladesh.

Member E. Basher  
(Ex-Officio) 22.1.98

3. Dr. Enamul Basher  
Professor  
Department of Electrical & Electronic Engg.  
BUET, Dhaka-1000  
Bangladesh.

Member E. Basher  
22.1.98

4. Dr. Md. Abdus Samad  
Professor  
Department of Electrical & Electronic Engg.  
and Head,  
Department of Communication Engg.  
BIT, Khulna-9203  
Bangladesh.

Member Abdus Samad  
(External) 22.1.98

# Contents

	<b>page no.</b>
ACKNOWLEDGEMENT	i
ABSTRACT	iii
LIST OF FIGURES	vi

## CHAPTER 1

1.0	Introduction	1
1.1.1	Operation of Induction motors at rated and variable loads	2
1.1.2	Method of maximum efficiency estimation of Induction motor	5
1.2	A.C Voltage Controller	7
1.3	Pulse width modulation techniques	8
1.4	Review of microcomputer controlled static conversion	21
1.5	Objective of the thesis	24
1.6	Thesis organization	25

## CHAPTER 2

	<b>page no.</b>
2.0 Introduction	27
2.1 Slip at maximum efficiency (Without considering constant losses)	27
2.2 Slip at maximum efficiency (Considering constant losses)	30
2.3 V/I Control strategy for maximum efficiency operation	32
2.4 Experimental Verification of V/I Control Strategy	34

## CHAPTER 3

	<b>page no.</b>
3.0 Introduction	45
3.1 Switching Point Calculation of sine PWM switching	48
3.2 PWM waveform generation by Microcomputer	51
3.2.1 Composite byte Generation	58
3.2.2 On Line real time pulse generation	65
3.2.3 Generation of pulses at the parallel port	68
3.2.4 Synchronization of PWM wave with Line to Neutral voltage	70

	<b>page no.</b>
3.2.5 Computer generated PWM pulses	74
3.3 Interface of Microcomputer with three phase Voltage controller & synchronization.	74

## CHAPTER 4

	<b>page no.</b>
4.0 Conclusion	88
4.1 Recommendations on future work.	90
<b>REFERENCES</b>	91
<b>Appendix A : Motor test data</b>	95
<b>Appendix B : PWM pulse Generation program</b>	99

## ACKNOWLEDGEMENT

I would like to thank Professor Mohammad Ali Choudhury, without whose guidance, initiatives and constant efforts this thesis work would not have realized. His suggestions, supervision and initiatives to my thesis engaged me to carry out the research which I will remember.

I also express my deep sense of gratitude to Dr. A.B.M. Siddique Hossain, Professor and Ex-Head of the Department of Electrical and Electronic Engineering, BUET, Dhaka, for his kind cooperation and support during the course of my study.

I wish to express my sincere thanks and regards to Professor Dr. Enamul Basher, Professor and Head of the department of Electrical and Electronic Engineering, BUET, Dhaka, for his encouragement and cooperation to complete this thesis.



I am personally indebted to Mr. Kazi Mujibur Rahman, Assistant professor, Department of Electrical and Electronic Engg., BUET, Dhaka, for his valuable suggestion.

I am thankful to my employer BEXIMCO for granting me leave and support during this program at BUET. My special thanks are to the management of PADMA Textile Mills Ltd. for allowing me time for carrying out the research on my M. Sc. Engg. thesis.

Finally, I wish to express my sincerest thanks to all my teachers, Colleagues and well wishers those who assisted me during my research work.

## **Abstract**

Induction motors are work horse of industries and are essentially constant speed machines at utility supply voltage with rated loads. Advent of modern power electronics has made possible the use of these motors in variable speed applications incorporating inverter/voltage controller/cycloconverter control. Induction motors offer maximum efficiency near their rated speed at rated load condition. Above rated speed, their performance may be controlled by V/f control using modern inverters. However, the open loop control strategy is still being investigated for lower than rated speed with reduced load. Present methods available in the literature being used for such operation of these motors are complicated and not satisfactory. As a result for better energy utilization and management, energy efficient motors are being proposed.

In this thesis, efforts have been made to find a method to obtain maximum attainable efficiency of these motors in open loop control for various loading. A simple control strategy has been developed for obtaining maximum achievable efficiency of these motors at loads lower than rated values. The strategy provides the expression of slip value in terms of motor parameters and fraction of load. Maintaining this slip will ensure maximum efficiency of a motor at that particular load. Using this slip value a V/I relationship of the motor in terms of motor parameters is derived which will ensure maximum attainable efficiency of these motors.

In normal practice, the V/I ratio dictated by the formulas developed can be maintained for a motor by power converters. In this thesis work, effort has been made to implement the scheme at lower than rated speed by a three phase pulse width modulated (PWM) voltage controller. Microcomputer control of a three phase PWM voltage controller has been developed for the implementation of the control

strategy proposed in the thesis. In implementation of microcomputer based PWM voltage controller, simple algebraic equation are being used to generate the PWM gating pulses. The synchronization problem of gate pulse with input sine supply voltage is solved using a new technique on a previously reported PWM generation technique using microcomputer alone having parallel port as the output. Necessary power circuit and interface circuits were designed and fabricated as required for the implementation of a 3-phase PWM voltage controller for the purpose of verification of the proposed open loop control strategy to obtain maximum achievable efficiency of an induction motor at variable loads.

## LIST OF FIGURES

<u>Figure (Number &amp; Title)</u>	<u>Page no</u>
1.1 : Per phase equivalent Circuit of an induction motor	3
1.3.1 : Single Pulse-width Modulation	10
1.3.2 : Multiple Pulse-width Modulation	11
1.3.3 : Sinusoidal Pulse-width Modulation	12
1.3.4 : Modified sine Pulse-width Modulation	14
1.3.5 : Staircase Modulation	15
1.3.6 : Stepped Modulation	17
1.3.7 : Trapezoidal Modulation	18
1.3.8 : Delta Modulation	19
1.3.9 : Hysteresis-band Current controlled PWM	20
2.1 : Equivalent Circuit of an induction motor	28
2.2 : Graphical presentation of Efficiency Vs Slip and Efficiency Vs V/I ratio of a 380V, 175W, 3-phase Induction motor for constant load of 0.16 N-M (Data-1 of appendix A)	37
2.3 : Graphical presentation of Efficiency Vs Slip and Efficiency Vs V/I ratio of a 380V, 175W, 3-phase Induction motor for constant load of 0.25 N-M (Data-2 of appendix A)	38

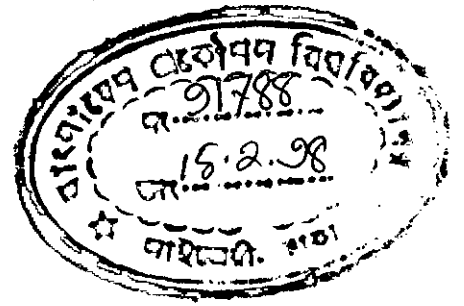
<b><u>Figure (Number &amp; Title)</u></b>	<b><u>Page no</u></b>
2.4 : Graphical presentation of Efficiency Vs Slip and Efficiency Vs V/I ratio of a 380V, 175W, 3-phase Induction motor for constant load of 0.40 N-M (Data-3 of appendix A)	39
2.5 : Graphical presentation of Efficiency Vs Slip and Efficiency Vs V/I ratio of a 380V, 175W, 3-phase Induction motor for constant load of 0.50 N-M (Data-4 of appendix A)	40
2.6 : Graphical presentation of Efficiency Vs Slip and Efficiency Vs V/I ratio of a 380V, 175W, 3-phase Induction motor for constant load of 0.60 N-M (Data-5 of appendix A)	41
2.7 : Graphical presentation of Efficiency Vs Slip and Efficiency Vs V/I ratio of a 380V, 175W, 3-phase Induction motor for constant load of 0.75 N-M (Data-6 of appendix A)	42
2.8 : Graphical presentation of Efficiency Vs Slip and Efficiency Vs V/I ratio of a 380V, 175W, 3-phase Induction motor for constant load of 0.90 N-M (Data-7 of appendix A)	43
2.9 : Graphical presentation of Efficiency Vs Slip and Efficiency Vs V/I ratio of a 380V, 175W, 3-phase Induction motor for constant load of 1.0 N-M (Data-8 of appendix A)	44

<b><u>Figure (Number &amp; Title)</u></b>	<b><u>Page no</u></b>
3.1 : Three phase MOSFET voltage controller	46
3.2 : Typical PWM gating signals for power module of static voltage controller	47
3.3 : Expanded view of triangular carrier modulation process.	49
3.4 : Fundamental subsystems of a microcomputer system	54
3.5 : The internal block diagram of microcomputer central processing unit (CPU)	55
3.6 : Block diagram of the system unit of a microcomputer	56
3.7 : Block diagram of a printer adapter of a microcomputer	59
3.8 : Connector Specification of a parallel port	60
3.9 : Data-pin specification of 25-pin D-shell parallel I/O Port	61
3.10 : Timing diagram of switching pulses showing the technique of their generation at the corresponding data pins, one for each bit in a bite to be at Ox378	63
3.11 : Timing diagram of switching pulses showing the technique of their generation at the corresponding data pins, one for each bit in a bite to be at Ox378	64

<u>Figure (Number &amp; Title)</u>	<u>Page no</u>
3.12(a):Flow chart of the main program used for On-Line Generation of PWM gating pulse.	66
3.12(b):Flow chart of the main program used for On-Line Generation of PWM gating pulse.	67
3.13 : Flow chart of the subfunction Genpulse ( )	69
3.14 : Interface circuit for synchronized PWM pattern	70
3.15 : Hardware schematic of implementation of synchronization of PWM waveforms with supply voltage.	71
3.16(a): Flow chart of determination of three phase PWM waveform from single phase pattern synchronized with line to neutral voltage.	72
3.16(b): Flow chart of determination of three phase PWM waveform from single phase pattern synchronized with line to neutral voltage.	73
3.17 : Output pulse available at parallel port of pin nos. 2 &7 (60 degree apart).	75
3.18 : Three phase voltage controller circuit with MOSFET switching devices.	76



<u>Figure (Number &amp; Title)</u>	<u>Page no</u>
3.19 : Synchronizing with phase A	77
3.20 : Output waveform of voltage controller at $E_m=0.1$ , $f_c=450\text{Hz}$ , $f_m=50.0\text{ Hz}$ .	78
3.21 : Output waveform of voltage controller at $E_m=0.1$ , $f_c=550\text{ Hz}$ , $f_m=50.0\text{ Hz}$ .	79
3.22 : Output waveform of voltage controller at $E_m=0.1$ , $f_c=750\text{ Hz}$ , $f_m=50.0\text{ Hz}$ .	80
3.23 : Output waveform of voltage controller at $E_m=0.1$ , $f_c=1000\text{ Hz}$ , $f_m=50.0\text{ Hz}$ .	81
3.24 : Output waveform of voltage controller at 'a' = 0.25, $E_m=0.25$ , $f_c=450\text{ Hz}$ , $f_m=50.0\text{ Hz}$ .	82
3.25 : Output waveform of voltage controller at 'a' = 0.50, $E_m=0.50$ , $f_c=450\text{ Hz}$ , $f_m=50.0\text{ Hz}$ .	83
3.26 : Output waveform of voltage controller at 'a' = 0.75, $E_m=0.75$ , $f_c=450\text{ Hz}$ , $f_m=50.0\text{ Hz}$ .	84
3.27 : Output waveform of voltage controller at 'a' = 0.90, $E_m=0.90$ , $f_c=450\text{ Hz}$ , $f_m=50.0\text{ Hz}$ .	85



## CHAPTER 1

### 1.0 Introduction:

Squirrel cage induction motors are used extensively in industrial, commercial and domestic applications because of their simple, rugged and maintenance free construction & operation. These motors are fairly efficient. With the advent of solid state voltage and frequency converters like voltage controller, cycloconverter and inverters, induction motors are finding applications requiring speed adjustment, where, expensive dc motors have so far been the only work horse.

Induction motors have their maximum efficiency when they are operated at their rated voltage and at a certain load conditions. At any other load, the efficiency of these motors fall (either with increase or decrease in load). Maximum efficiency which occur at rated voltage cannot be achieved for these motors at other loads . However, researchers are still investigating ways to achieve maximum achievable efficiency of induction motors at variable load condition to save energy cost of operating these motors. The main focus in their research has been to adjust voltage, frequency or voltage-frequency of a motor to obtain maximum achievable efficiency at any load.

In normal practice, power converters like ac voltage controllers and inverters are used to implement efficiency enhancement schemes. AC voltage controllers are used in limited manner to control induction motors below their rated speeds, whereas, inverters are used for wide range of load and speed variation. Voltage controllers use rms output

voltage control and inverters use both voltage and frequency control to achieve their control.

In this thesis, a new scheme of voltage to current (V/I) ratio control is proposed to obtain maximum achievable efficiency of an induction motor operating at variable loads. Practical implementation of the scheme can be achieved by voltage controllers having pulse width modulated (PWM) control using microcomputers. Normal phase controlled voltage controller can also be used for the purpose. But as the proposed scheme will use calculations on monitored line quantities and machine parameters in decision making by computer, it is desirable that improved waveforms of voltage controllers be incorporated in the scheme by modern PWM techniques.

### **1.1.1 Operation of Induction motors at rated and variable loads.**

Induction motors are substantially constant speed motors. Introduction of high power static converters like voltage controllers, inverters and cycloconverters have made possible their use in applications requiring adjustable speeds. Variable speed operation of normal induction motors are also desirable as these motors do not operate at maximum achievable efficiency with variable load. The efficiency of an induction motor is at maximum when it is operated from a rated voltage source with a particular load connected to its shafts. In practical situation i,e in fluid pumping, the motor in use may not be handling same load at all the time. Whenever the load deviates , the efficiency of an induction motor decreases both for increase in the load or decrease in

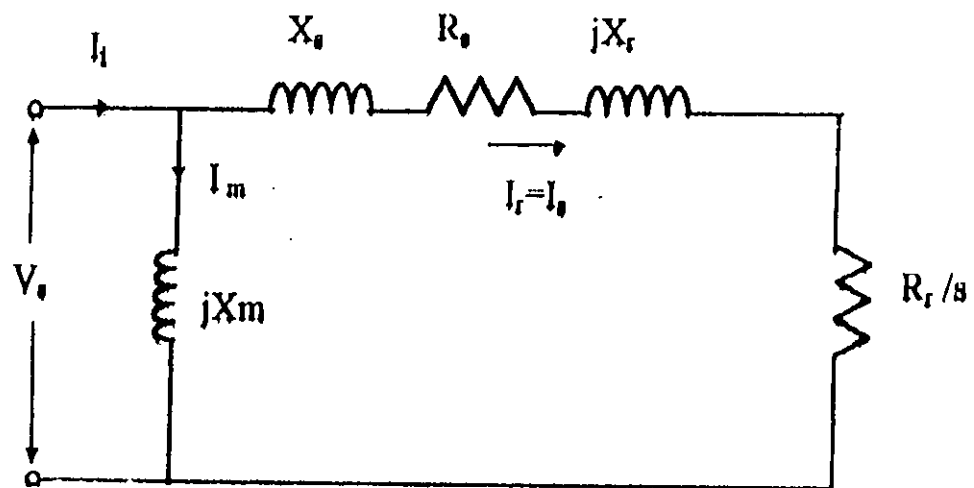


**Figure 1.1 : Per Phase equivalent Circuit of an Induction Motor.**

the load. It has been a constant effort of the researchers to find various ways to achieve the maximum possible efficiency of induction motors at changed loads. This is not achievable at rated voltage. The maximum possible efficiency at any other load is less than the maximum efficiency of the motor due to change in losses. Together with the motor, loads like pumps may also demand change in operating quantities to have a maximum achievable efficiency operation. Hence it has been constant effort of researcher to find ways to get enhanced efficiency operation either by change in frequency or by change in supply voltage.

An induction motor may be characterized by an equivalent circuit as shown in figure

1.1. Following approximate performance expression can be derived [1] ,

$$I_r = \frac{V_1}{\sqrt{\left(\frac{R_2}{S}\right)^2 + (X_2)^2}} \quad 1.1.1$$

$$T_d = \frac{3}{\omega} * \frac{V_1^2 \left(\frac{R_2}{S}\right)}{\left(\frac{R_2}{S}\right)^2 + X_2^2} \quad 1.1.2$$

$$\Phi_r = \frac{1}{4.44KN} \left(\frac{V_1}{f}\right) \quad 1.1.3$$

Where, all symbols are in standard notations. The approximate efficiency equation of the motor is,

$$\eta = \frac{P_{out}}{P_{in}} \quad 1.1.4$$

$$\text{or, } \eta = \frac{3I_r^2 \frac{R_2(1-S)}{S}}{3I_2^2 \frac{R_2}{S} + 3I_s^2 R_1} \quad 1.1.5$$

$$\text{or, } \eta = \frac{1-S}{1+S \frac{R_1}{R_2} \left( \frac{I_1}{I_2} \right)^2} \quad 1.1.6$$

As evident from the equation 1.1.6, the efficiency of the motor depends on mainly the rotor and stator currents and the slip of the motor. Again the currents and slip are dependent on applied voltage and frequency of the supply to the motor. So the effort is mainly concentrated on the voltage and frequency control of induction motors to enhance their efficiency at operating loads. To formulate an efficiency enhancement scheme of an induction motor, it is always necessary to estimate the efficiency of the motor.

### 1.1.2 Method of maximum efficiency estimation of Induction motor

In order to estimate energy losses of an induction motor it is essential to determine its efficiency. A large amount of energy can be saved if efficient motors are used. As a result, emphasis is being placed to enhance motor efficiency during their operation. Usually tests are made to find efficiency of induction motors before installation. However, it is also necessary to monitor their efficiency in-situ to implement any efficiency enhancement scheme. Conventional methods [2] of determining efficiency of

an induction machine is to obtain equivalent circuit parameters from standard tests at different slips or by direct loading [3]. These methods are usually used in manufacturing plants or in laboratories. No accurate in-situ efficiency measurement techniques are available so far. In reference [4] the authors have developed a method to calculate the efficiency of the induction motor during operation. In this method the authors proposed to measure input power and matched characteristics of an induction motor to determine by computer in site. The method provides the estimate of the efficiency based on known characteristic curves. In reference [5] the authors put forward a method based on calculation of two quantities, one a measured efficiency value under an arbitrary loading condition and the other under no load condition. The method uses power, current and speed of the motor during two conditions without measurement of loads.

In this thesis it is our objective to achieve enhanced efficiency operation of induction motor below its rated speed by voltage control. To implement such scheme, a control scheme is to be adopted which will ensure such enhanced efficiency operation. A new method of estimating efficiency from motor's input voltage, current and parameters is suggested for this purpose in this thesis. Voltage control of the motor is to be achieved by pulse width modulated voltage controller to have better wave shape of motor's voltage and current and also to reduce harmonic losses that would have occurred due to the presence of low frequency components. Also, the Pulse width modulated scheme

will be implemented by microcomputer generation of the switching signals for the static voltage controller.

## **1.2 A.C Voltage controller.**

The Power flow of ac supply to load can be controlled by a controlled static switch connected between ac supply and load. This type of power circuit is called ac voltage controllers. Usual application of ac voltage controllers are, speed control of polyphase induction motors, heating , transformer tap changing etc. Normally two types of controls are used for power transfer, these are ,

1. On-off control
2. Phase control

In on-off control, power is connected to the load for few cycles, by turning on the power switch followed by disconnecting the switch for few cycles. In phase control, static switches connect the load to the ac source for a portion of each cycle of input voltage. The ac voltage controller can be classified as follows,

1. Single phase controller
2. Three phase controller

Each of the above may again be subdivided in the following categories,

- (a) Unidirectional or half wave control and
- (b) Bi-directional or full wave control.



The three phase controllers have many configuration depending on static switch connection. Switches are line commutated because the input voltage is ac. Normally thyristors are used in voltage controllers. In applications requiring up to the 400 Hz, TRIACs are also used if available voltage and current ratings are satisfied. Due to line and natural commutation, ac voltage controller circuits are simple. The nature of output waveforms is nonsinusoidal and the analysis involving explicit expressions for the performance assessment is not simple, especially for phase angle controlled converters with RL loads. The investigation of this thesis provides us with a scheme in which maintaining V/I ratio of a motor may allow one to operate induction motor at a maximum attainable efficiency at various loads. This control scheme may be incorporated in a drive by a microcomputer controlled static converter, particularly, by a voltage controller in the simplest way. Since a microcomputer is necessary for the necessary calculations of V/I ratios and generation of control signals, pulse width modulation control of the three phase voltage controller is also suggested in the implementation. Pulse width modulation of power converters have many advantages over their normal counter parts [6]. It is therefore expected that PWM microcomputer controlled voltage controller will meet the objectives of research goals of this thesis.

### **1.3 Pulse width modulation techniques (PWM)**

In pulse width modulated static converters, switching devices are switched on and off many times within a half cycle to generate variable voltage output which normally is

low in harmonic content. There are several PWM techniques. The commonly used techniques are [7],

- a) Single pulse width modulation.
- b) Multiple pulse width modulation.
- c) Sinusoidal pulse width modulation.
- d) Modified sine pulse width modulation.
- e) Delta modulation.
- f) Optimum pulse width modulation and
- g) Hysteresis current controlled pulse width modulation.

In the single pulse width modulation control, there is only one pulse per half cycle. The width of the pulse is varied to control the inverter output voltage. The frequency change is also achieved in the same circuit (fig 1.3.1). In single pulse width modulation the harmonics at the output increase as the widths of the pulses are reduced. The harmonic contents at lower output voltages can be significantly reduced by using several pulses in each half cycle (fig.1.3.2). This is termed as multiple pulse width modulation. The most commonly used technique is sinusoidal pulse width modulation (fig.1.3.3). In this technique an isosceles triangle carrier wave is compared with a sine wave and cross-over points determine the point of commutation [8]. Except at low frequency range, the carrier is synchronized with the modulating signal, and an even integral ratio is maintained to improve the harmonic content. The fundamental

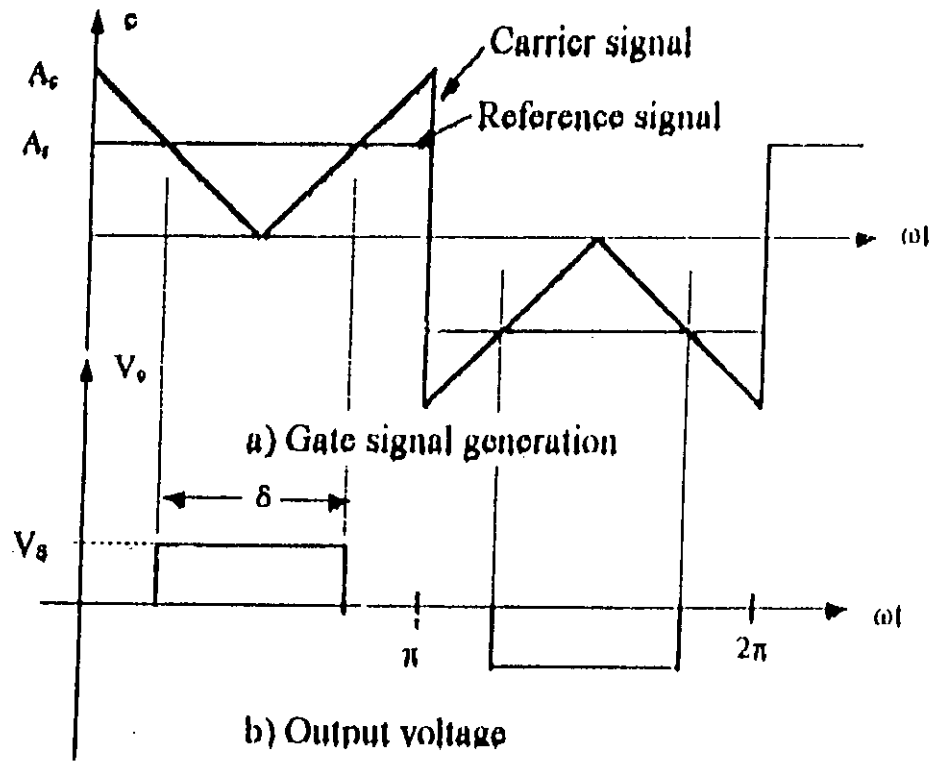
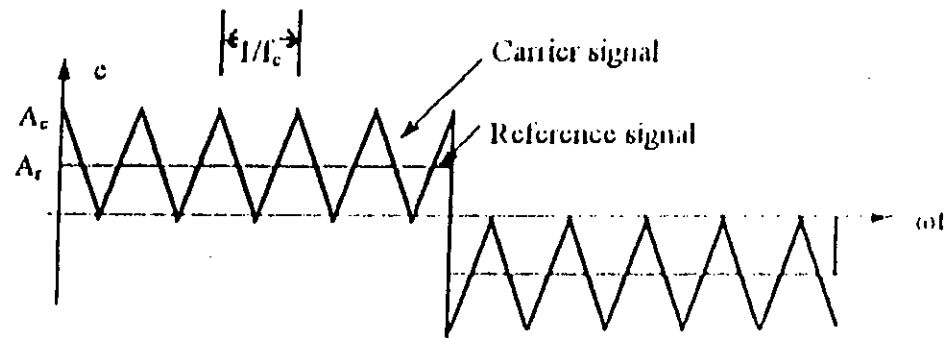
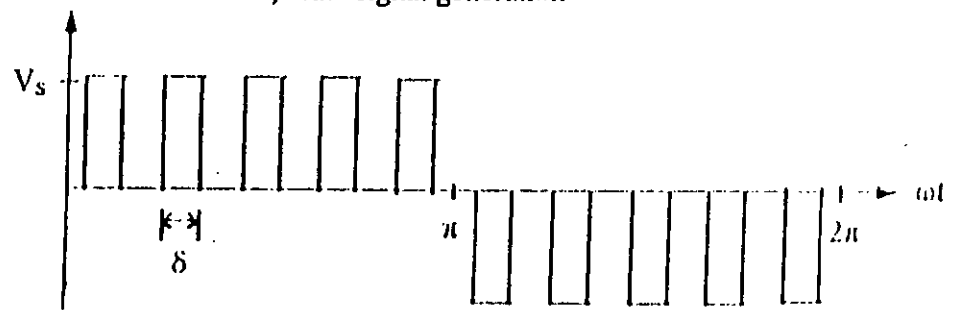


**Figure 1. 3.1 : Single Pulse-width Modulation.**



a) Gate signal generation



b) Output voltage

**Figure 1.3.2 : Multiple Pulse-width Modulation.**

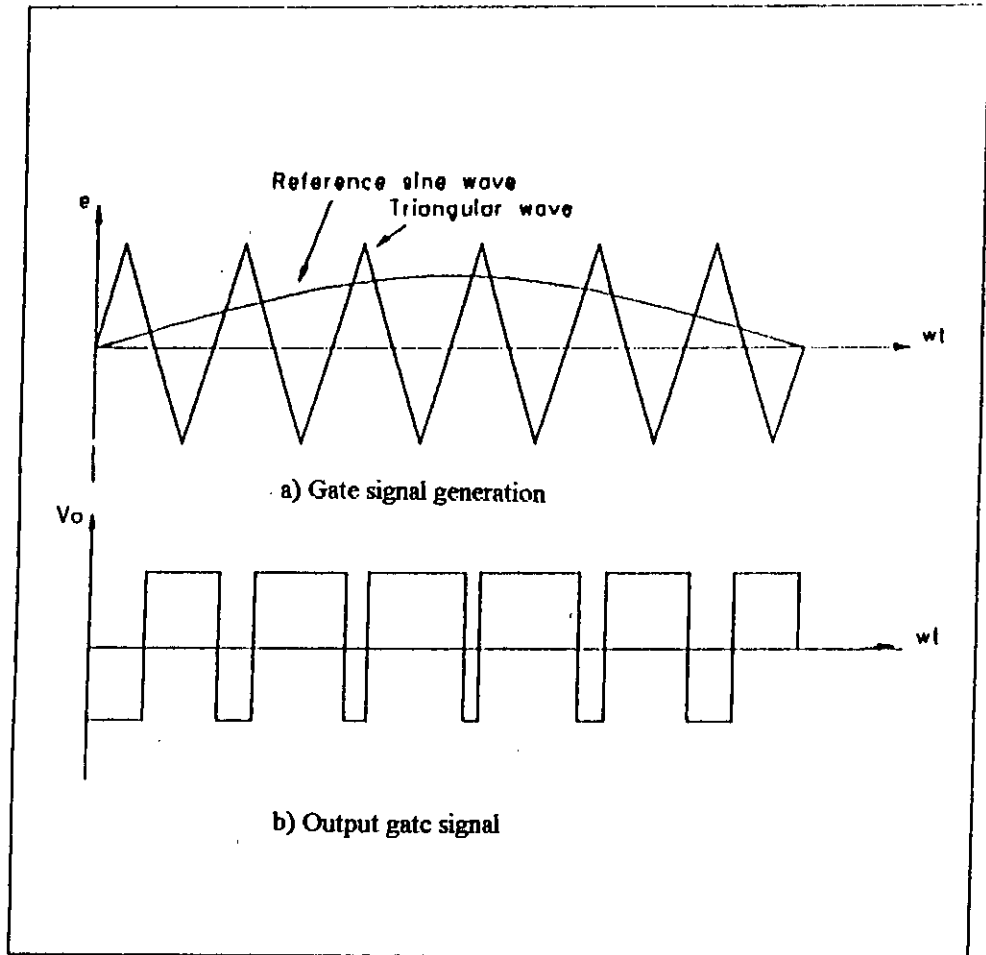


**Figure 1.3.3 : Sinusoidal Pulse-width Modulation.**

output voltage is varied by variation of the modulation index. If the modulation index is less than unity, only the carrier frequency harmonics with the fundamental frequency related side bands appear at the output. This type of waveform results in less harmonic heating and torque pulsation. In sinusoidal pulse width modulation (SPWM) the width of the pulses that are nearer to the peak of the sine wave don't change significantly with the variation of modulation index. A modified technique is employed, called modified sinusoidal pulse width modulation, in which the carrier wave is applied during the first and last 60 degree intervals per half cycle. In this technique the fundamental component increases and the harmonic characteristics are improved. It reduces the number of switching points and thereby reduces switching losses (fig 1.3.4). Some better techniques have been developed by the researchers recently. These include,

- 1) Staircase modulation.
- 2) Stepped modulation.
- 3) Harmonic injection modulation.
- 4) Delta modulation.
- 5) Hysteresis Current controlled Modulation.

In staircase modulation [9], the modulating signal is a staircase wave, as shown in figure (1.3.5). The levels of staircase are calculated to eliminate specific harmonics. Staircase modulation technique is recommended for greater than 15 pulses per cycle. This type of control provides a high quality output voltage with a fundamental value

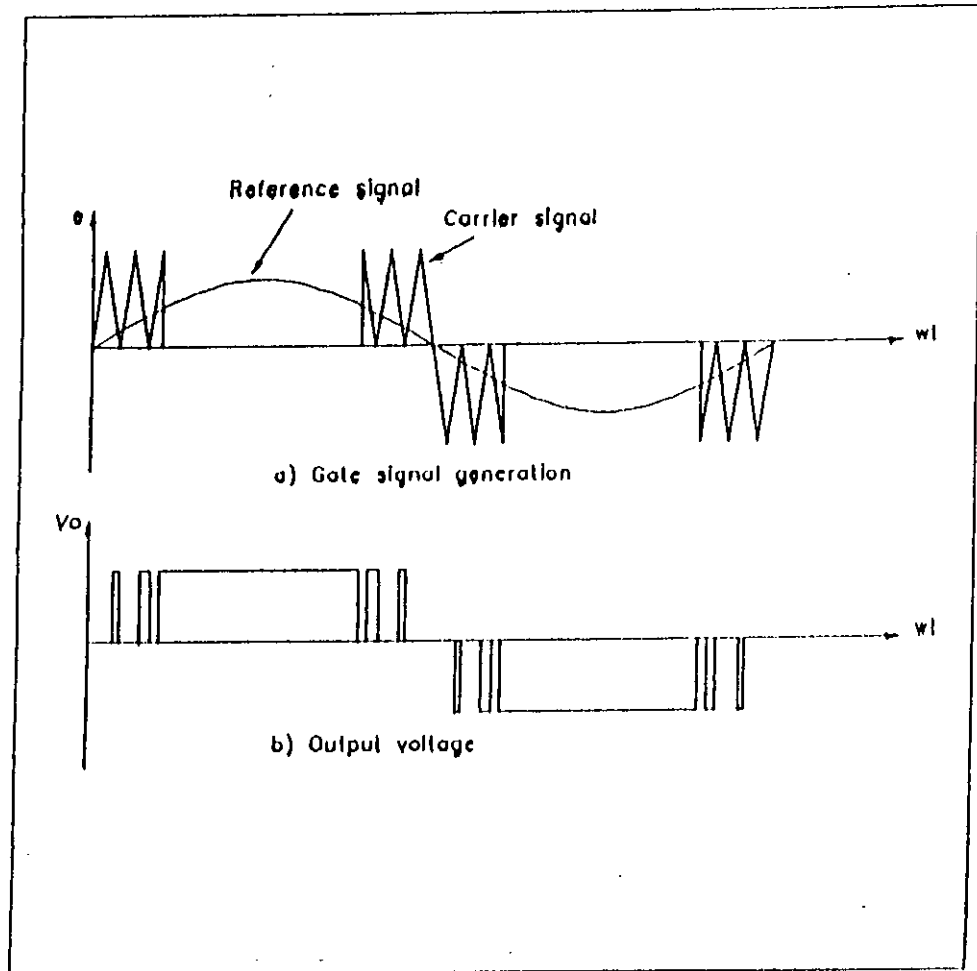


**Figure 1.3.4 : Modified sine Pulse-width Modulation.**

Q.S

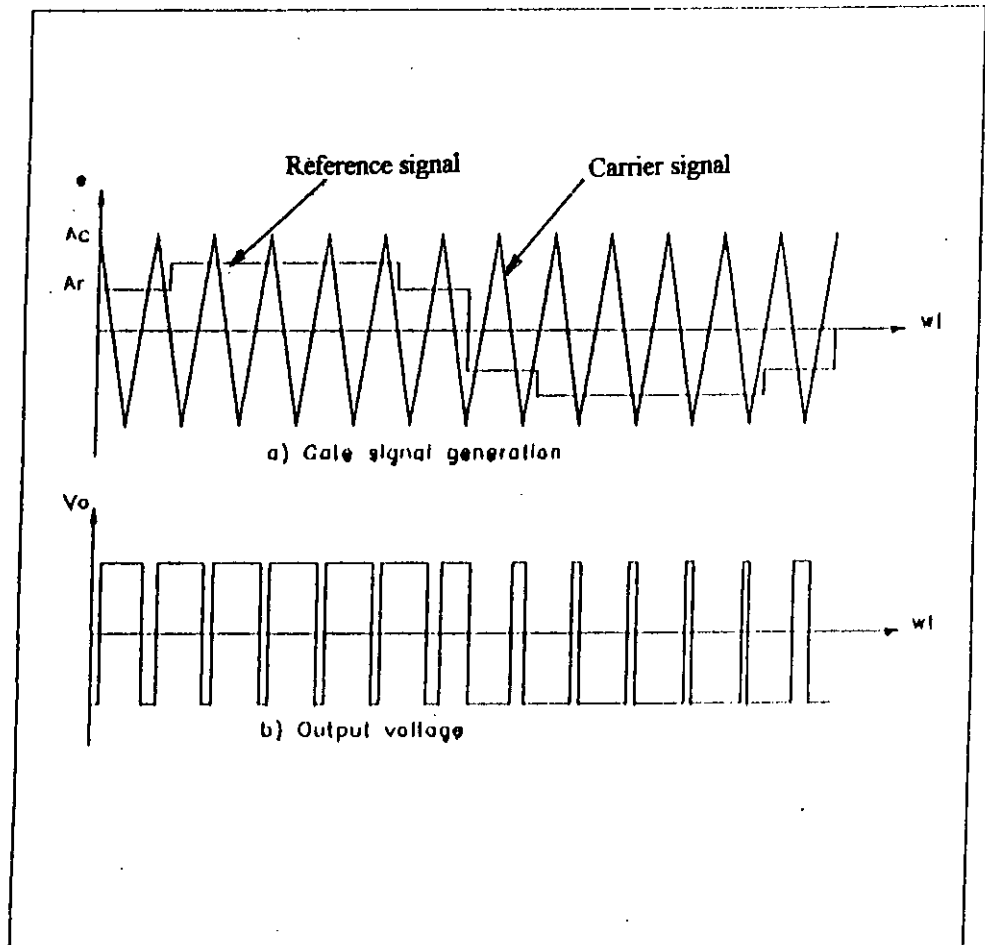


**Figure 1.3.5 : Staircase Modulation.**



upto  $0.94 V_s$  . In stepped modulation [10] the modulating sine wave is divided into specified intervals to eliminate specific harmonics (fig.1.3.6). In trapezoidal modulation the gated signals are generated by comparing a triangular carrier wave with a modulating trapezoidal wave [7,11] as shown in figure (1.3.7). The trapezoidal wave can be obtained from a triangular wave by limiting its magnitude to  $\pm A_R$  , which is related to the peak value  $A_{Rm}$  by  $A_R = \sigma A_{Rm}$  , where,  $\sigma$  is called the triangulation factor, because the waveform becomes a triangular wave when  $\sigma=1$ . Trapezoidal modulation increases the fundamental output voltage upto  $1.05 V_s$ , but the output contains low order harmonics. In harmonic injected modulation, the modulating signal is generated by injecting selected harmonics to the sine wave. It provides a higher fundamental amplitude and low distortion of the output voltage. In delta modulation [12], a triangular wave is allowed to oscillate within a defined window  $\Delta V$ , above and below the reference sine wave  $V_r$ . The inverter switching function is generated from the vertices of the triangular wave  $V_c$  (fig.1.3.8). The ratio of voltage to frequency can be conveniently controlled using delta modulation, particularly in the applications of ac motor control.

The optimal PWM techniques are based on the optimization of particular criteria [13,14] like minimization or elimination of desirable harmonics, peak current and harmonic current distribution etc. It is opposite in nature of natural or uniform sampling method and therefore optimal PWM techniques require the PWM wave to be

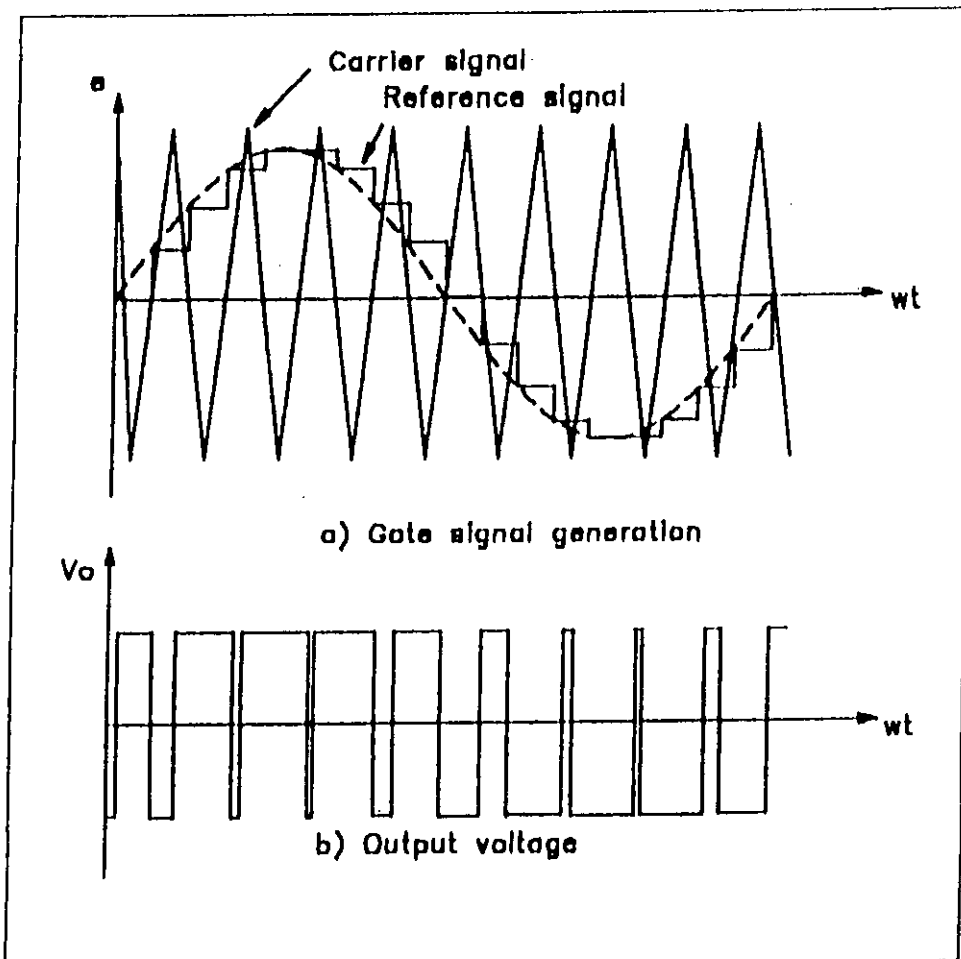
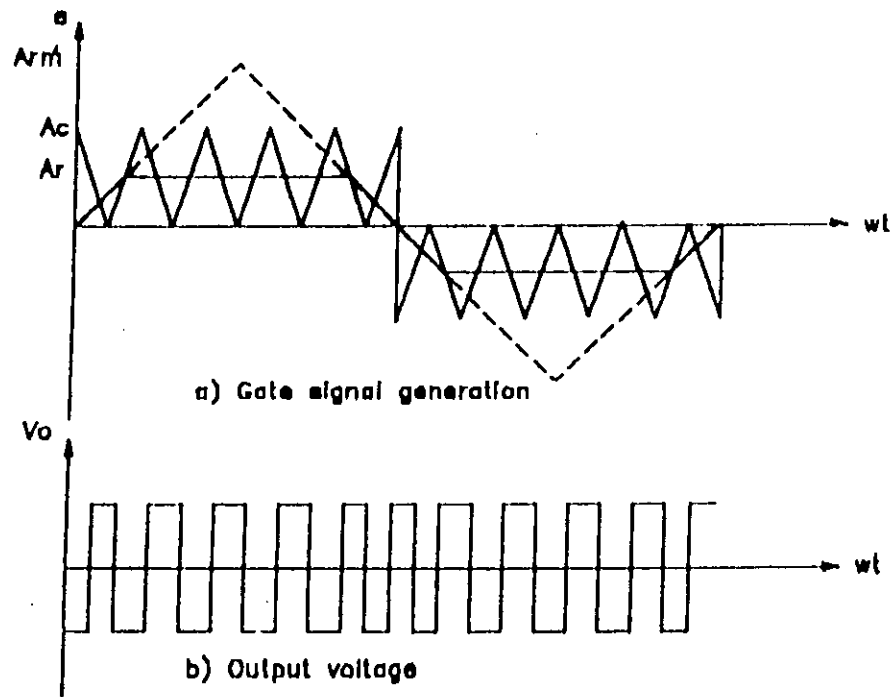
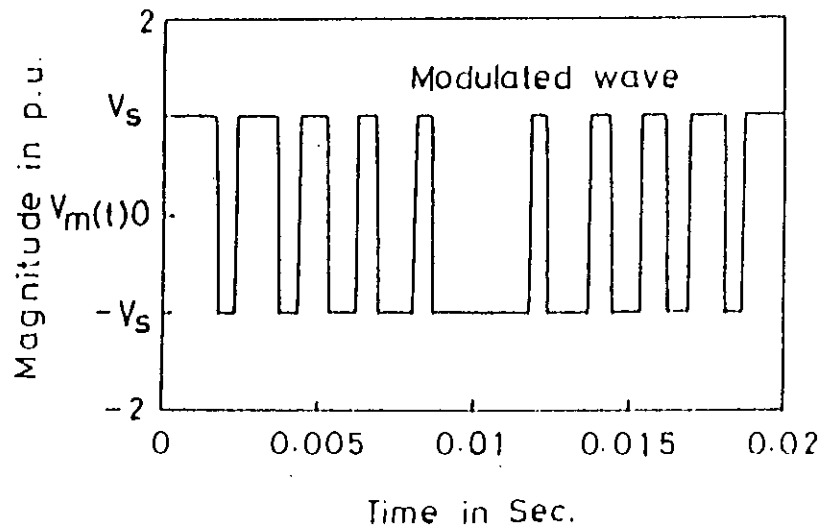
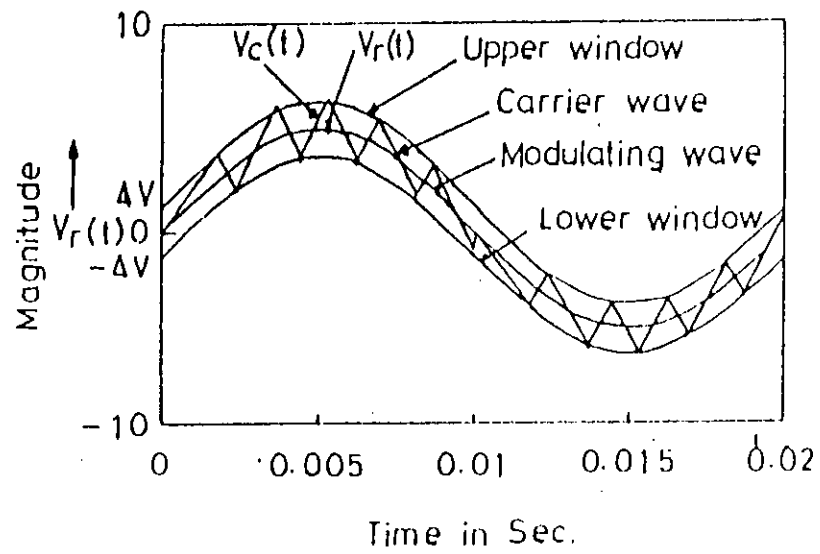


Figure 1.3.6 : Stepped Modulation.



**Figure 1.3.7 : Trapezoidal Modulation.**



**Figure 1.3.8 : Delta Modulation.**

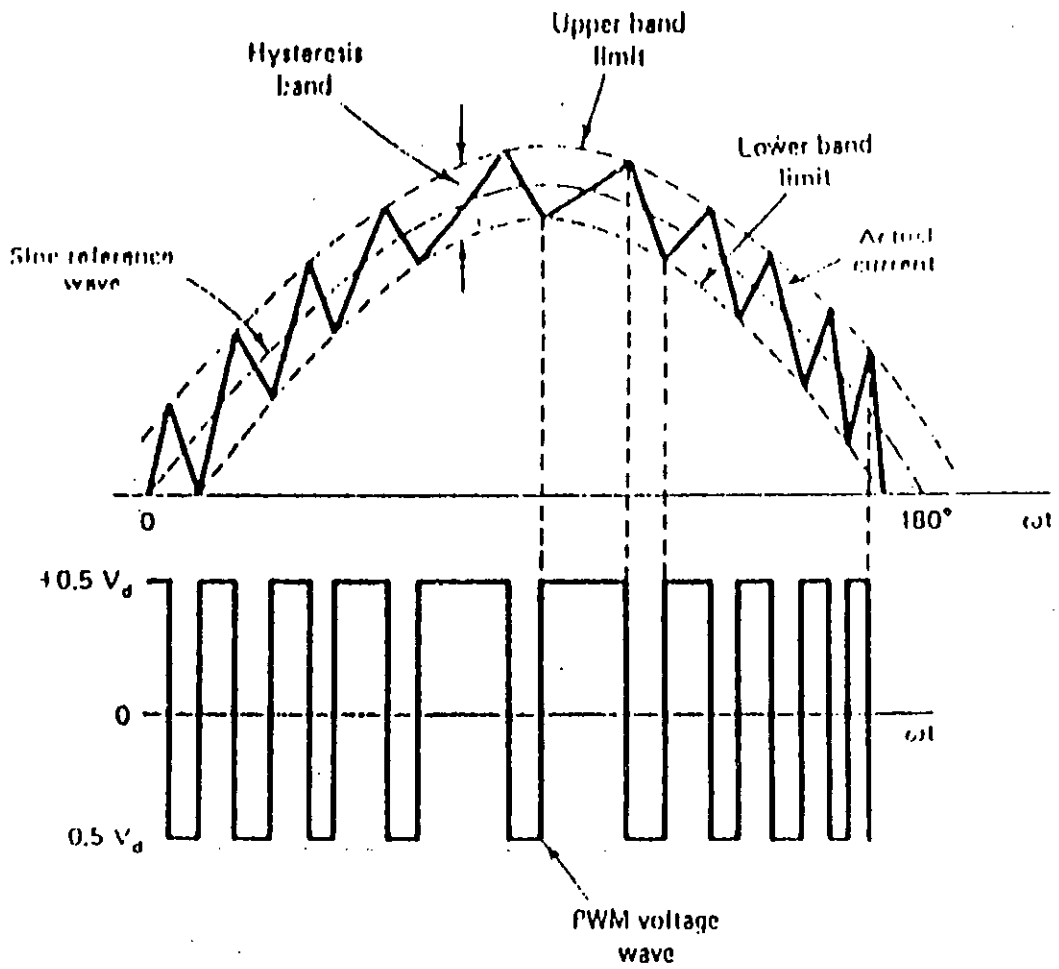


**Figure 1.3.9 : Hysteresis-band Current controlled PWM**

specified a priori in terms switching instants and realization of ultimate data by their determination through numerical techniques. Optimal PWM strategy has a certain methodology and require microcomputer for computation of data to get optimal result of the target. Therefore, a high speed microprocessor is needed for efficient/successful adaptation of optimal PWM schemes.

High performance ac machine drives use current controlled PWM (fig. 1.3.9). Motor torque and flux are directly related to the current. To get regulated voltage output a feed back control loop is provided for necessary voltage compensation. In current controlled hysteresis band PWM method, a current feed back is applied for necessary voltage compensation resulting regulated output. The magnitude and frequency of the desired current wave are determined by the outer control loop. The actual current wave is forced to track the prescribed band by back and forth switching of upper and lower transistor independent of dc voltage fluctuation.

## **1.4 Review of microcomputer controlled static convertors**

Introduction of microcomputers in 1970's has integrated and diversified the control of power conversion by static convertors. Initially they have been used in the implementation of logic control functions. As technology improved and the microcomputers have become faster, their application expanded to general control systems. In power Electronics their use may be in many areas such as,

- a) Gate or Base drive control of static convertors,

- b) Adaptive and Feedback control schemes,
- c) Sequential control,
- d) Protection and Fault detection schemes,
- e) Signal monitoring and wave shaping,
- f) Data acquisitions,
- g) Diagnostic's and
- h) Computation, quality control etc.

Conventional gate or base drive by phase control or square wave signals of SCRs, BJTs, GTOs and MOSFETs of static converters has long been implemented. At present, to minimize harmonic losses and to improve application performance, various PWM techniques are being investigated. These schemes when implemented by microcomputers become more reliable, efficient, versatile and rugged. Microcomputers have now been accepted universally in power electronics and drive systems and their application is on increase continuously in time critical applications such as switching regulators. In future, they will play vital roles not only in high level supervisory control but also in low level power control, specially, in drives and power systems.

In 1982, a firing scheme was used based on microprocessor to control a three phase thyristor converter using look up table algorithm [15]. In the same year, a six pulse converter firing pulse generator was suggested which used an eight bit microprocessor [16]. In 1985, a fast response microprocessor based firing scheme and control

technique for a phase controlled rectifier was developed and tested [17]. During the same period, microcomputer control of static choppers and inverters were also suggested. In particular complicated PWM switching strategies were also implemented on OFF line basis to control inverters.

In 1982 [18], digital control systems applying the microprocessors have been investigated to provide compact, low cost and maintenance free thyristor control. A circuit for DC to DC SCR chopper was presented in 1983 [19]. In 1981 [20], microprocessor controller for an SCR converter with improved power factor was presented. In 1984 [21], microcomputer based control of a sinusoidal photovoltaic power conditioning system was developed. The control functions were implemented using Intel 8751 single-chip microcomputer based hardware and software.

In the PWM waveform generation side several microprocessor based systems were investigated in 1978 [22]. Implementation of a three phase sine PWM inverter control strategy using microprocessor was presented in 1982 [23]. To save CPU time, the efficient DMA technique was used for transferring switching pattern from memory to the pulse amplifier and isolation circuits of individual thyristors in the inverter bridge. The memory requirement is minimum. Interest continues in microcomputer based PWM schemes for AC drive systems in recent years. A high performance Intel 8086 microcomputer based pulse width modulator had been described in the year 1983 [24]. It operates on the computation intensive uniform sampling method in the low



frequency region, whereas, the higher frequency region is based on look up table method . Recently an on-line microcomputer based PWM switching pattern generation has been reported using solution of simple algebraic equation [25]. The technique is simple and easy to implement having added advantages of On-line modulation parameter change and diagnostic option.

## **1.5 Objective of the Thesis.**

In this thesis, a new control strategy is proposed to operate induction motors at their maximum achievable efficiencies at different loads. The control strategy will be to maintain a certain  $V/I$  ratio of the input to achieve the desired operation of the motors. The scheme will require the terminal voltage and current sensing for the control. However, it will not require the speed feed back and on-line efficiency measurements as required by methods so far reported. The second objective of this thesis is to verify the developed control strategy at lower than rated voltage operation of an induction motor at variable load. The desired  $V/I$  value will be maintained by a pulse width modulated voltage controller. In the process of verification it is also desired to implement the pulse width modulated control of a voltage controller by a microcomputer. The implementation of SPWM switching technique will use a simple algebraic equation as reported in reference [25] to generate switching pulses. A novel method to obtain three phase gating signals and synchronization of these pulses with supply voltage ( 50 Hz) will also be implemented.

## **1.6 Thesis organization:**

In the present work a mathematical relationship is developed for a control strategy to achieve maximum efficiency operation of an induction motor at variable load. To verify the applicability of the control scheme, operation of an induction motor supplied from a PWM voltage controller is suggested. The mathematical control strategy is verified by theoretical and experimental observations for sinusoidal supply in the laboratory. The PWM voltage controller operation has also been successfully implemented.

Chapter 1 of the thesis serves the introduction of the subject matter of the thesis with brief review of induction motor control by variable voltage, PWM voltage controller, PWM techniques and the microcomputer control of static converters. This chapter also introduces the objective of the thesis in brief.

The theoretical model for the control strategy to get maximum efficiency operation of an induction motor is presented in chapter 2 of the thesis. This chapter also includes the experimental verification of the proposed control strategy by laboratory experiments with sinusoidal supply. The control strategy suggests to maintain certain  $V/I$  ratio of the supply to achieve the maximum efficiency of an induction motor. In common sense, maintaining constant  $V/I$  would result in constant slip operation of an induction motor. If this slip is maintained constant, then the maximum efficiency

operation is supposed to be achieved. The relationship developed in chapter 2 of the thesis holds good for all values of the load.

Chapter 3 of the thesis is devoted to describe microcomputer control of a three phase voltage controller. A simple algebraic equation is used by the microcomputer to generate PWM switching signals. A new method of composite bit mapping technique has been adopted to obtain three phase switching signals and a new synchronization technique is developed to obtain synchronized switching signals with power supply voltage. The bit mapping scheme and synchronizing technique are also described in chapter 3.

In chapter 4, concluding remarks with detail discussion, the achievements and failures of the thesis and suggestions for future work are made.

## CHAPTER 2

### 2.0 Introduction

Induction motors are operated from inverters with V/f control to improve their efficiencies at variable load condition. In motors operating at below rated load and below rated speed, it is desirable to avoid expensive inverters and complicated control schemes. In this thesis, attempt is being carried out to find out a simplified control strategy to obtain maximum attainable efficiency of an induction motor at below rated load conditions in open loop manner by voltage control only.

In this chapter, theoretical and analytical method for predicting maximum attainable slip and efficiency is presented. The formulations are presented in closed forms without the necessity of iterative solution involving motor parameters and performance curves as reported in earlier works [5].

### 2.1 Slip at maximum efficiency (without considering constant losses)

Simple relationship of slip at maximum attainable efficiency of induction motors can easily be obtained from the motor equations considering the equivalent circuit of figure 2.1. Motor's constant losses have been neglected in the following treatment for simplification.

$$\text{Power out put of the Motor, } P_{\text{out}} = 3I_2^2 \frac{R_2(1-S)}{S} \quad (2.1)$$

Power input of the motor,  $P_{in} = 3I_2^2 \frac{R_2}{S} + 3I_1^2 R_1$  (2.2)

From equation (2.1) and (2.2), efficiency is given by,

$$\eta = \frac{3I_2^2 \frac{R_2(1-S)}{S}}{3I_2^2 \frac{R_2}{S} + 3I_1^2 R_1} \quad (2.3)$$

$$= \frac{1-S}{1+S \frac{R_1 \left(\frac{I_1}{I_2}\right)^2}{R_2}} \quad (2.4)$$

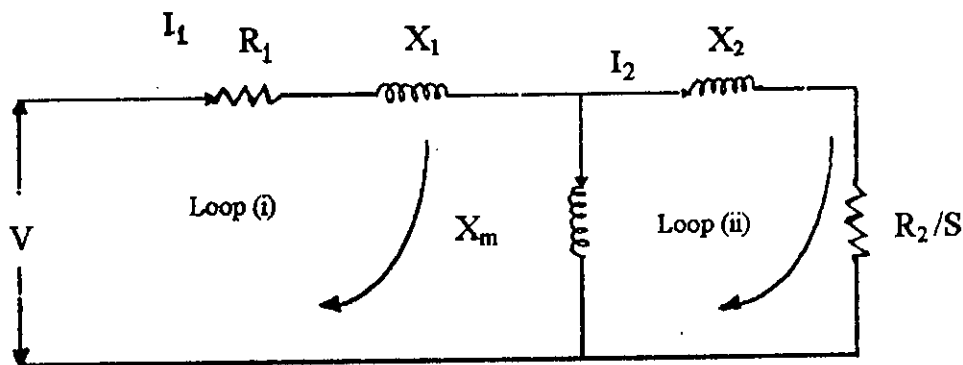


Figure 2.1 : Equivalent circuit of an Induction motor.

Also, from the equivalent circuit of an induction motor considering the following

analysis, we obtain a relationship of  $\left|\frac{I_1}{I_2}\right|^2$  in terms of slip and rotor resistance  $R_2$ .

From second loop,

$$0 = -jI_1 X_m + I_2 \left\{ \frac{R_2}{S} + j(X_2 + X_m) \right\} \quad (2.5)$$

From (2.5) relation of current ratio can be expressed as,

$$\frac{I_1}{I_2} = \frac{\frac{R_2}{S} + J(X_2 + X_m)}{JX_m} \quad (2.6)$$

which can be rewritten as,

$$\frac{I_1}{I_2} = -J \frac{R_2}{SX_m} + \frac{X_2 + X_m}{X_m} \quad (2.7)$$

and simplified to,

$$\frac{I_1}{I_2} = 1 - J \frac{R_2}{SX_m} \quad (2.8)$$

Since  $\frac{X_2}{X_m} \ll 1$

Equation (2.8) can be written as,

$$\left| \frac{I_1}{I_2} \right|^2 = 1 + \frac{R_2^2}{(SX_m)^2} \quad (2.9)$$

Combining (2.4) & (2.9) we obtain,

$$\eta = \frac{1-S}{1 + \frac{R_1}{R_2} \left( \frac{I_1}{I_2} \right)^2 S} = \frac{1-S}{1 + \left( 1 + \frac{R_2^2}{[SX_m]^2} \right) \frac{R_1}{R_2} S} \quad (2.10)$$

Which can be simplified to,

$$\eta = \frac{(S-S^2) X_m^2 R_2}{SR_2 X_m^2 + R_1 X_m^2 S^2 + R_2^2 R_1} \quad (2.11)$$

For maximum efficiency operation following condition prevails,

$$\frac{d\eta}{dS} = 0 \quad (1.12)$$

which gives,

$$(SR_2 X_m^2 + R_1 S^2 X_m^2 + R_1 R_2^2)(1-2S) = (S-S^2)(R_2 X_m^2 + 2R_1 S X_m^2) \quad (2.13)$$

or

$$S^2(R_2 X_m^2 + R_1 X_m^2) + R_1 R_2^2(2S-1) = 0 \quad (2.14)$$

or,

$$S^2(R_2 + R_1) + \frac{R_1 R_2^2}{X_m^2}(2S-1) = 0 \quad (2.15)$$

Since  $\frac{1}{X_m^2} \gg \frac{2S}{X_m^2}$ , Equation (2.15) can be approximately written as,

$$S^2(R_2 + R_1) = \frac{R_2^2 R_1}{X_m^2} \quad (2.16)$$

Equation (2.16) yields the value of slip at maximum efficiency to be,

$$S_{\eta, \max} = \frac{R_2}{X_m} \sqrt{\frac{R_1}{R_1 + R_2}} \quad (2.17)$$

The above expression for slip at maximum efficiency is derived without considering the constant losses of the motor. The expression of slip at maximum efficiency operation considering the constant losses can also be derived.

## 2.2 Slip at maximum efficiency (considering constant losses) :

Efficiency of an induction motor is given by

$$\eta = \frac{P_{OL}}{P_{OL} + 3I_1^2 R_1 + 3I_2^2 R_2 + W_c} \quad (3.18)$$

where,

$P_{OL}$  = Output power at any load L of full load and

$W_c$  = Constant losses including friction windage and core losses.

The above can be expressed as follows considering the equivalent circuit of the motor

$$P_{OL} = 3I_2^2 R_2 \frac{1-S}{S} - W_c \quad (2.19)$$

$$\text{or, } I_2^2 = \frac{S(W_c + P_{OL})}{3(1-S)R_2} \quad (2.20)$$

Hence the efficiency expression can be written as ,

$$\eta = \frac{P_{OL}}{P_{OL} + 3R_1 \left[ \left( \frac{R_2}{SX_m} \right)^2 + \left( \frac{X_2 + X_m}{X_m} \right)^2 \right] \frac{S(W_c + P_{OL})}{3(1-S)R_2}} * \frac{1}{\frac{3(W_c + P_{OL})}{3(1-S)R_2} R_2 + W_c} \quad (2.21)$$

which can be simplified to,

$$\eta = \frac{P_{OL}}{P_{OL} + W_c} \left[ \frac{1-S}{1 + \left( \frac{R_1}{R_2} \right) S \left[ \left( \frac{R_2}{SX_m} \right)^2 + \left( \frac{X_2 + X_m}{X_m} \right)^2 \right]} \right] \quad (2.22)$$

Since for a given load  $\frac{P_{OL}}{P_{OL} + W_c} = \text{constant } t = K(\text{say})$ , efficiency can be expressed as,

$$\eta = K \left[ \frac{1-S}{1 + \left( \frac{R_1}{R_2} \right) S \left[ \left( \frac{R_2}{SX_m} \right)^2 + \left( \frac{X_2 + X_m}{X_m} \right)^2 \right]} \right] \quad (2.23)$$



which shows maximum efficiency  $\eta_{\max}$  is independent of K or on load fraction and constant losses and as in equation (2.17)  $\eta_{\max}$  will occur at slip  $S_{\eta,\max}$  which can approximately obtained as equation (2.24) as follows,

$$S_{\eta,\max} = \frac{R_2}{X_m} \sqrt{\frac{R_1}{R_1 + R_2}} \quad (2.24)$$

### 2.3 V/I Control strategy for maximum efficiency operation .

Focus has been made on the steady state impedance relationship of the motor in order to obtain a simple control strategy to maintain maximum attainable efficiency at any load. The input impedance of an induction motor is the ratio of input voltage to the input current which in terms of motor parameters become slip dependent. The approximate efficiency relationship of the motor is,

$$\eta = 1 - S \quad (2.25)$$

From the above relationship, it may seem that maintaining the constant slip operation at the value of full load slip would result in motors maximum efficiency all the time. The slip relationship for maximum attainable efficiency considering constant losses and variable load has been derived in the previous section. If the slip relationship of equation (2.17) or (2.24) can be maintained then it is possible to obtain maximum efficiency operation of the motor at other than rated load. It is our objective to obtain a simple V/I control scheme which will allow us to achieve the mentioned goal without feedback and without frequency control at speeds below rated speed. To develop a V/I

control scheme the following treatment is followed to obtain a V/I relationship in terms of motor's steady state parameters and slip at maximum efficiency.

From loop ( i ) and (ii) of the equivalent circuit of figure 2.1,

$$V = [R_1 + j(X_1 + X_m)]I - jX_m I_2 \quad (2.26)$$

where,  $I_1 = I$  (input current)

$$0 = -jX_m I + \left[ \frac{R_2}{s} + j(X_2 + X_m) \right] I_2 \quad (2.27)$$

From (2.26) we can write,

$$I_2 = \frac{jX_m I}{\left[ \frac{R_2}{s} + j(X_2 + X_m) \right]} \quad (2.28)$$

Replacing (2.41) in (2.39) we get,

$$V = [R_1 + j(X_1 + X_m)]I - jX_m \frac{jX_m I}{\left[ \frac{R_2}{s} + j(X_2 + X_m) \right]} \quad (2.29)$$

From which V/I can be obtained as,

$$\frac{V}{I} = [R_1 + j(X_1 + X_m)] + \frac{X_m^2}{\left[ \frac{R_2}{s} + j(X_2 + X_m) \right]} \quad (2.30)$$

Since all quantities of the V/I ratio (i.e impedance of the motor) is constant except S, putting the value of S for maximum efficiency in the above expression will yield a V/I

ratio maintaining of which will ensure operation of the motor at the set slip of maximum efficiency.

Equation (2.30) indicates that by adjusting  $V/I$  ratio of a motor, the slip  $S$  can be attained at desirable values. In the previous section the relationship has been developed for  $S_{\eta_{max}}$  for various loading on the motor. Hence, if we can predetermine the target slip from equation (2.24) as the load is changed, we may resort to change in the voltage until the desired  $V/I$  is obtained as given by (2.30). This in the long run will ensure the maximum attainable efficiency operation of the motor at the changed load.

In other word, if the expression for slip at maximum efficiency is put in relation (2.30), a  $V/I$  ratio in terms of motor constants and load is predetermined, maintaining of which will ensure the maximum attainable efficiency operation of the motor at a load  $L$ , where  $L$  is the fraction of full load.

## **2.4 Experimental Verification of V/I Control Strategy**

A three phase wound rotor 380 volt, 175 watt machine was tested for the verification of the  $V/I$  control strategy developed in the previous section. The motor parameters were determined by standard block rotor and no load tests. The parameters were found as,

$$R_1 = 46 \text{ ohm/phase}$$

$$R_2 = 92 \text{ ohm/phase}$$

$$X_1 = 36 \text{ ohm/phase}$$

$$X_2 = 36 \text{ ohm/phase}$$

$$X_m = 580 \text{ ohm/phase}$$

With the parameters, the slip at which maximum efficiency should occur may be obtained from equation (2.24). This slip value put in the V/I relationship equation (2.30) of the motor, the impedance of the motor or V/I ratio was found to be 550. As outlined in the previous sections, maintaining this ratio should maintain the maximum attainable efficiency of the motor at any operating load. To verify this an experiment was designed with the same motor with a dynamometer as load, the motor having the provision for variable sinusoidal voltage supply from a three phase variac. The motor was tested for several load conditions (0.16 N-M to 1.00 N-M). For each loading (say 0.16 N-M) the load was kept constant by dynamometer knob adjustment while the supply voltage to the motor was changed by the variac. Readings were taken for V, I, Input power, Output power and the Speed of the motor. These were recorded and are presented in appendix 1. For each loading condition (constant load) efficiency, slip and a V/I ratio of the motor were calculated from experimental data and they are plotted in figures 2.2 to 2.9. It is evident from these figures (efficiency vs slip) that the maximum attainable efficiency of this test motor occurs near the predicted slip of 9.15. Also from the efficiency vs V/I ratio curves, it is evident that the V/I ratio is almost equal to 550. Similar experiments on other motors will also justify the validity of the slip and V/I

ratio of induction motor expression for maintaining the maximum attainable efficiency at various loads by voltage variation only. Hence, it can be inferred that by resorting to a suitable voltage control strategy and maintaining a particular  $V/I$  ratio determined by the motor parameters, an induction motor can be operated at its maximum attainable efficiency at a certain load and below rated speed operation of the motor. In this thesis, a PWM voltage control scheme controlled by microcomputer is developed for this purpose which is described in the following chapter.

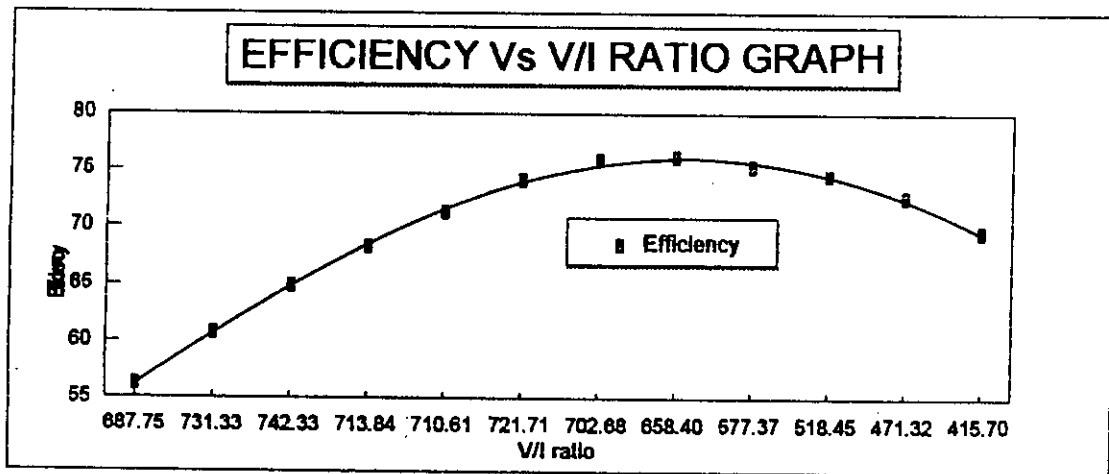
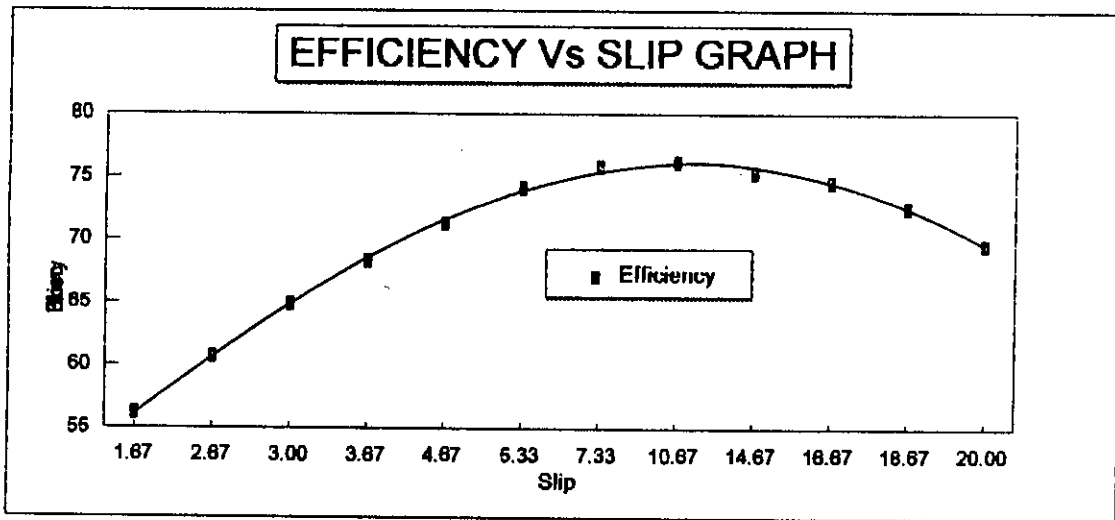


**FIG. 2.2 : Graphical presentation of Efficiency Vs Slip and Efficiency Vs V/I ratio of a 380 V, 175 W, 3-phase Induction motor for constant load of 0.16 N-M**

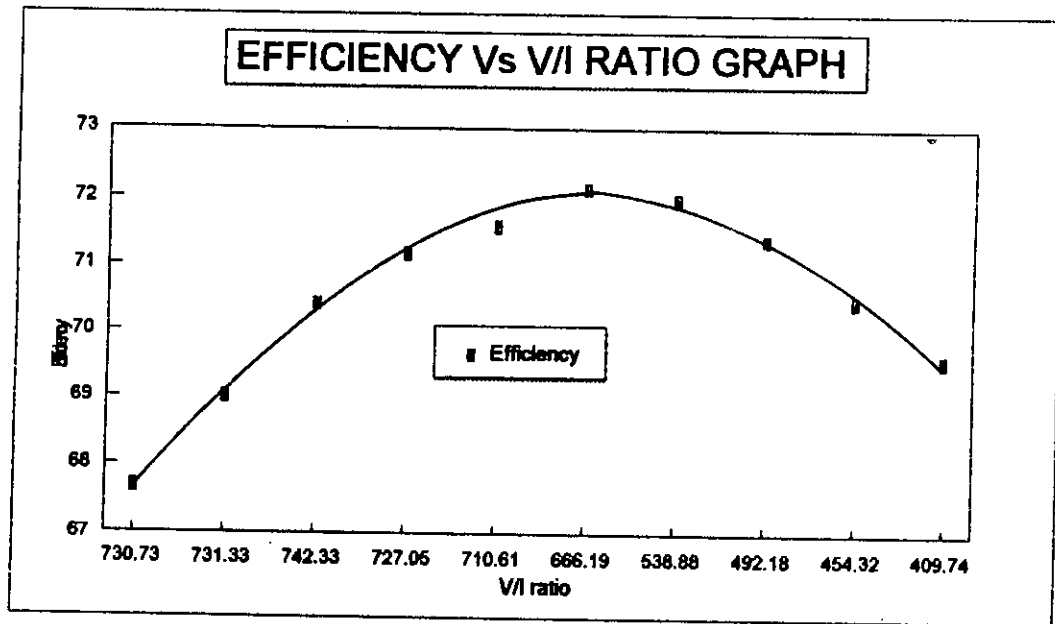
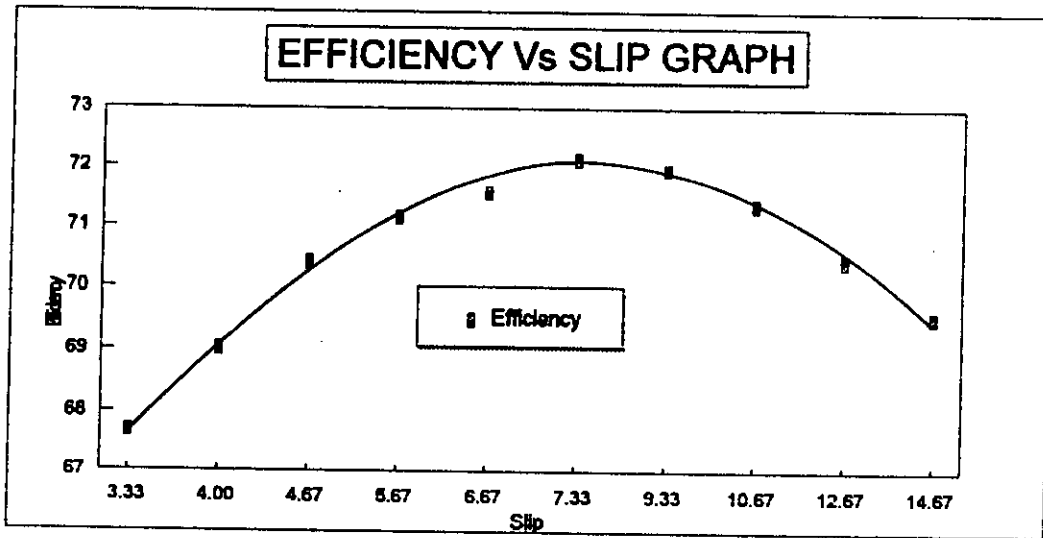


**FIG. 2.3 : Graphical presentation of Efficiency Vs Slip and Efficiency Vs V/I ratio of a 380 V, 175 W, 3-phase Induction motor for constant load of 0.25 N-M**

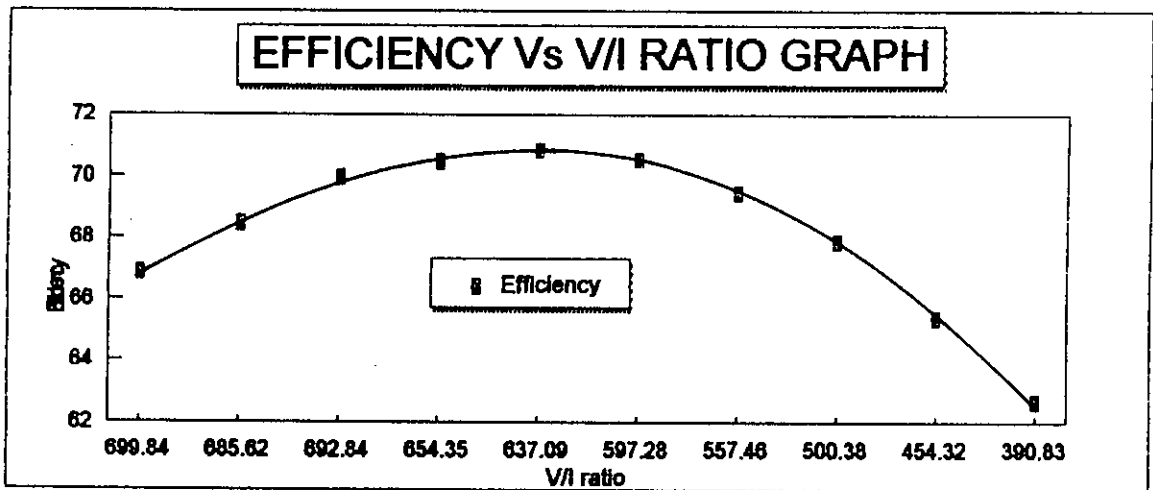
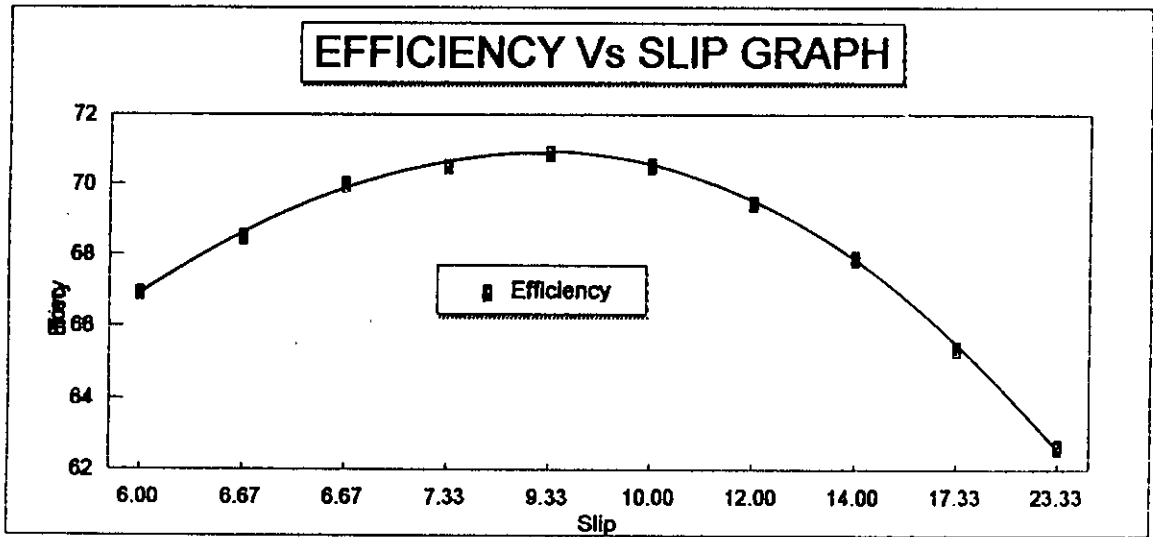


**FIG. 2.4 : Graphical presentation of Efficiency Vs Slip and Efficiency Vs V/I ratio of a 380 V,175 W, 3-phase Induction motor for constant load of 0.40 N-M**



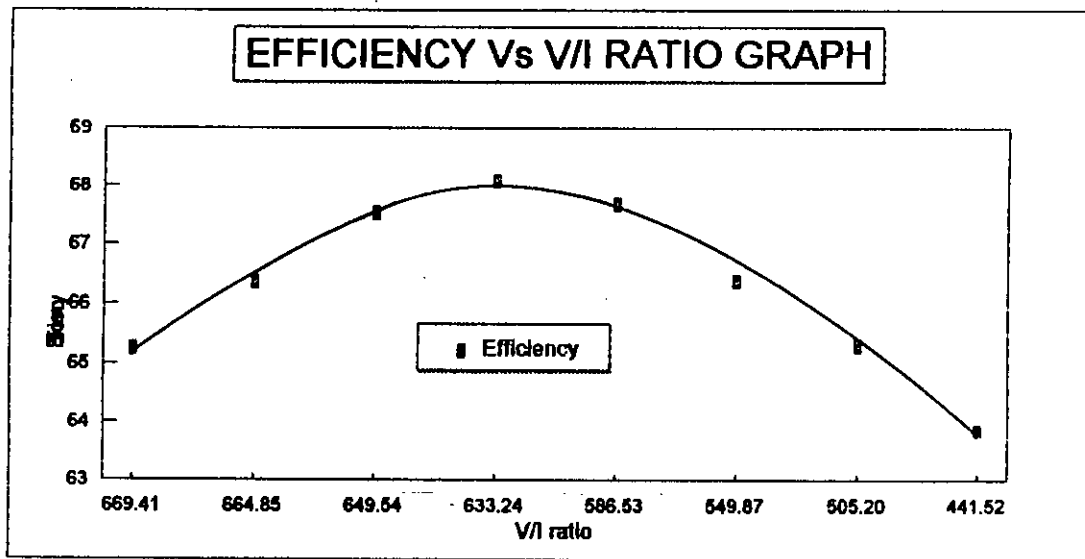
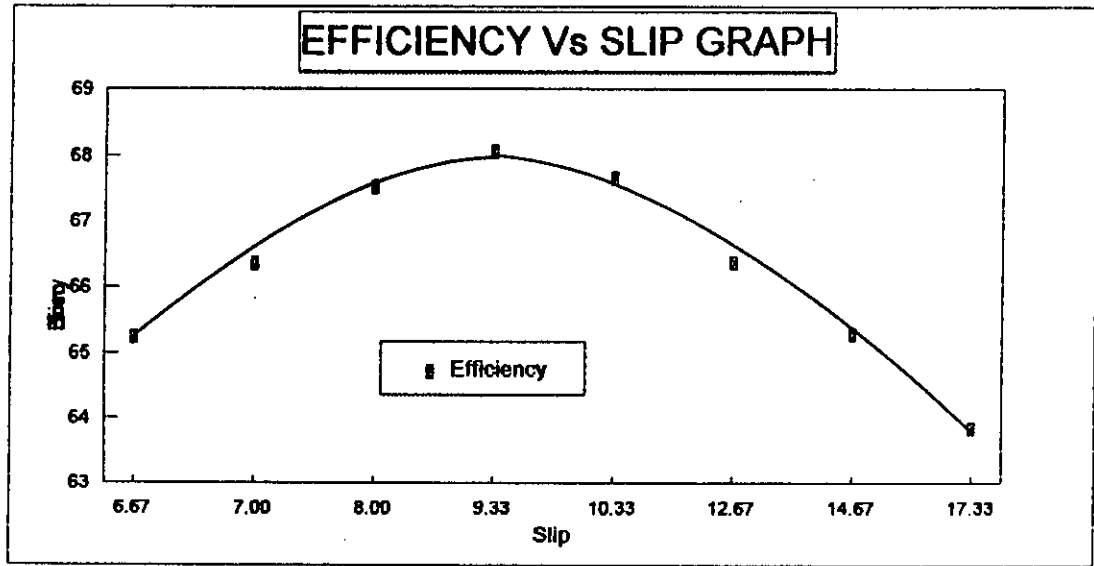


**FIG. 2.5 : Graphical presentation of Efficiency Vs Slip and Efficiency Vs V/I ratio of a 380 V, 175 W, 3-phase Induction motor for constant load of 0.50 N-M**

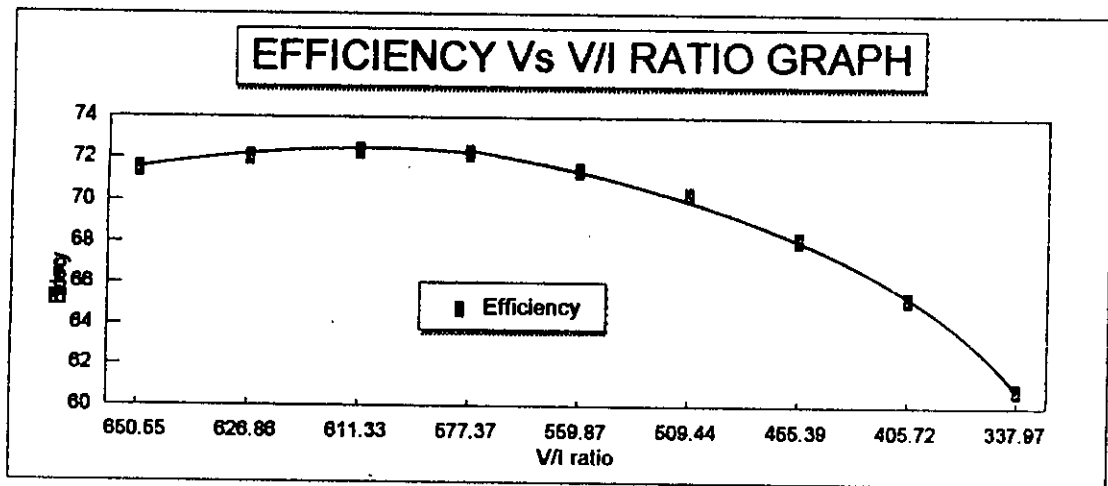
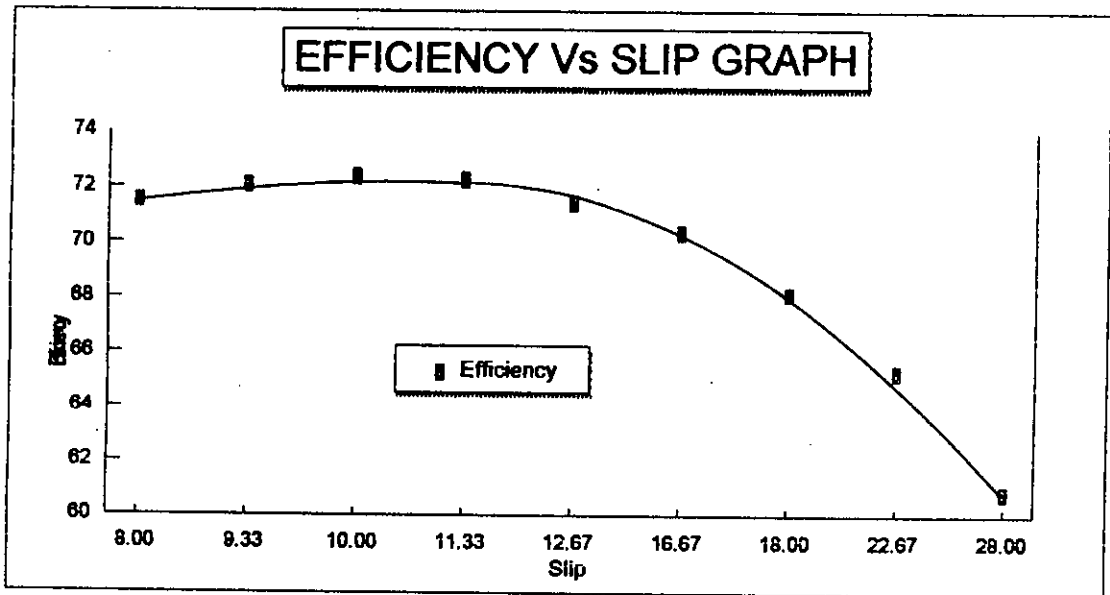


**FIG. 2.6 : Graphical presentation of Efficiency Vs Slip and Efficiency Vs V/I ratio of a 380 V, 175 W, 3-phase Induction motor for constant load of 0.60 N-M**

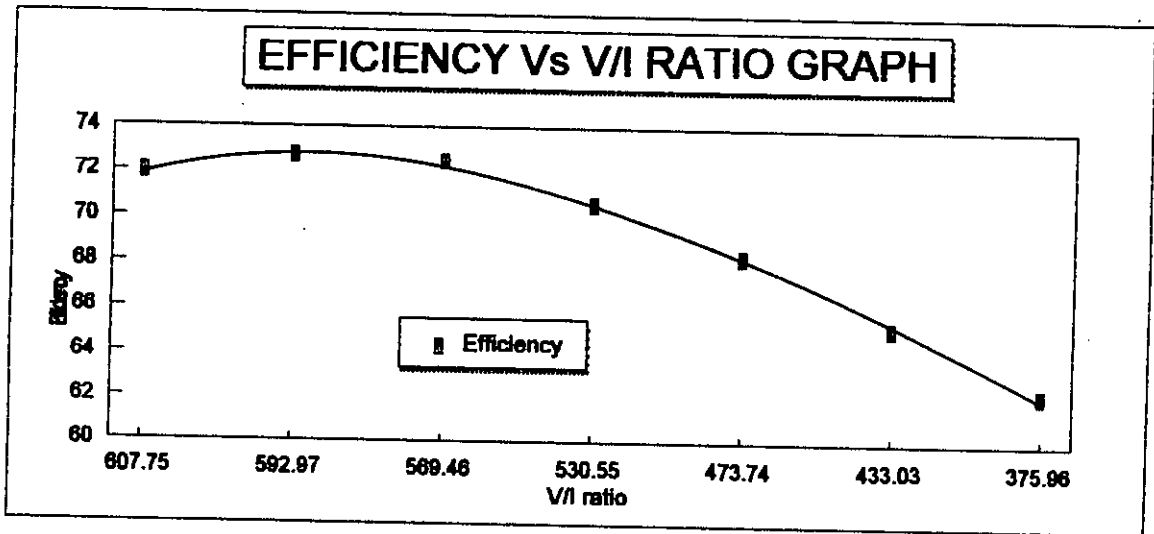
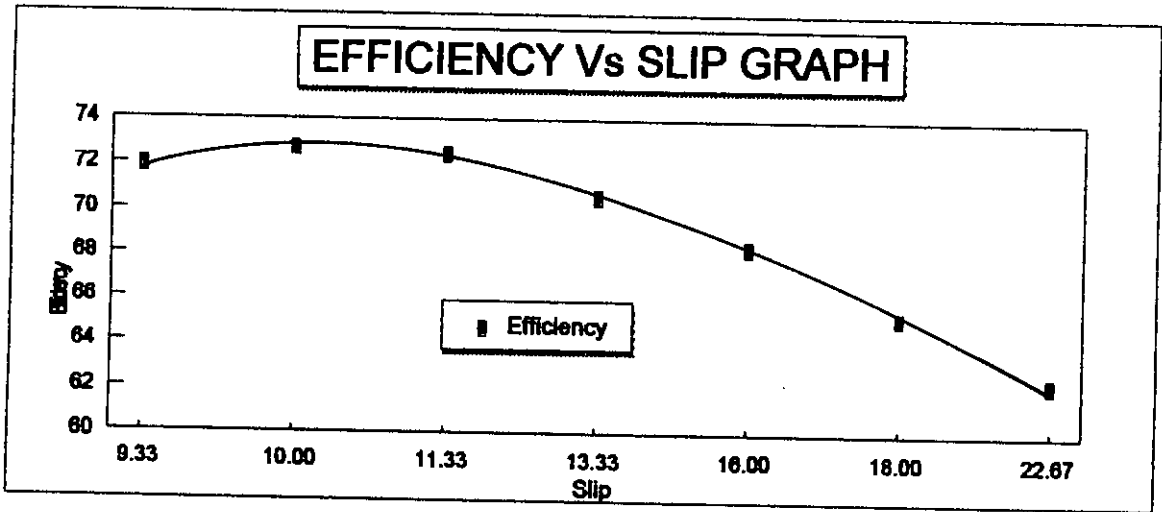


**FIG. 2.7 : Graphical presentation of Efficiency Vs Slip and Efficiency Vs V/I ratio of a 380 V, 175 W, 3-phase Induction motor for constant load of 0.75 N-M**

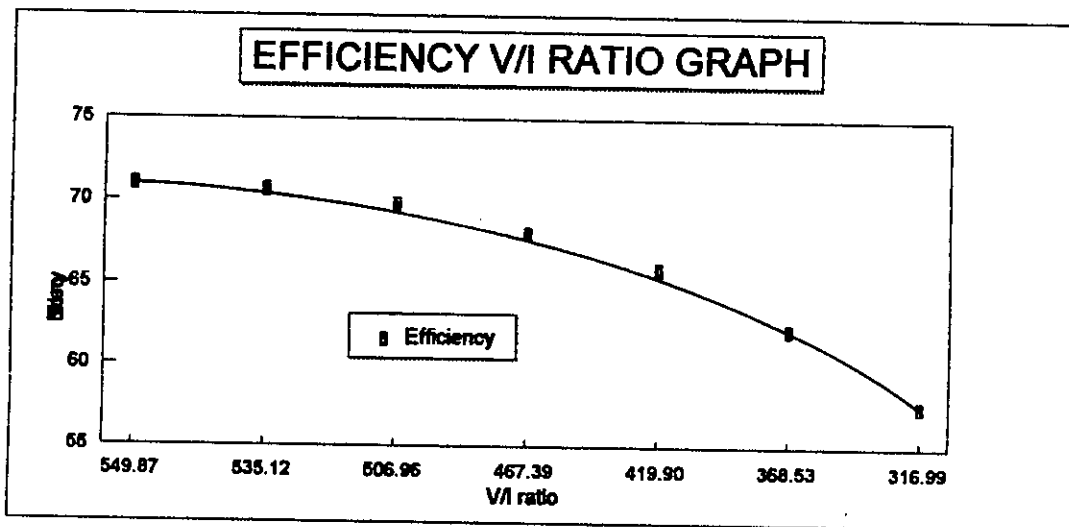
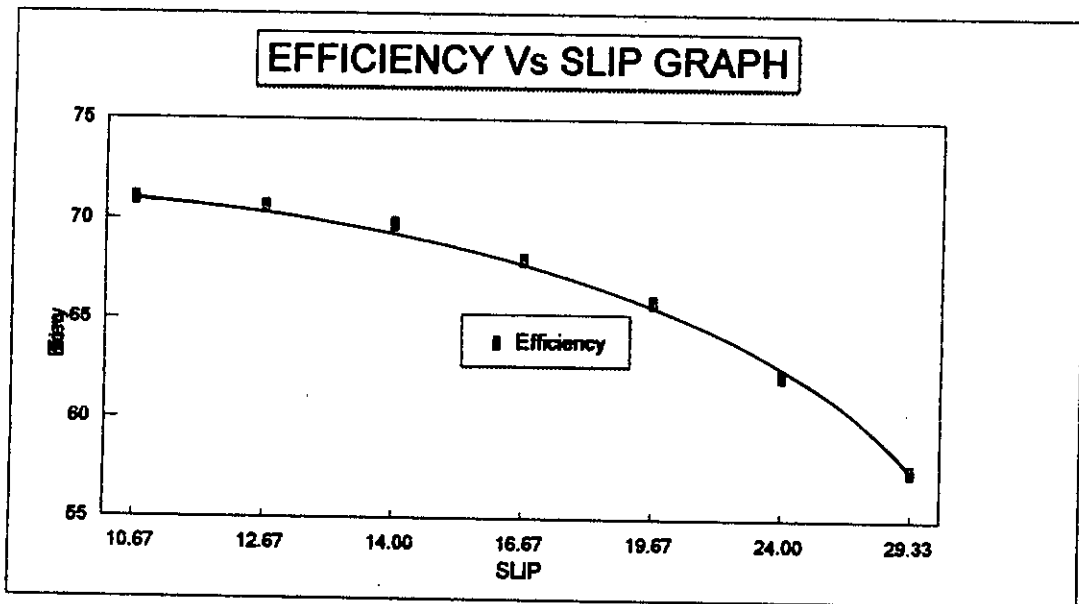


**FIG. 2.8 : Graphical presentation of Efficiency Vs Slip and Efficiency Vs V/I ratio of a 380 V,175 W, 3-phase Induction motor for constant load of 0.90 N-M**

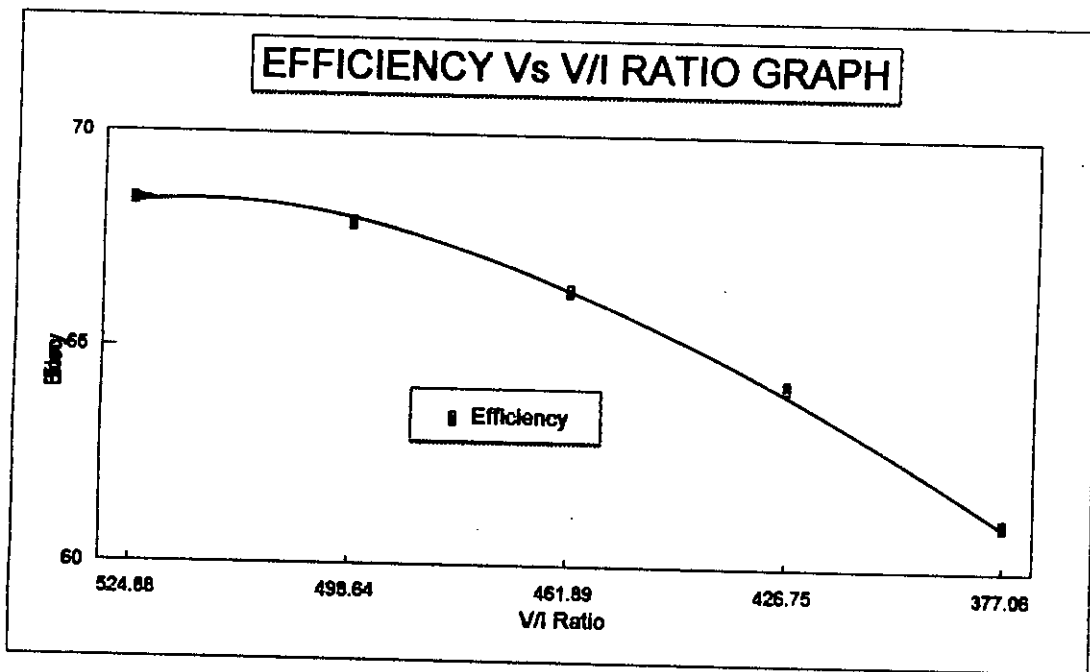
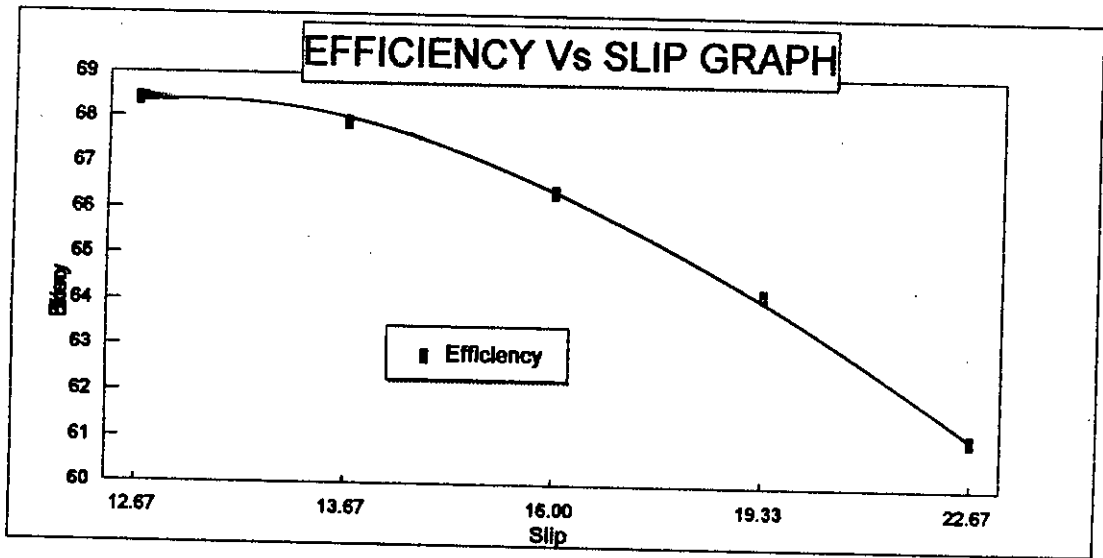


**FIG. 2.9 : Graphical presentation of Efficiency Vs Slip and Efficiency Vs V/I ratio of a 380 V, 175 W, 3-phase Induction motor for constant load of 1.0 N-M**

## CHAPTER -3

### 3.0 Introduction.

The voltage to current ratio strategy to obtain maximum achievable efficiency of an induction motor at various load conditions can be implemented by static voltage controllers. Normal static voltage controllers are phase controlled and contain significant low order harmonics. These harmonics are the cause of losses and uneven torque in ac motors. To reduce the magnitudes of low order harmonics, filters may be used. For power applications the filters become large. One of the most effective method of reducing harmonics of static converter applications is to use pulse width modulated switching. Pulse width modulation allows voltage control of static converter waveforms and frequency control where necessary. In this thesis, sine pulse width modulated scheme of a three phase voltage controller by software control is proposed. Superiority of microcomputer based generation of switching signals by software modules over general hardware system is perceivable from the view point of improved reliability, stability, flexibility and fast calculations. The scheme outlined in this thesis can perform on line calculation of switching points of PWM strategy providing smooth control of various parameters without interruption of the system. In the reported scheme an intel 80386 DX-2 microcomputer or above may be used for the implementation, where, the switching patterns of six switches of a three phase voltage controller are available at the parallel port of the computer.

The implementation involves,

- a. Switching point calculation by microcomputer.
- b. Switching signal generation by microcomputer at the parallel port.
- c. Synchronization of the switching signal with line voltage.
- d. Interface circuit development to drive the gate or base of switches of static converters.
- e. The voltage controller implementation by six static switch modules.

The six switch module performing the function of a voltage controller driving a motor load is shown in fig. 3.1. Typical PWM gating signals for voltage control of static power module of figure 3.1 is shown in figure 3.2. It can be noted that the switching signals are to be synchronized with the line to neutral voltages of the supply voltage for

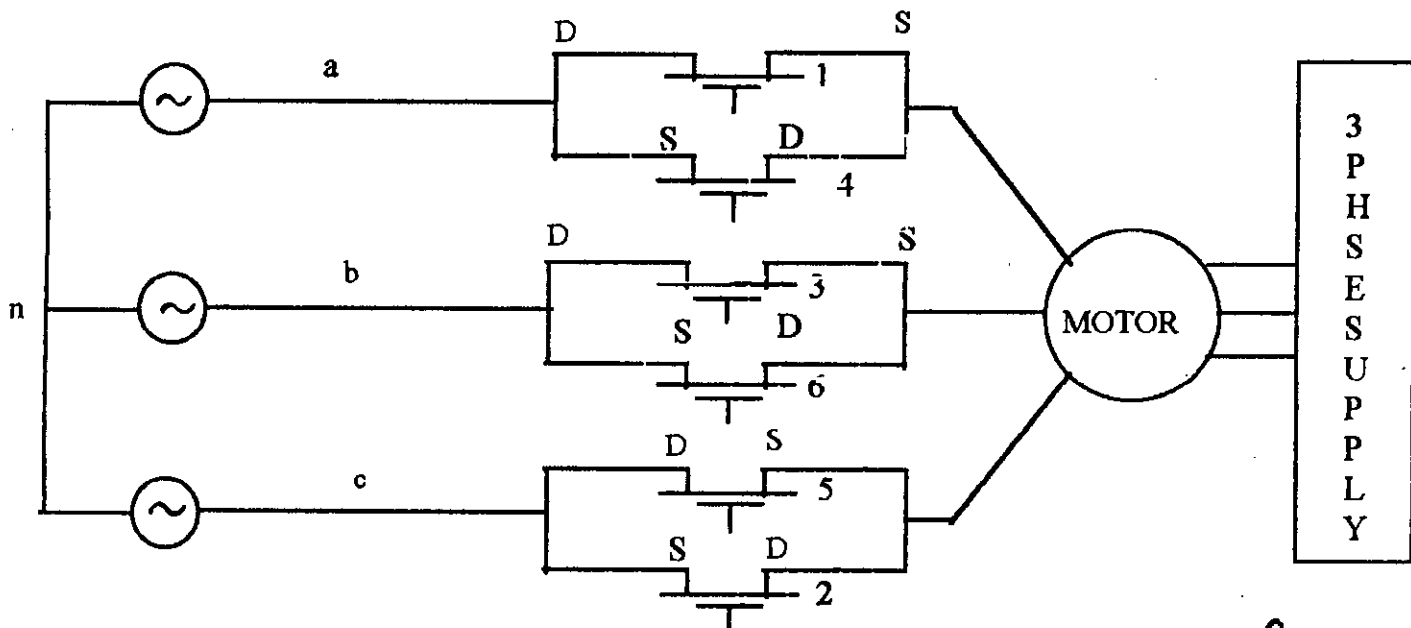


Figure 3.1: Three Phase MOSFET Voltage controller

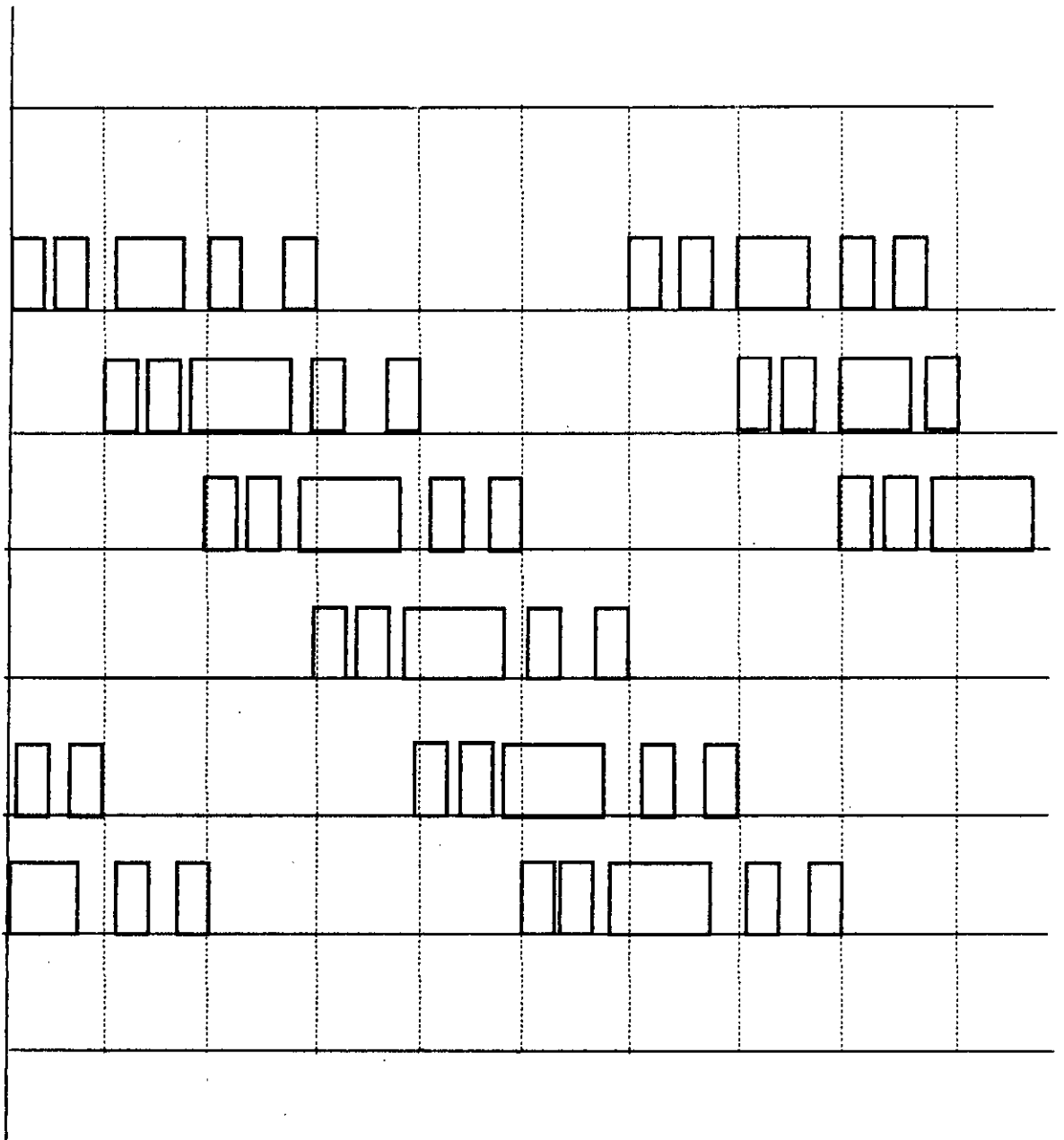


Figure 3.2 : Typical PWM gating signals for power module of the static voltage controllers

Q.



proper operation of the voltage controller. Expected gating signals for power module are shown in figure 3.2. Implementation details with practical results in the form of voltage controller waveforms are presented in the following sections.

### 3.1 SWITCHING POINT CALCULATION OF SINE PWM SWITCHING [25].

The calculation technique of switching points of sine PWM method has been suggested in reference [25]. The technique provides a simple algebraic equation for the calculation of SPWM waveform generation. Figure 3.3 shows the sine modulating & the carrier triangular waveforms. In figure 3.3, the mid point  $\theta_i$  of the  $i$ -th pulse of the switching point is,

$$\theta_i = \frac{(2i-1)\pi}{N} \quad (3.1)$$

As the width of the  $i$ -th pulse is directly proportional to  $E_m \sin\theta_i$  (instantaneous value of sine modulating wave) and inversely proportional to  $E_c$  (magnitude of the carrier wave), the widths can be related as,

$$\delta_i = K_i \frac{E_m}{E_c} \sin\theta_i = K_i m \sin\theta_i \quad (3.2)$$

where,  $\delta_i$  is the pulse width of the  $i$ th pulse,  $t_i$  and  $t_{i-1}$  are the  $i$ th and  $(i-1)$ th switching instants of the modulated wave. Slope of the rising edge of the triangular wave can be related as,

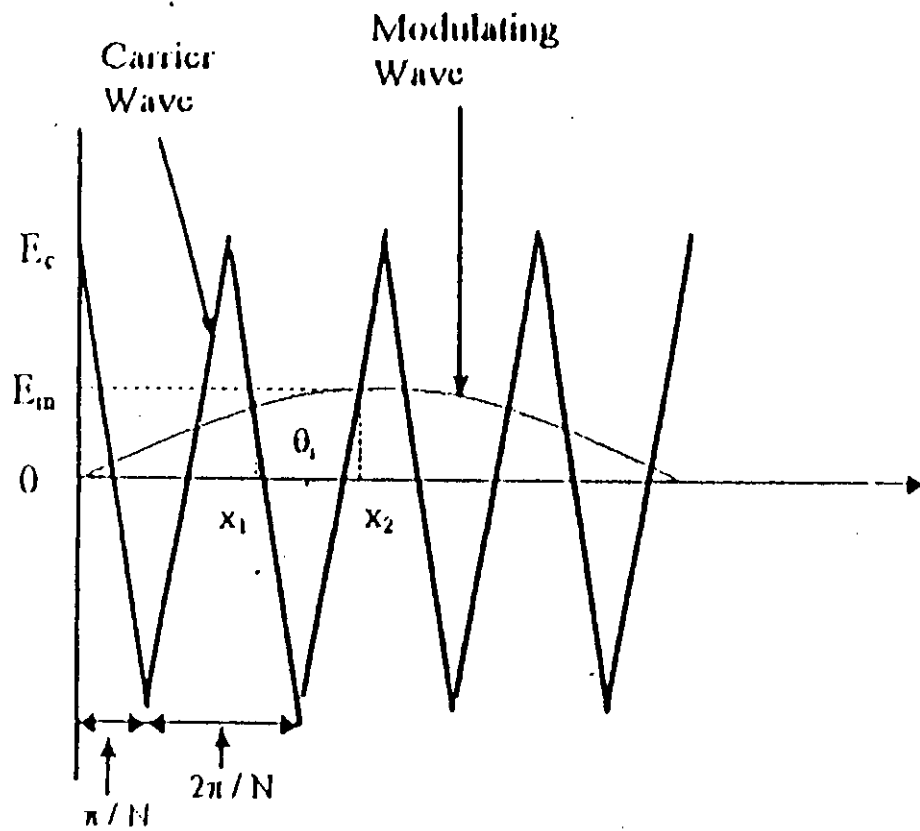


**Figure 3.3 : Expanded view of triangular carrier modulation process of a sine wave.**

$$S \left[ t_i - \left( \theta_i + \frac{\pi}{2N} \right) \right] = E_m \sin \omega t_i \quad (3.3)$$

and the slope of falling edge can be related as,

$$-S \left[ t_{i-1} - \left( \theta_i - \frac{\pi}{2N} \right) \right] = E_m \sin \omega t_{i-1} \quad (3.4)$$

Combining equations (3.3) and (3.4), we obtain,

$$(t_i - t_{i-1}) - \frac{\pi}{N} = \frac{E_m}{S} (\sin \omega t_i + \sin \omega t_{i-1}) \quad (3.5)$$

$$\frac{\delta_i}{\omega} - \frac{\pi}{N} = \frac{E_m}{S} (\sin \omega t_i + \sin \omega t_{i-1}) \quad (3.6)$$

With a fair degree of accuracy,  $E_m (\sin \omega t_i + \sin \omega t_{i-1})$  can be written  $2E_m \sin \theta_i$  (which is actually the value in regular sampled sine PWM switching). As a result equation (3.6) can be rewritten as,

$$\delta_i = \frac{2E_m}{S} \sin \theta_i + \frac{\pi}{N} = \frac{\pi}{N} \left( 1 + \frac{2NE_m}{S\pi} \sin \theta_i \right)$$

$$\delta_i = \frac{\pi}{N} (1 + m \sin \theta_i) \quad (3.7)$$

Once the width  $\delta_i$  of any pulse 'i' of the switching wave is known, the switching points can be calculated by,

$$t_{i-1} = \left( \theta_i - \frac{\delta_i}{2} \right) / 2\pi f_m \quad (3.8)$$

$$t_i = \left( \theta_i + \frac{\delta_i}{2} \right) / 2\pi f_m \quad (3.9)$$

In equations (3.1) to (3.9) the symbols have following meaning

$K_i$  = Constant of proportionality.

$S$  = Slope of the triangular wave =  $\frac{2NE_c}{\pi}$

$m$  = Modulation index =  $\frac{E_m}{E_c}$

$N$  = Ratio of the frequency of carrier wave to modulating wave =  $\frac{f_c}{f_m}$

$\delta_i$  = Width of the  $i$ 'th pulse.

As a simple equation is available for the determination of switchover points of modulated wave of sine PWM technique, the next step is to generate required PWM pulse pattern using the above switching equations.

### **3.2 PWM waveform generation by Microcomputer.**

It has been established in previous research [26,27,28,29, 30] that PWM waveform generation by microprocessors and microcomputers are superior to their analog electronic counterparts. However, the implementation so far has been restricted to look up table based microprocessor strategy in the absence of suitable mathematical formulation for quick solution of switching points at different modulation parameters. As a result, most of the previous works reported are EPROM based techniques incorporating digital ICs for interface. These techniques as they are EPROM based require large memory and do not contain smooth control of wide range of variation of

the control parameters even with the large memory size. They also fail to meet the steady state and transient performance specification of loads connected to static converters due to slow response time. An algebraic equation to determine switching points of sine PWM waveform in few nanoseconds opens the horizon of on line calculation of PWM pulses. This thesis uses the algebraic equation as described [25] in previous section to calculate the SPWM switching pulse to employ an on line microcomputer control of SPWM voltage controller. Unlike the traditional off line control, the proposed on line strategy uses a high speed microcomputer and its general facility of the printer port to generate required SPWM switching pulses for a static voltage controller. The modulation parameters can be changed from key board command 'on-line' without the interruption of the supply to the load. The method is fast and accurate and as a result meets the steady state and the transient performance requirement of the load. The proposed technique is described in the following sections keeping in mind the following feature of a modern fast microcomputer :

As any computer system consists of a combination of three types of subsystems : Central Processing Unit's (CPU), Direct-Memory subsystems having RAM and / ROM chips , and Input/output (I/O) interfaces for peripheral control. Between them, the CPU subsystems supports all the classical arithmetic, logical, and control functions of

the combined system. The Direct-Memory subsystems contain the programmed instructions to be executed by the individual CPU's on active data with which the CPU's are operating.

The I/O interfaces performs the critical communication links between the internal computer operations and the external input/output devices.

A typical block diagram of the fundamental subsystem of a microcomputer and internal block diagram of a CPU are shown in figures 3.4 and 3.5 respectively. The CPU is connected to the other elements through the address, data , and control buses. The width of the data bus normally determines the bit size of a computer. The address bus specifies the memory location, the control bus determines the operation from or a memory location, and the data bus bears data or instruction from the specified memory location.

The computer interface contains adapters to support speaker, keyboard, display monitor, printer, disk drivers etc. The printer adapter provides the parallel I/O port with a 25-pin D-shell connector. In this research, an INTEL 80386 DX-2 machine containing a 32-bit 80386 microprocessor is used.

The printer is connected from printer adapter or parallel adapter of input/output (I/O) channel. These are shown in the block diagram of System Unit of figure 3.6. The I/O channel supporting various adapter contains bi-directional data bus, address lines, interrupt, control lines for memory and I/O read or write, clock and timing lines, DMA

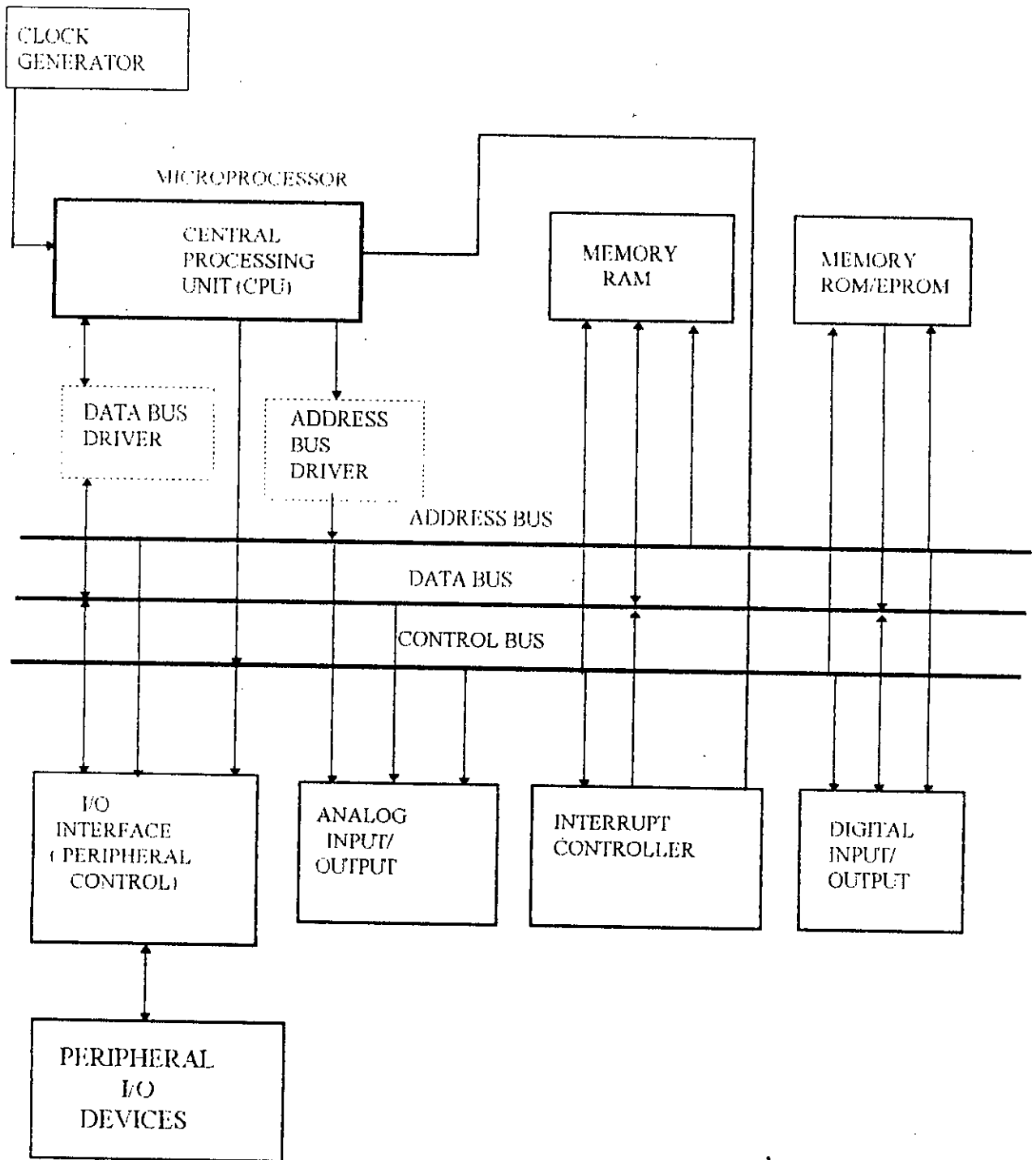


Figure 3.4 : Fundamental subsystems of a microcomputer system.

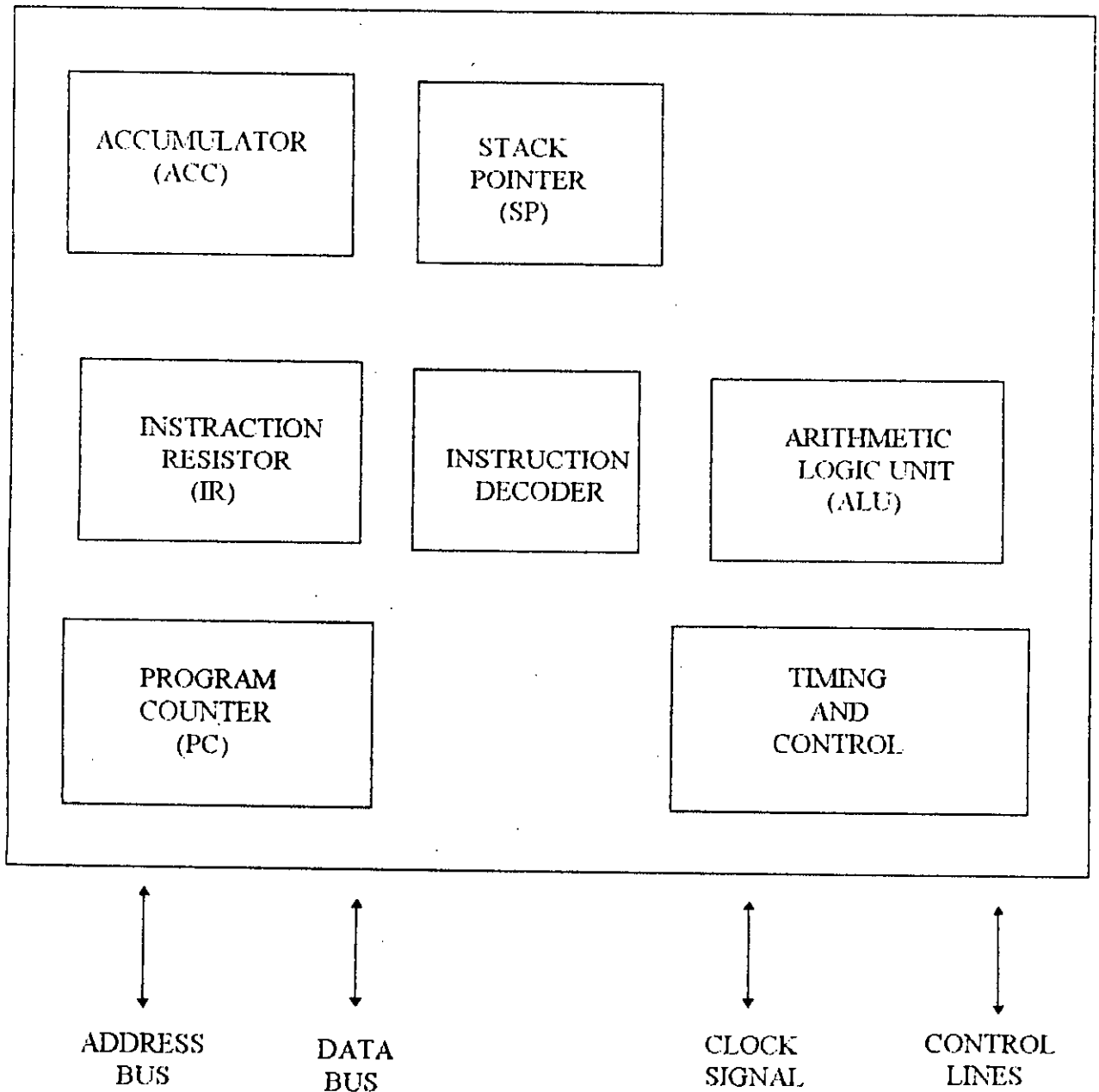


Figure 3.5 : The internal block diagram of a microcomputer central processing unit (CPU)



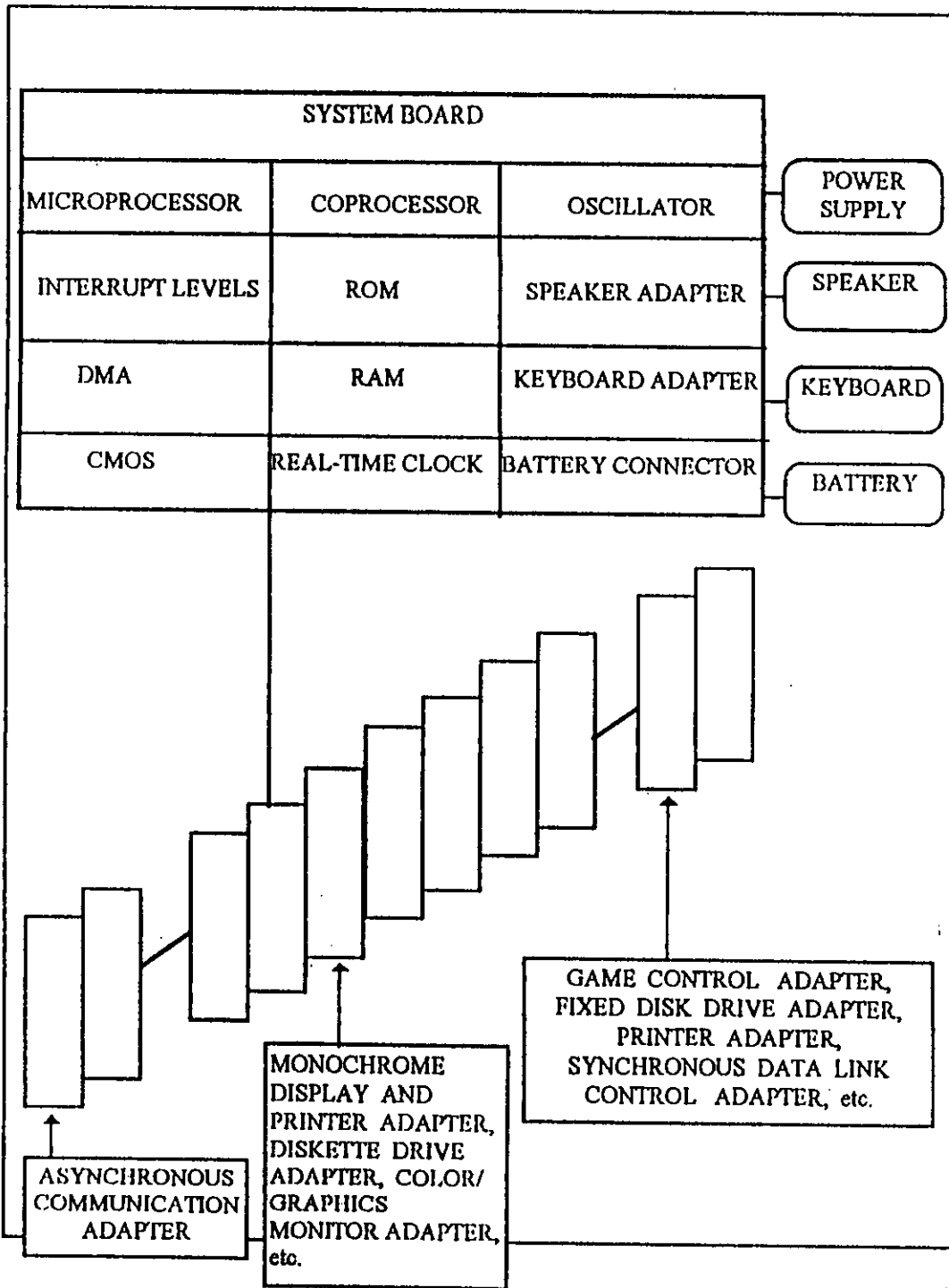


Figure 3.6 : Block diagram of the system unit of a microcomputer.

control lines, memory refresh timing control lines, channel-check line, and power and ground for the adapters. Four voltage levels are provided for I/O cards : +5 volt, -5 volt, +12 volt, -12 volt dc. The adapters are addressed according to the I/O address map. Of the connectors, the printer or parallel connector is the only parallel I/O port which is addressed as 378-37F in Hexadecimal range. Here, 3 indicates parallel port 1. If we write 2 instead of 3, it will address parallel port 2.

The simple communication ports, i.e. parallel printer and serial ports, are non-critical components in the personal computer machine. Of the two ports, parallel interface port is the easiest interface to understand. Although there is no well-defined standard for parallel and serial ports, the IBM style connector has become the de facto standard. Most IBM machines and clones use a 25-pin D-shell female connector which is marked either "parallel port" or "printer port" [31]. The parallel adapter or printer adapter makes possible the attachment of various devices that accept eight bits of parallel data at standard TTL levels. The block diagram of a printer adapter and connection specifications of a 25-pin D-shell connector are shown in figures 3.7 and 3.8 respectively [32].

The printer adapter or parallel adapter responds to five I/O instructions : two output and three input. The output instructions transfer data into 2 latches whose outputs are presented on pins of the 25-pin D-shell connector numbered as pin-2 to pin-9 for the corresponding data bit-0 to data bit-7 as shown in figure 3.9. Two of the three input

instructions allow the processor to read back the contents of the two latches. The third allows the processor to read the real time status of a group of pins on the connectors. When the printer adapter is used to attach a printer or any device that accept eight bits of parallel data at standard TTL levels, data or commands are loaded into an 8-bit latched output port and the strobe line is activated, writing data to the printer or passing pulses of required patterns to the interfaced device connected with the adapter. The SPWM switching pulses for a three phase voltage controller system will be available at the parallel connector.

### **3.2.1 Composite byte Generation.**

The switching pattern generation of three phase static converters by a microcomputer uses the algebraic equation to calculate the switching points for given modulation parameters. The switching points are then used to form a composite byte pattern resembling the switching waves for three phase static converter which are made available at the data pins of parallel port to be used for gating of static switches of the converter. For three phase voltage controllers additional requirement is to synchronize the waveforms with line supply voltage for proper gating of switching devices.

To produce the required pulses at the parallel port, composite byte pattern is generated by a software routine [33]. For three phase operation PWM patterns are shifted by 60 degrees from each other as shown in figure 3.10. When the whole pulse pattern is scanned with a sampling time of  $\Delta t$ , a composite byte of logic 1 for positive voltage

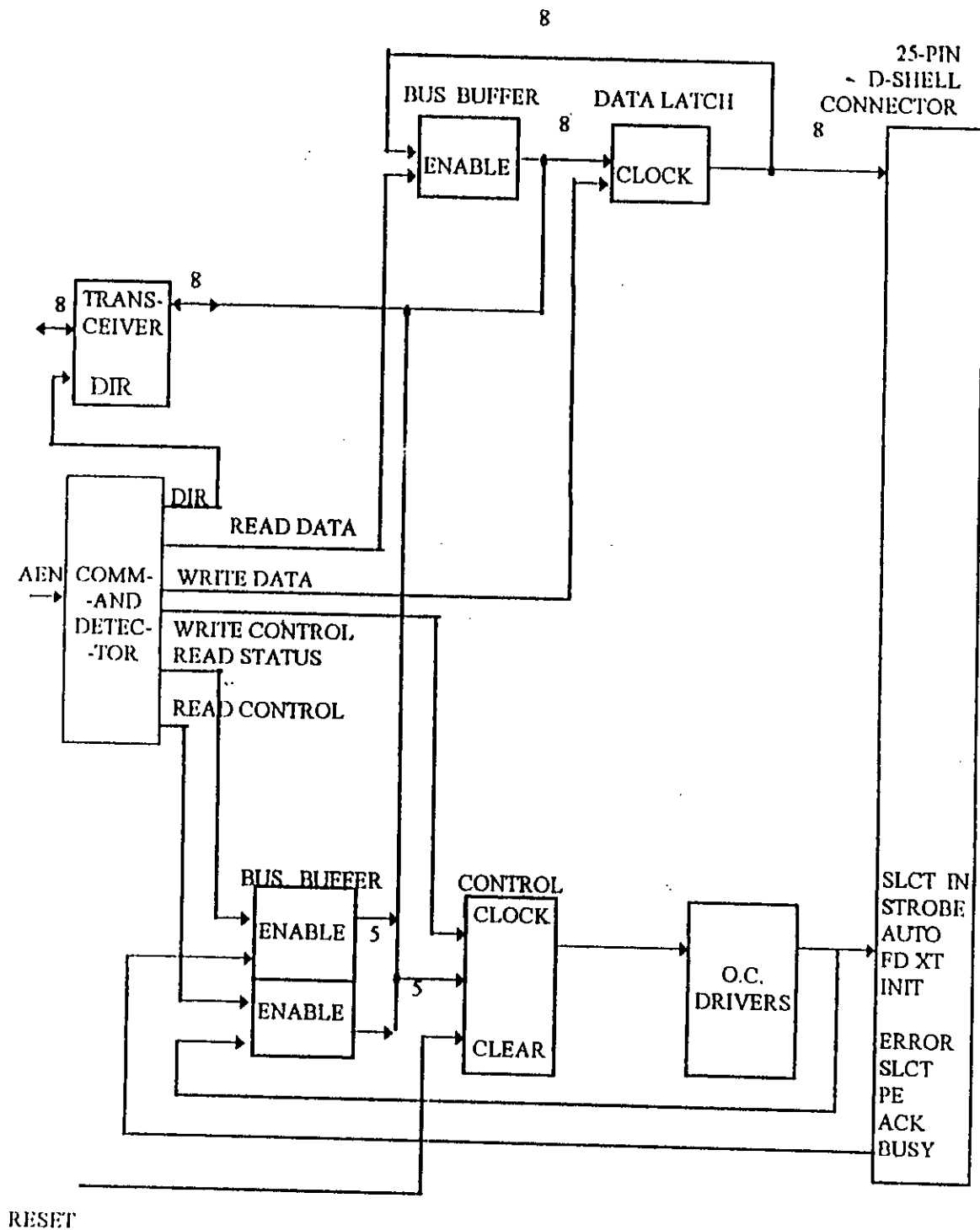
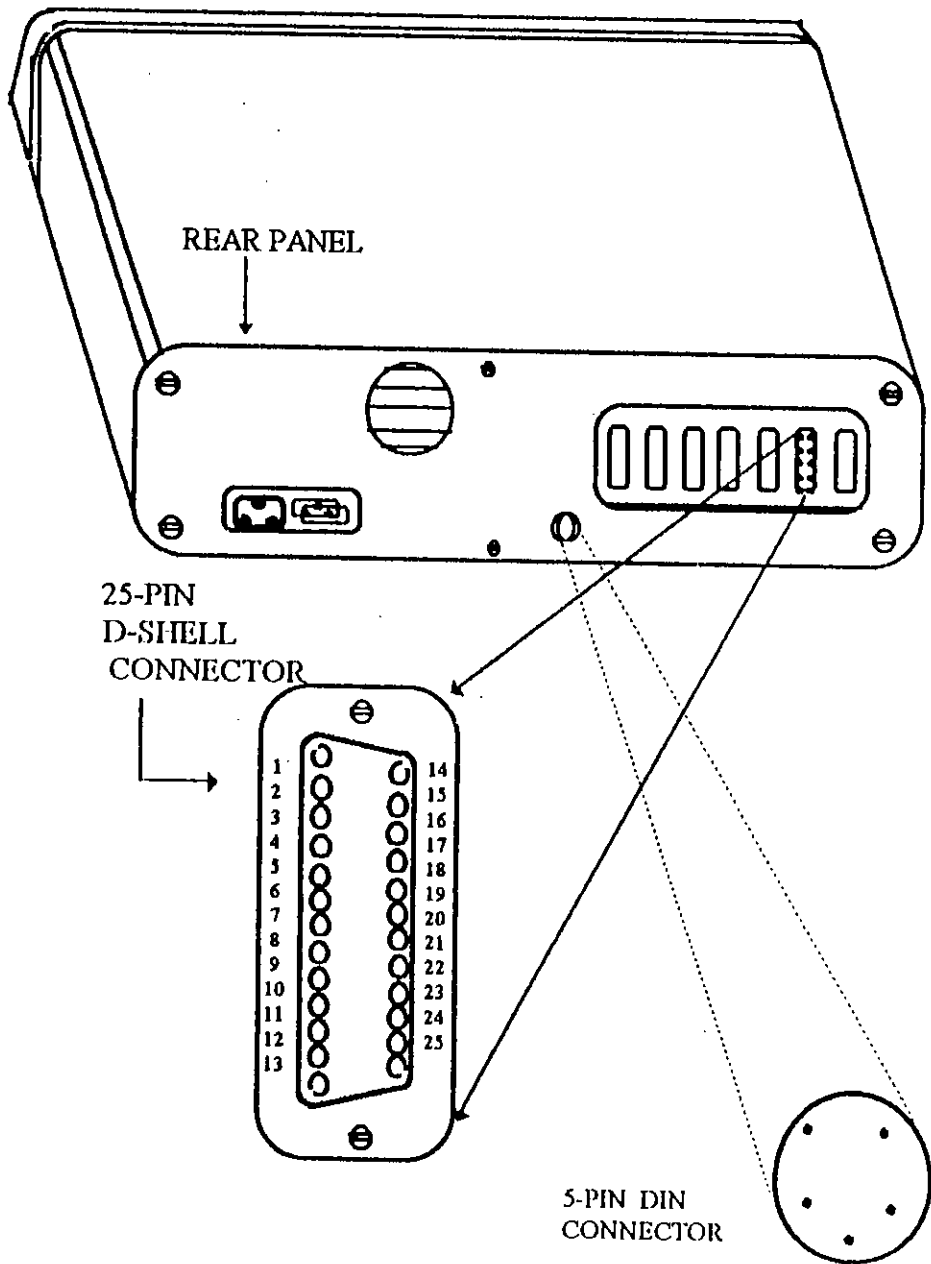
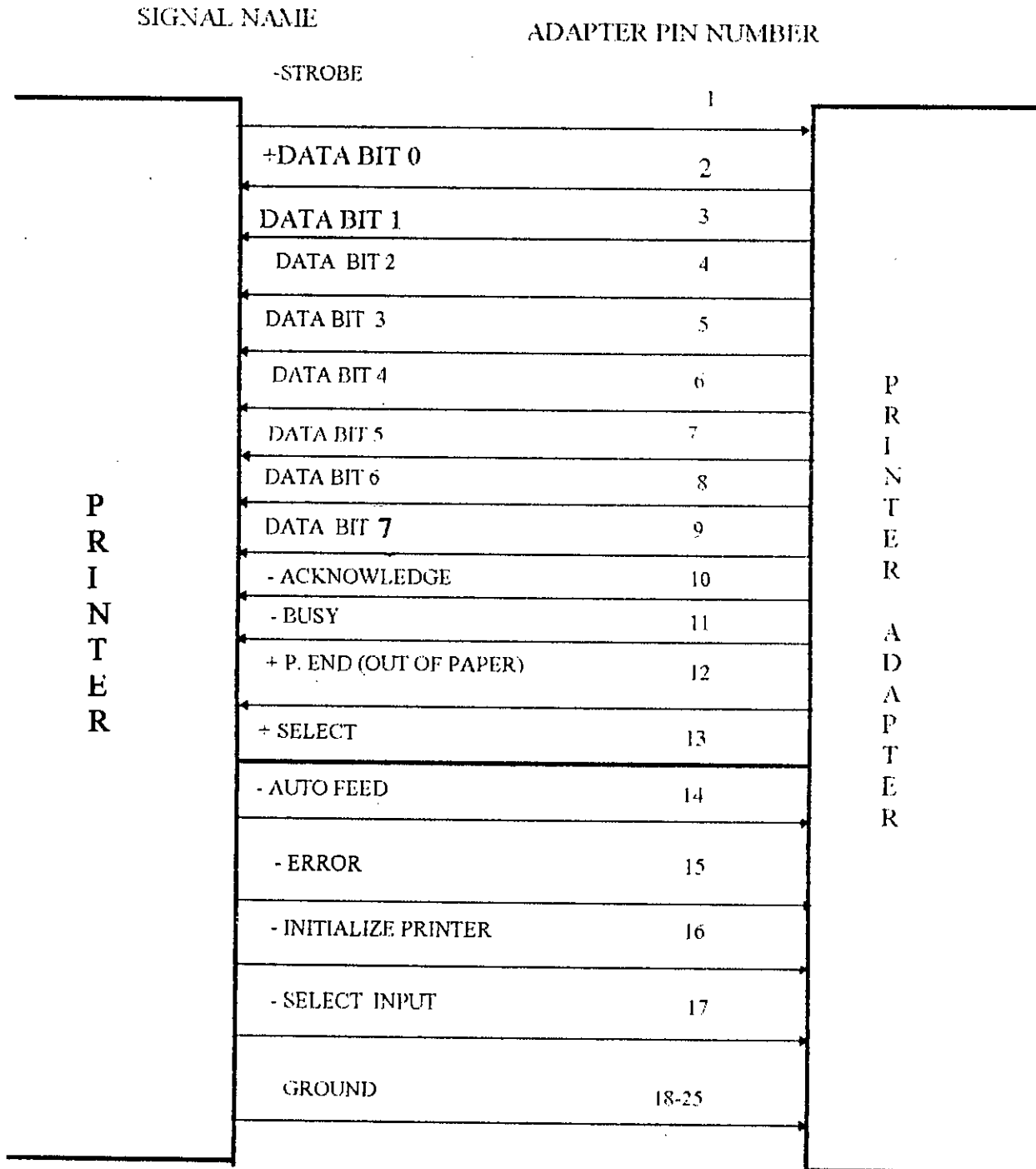


Figure 3.7 : Block diagram of a printer Adapter of a microcomputer.



**Figure 3.8 : Connector Specification of a Parallel I/O port.**

AT ATANDARD TTL LEVELS



NOTE : OUTPUT TO ADDRESS HEX 378 FOR PIN NUMBER-2 TO PIN NUMBER-9 & ALL OUTPUTS ARE SOFTWARE- GENERATED AND ALL INPUTS ARE REAL-TIME SIGNALS (NOT LATCHED)

Figure 3.9 : Data-pin Specification of 25-pin D-shell parallel I/O PORT.

and of logic '0' for negative voltage is obtained. If the decimal converted number of this binary composite byte can be sent to the address 0X378 to be sustained for a time span of  $del$ , then the pattern of this time segment will be reproduced at the eight data pins of the parallel port. These decimal numbers are stored in an array called  $deci[num\_seg]$ , where,  $num\_seg = t_m / del$ . From figure 3.11 the conversion equation of decimal numbers to create the array  $deci[num\_seg]$  can be obtained as,

$$deci[ r ] = b_{r2} 2^0 + b_{r3} 2^1 + \dots + b_{r7} 2^5 + 0 \times 2^6 + 0 \times 2^7$$

Where,  $r$  is the segment number = 0, 1, 2, ..... , and

$b_{rx}$  is the binary 1 and 0 of the 'element' of segment 'r' and pin 'x'.

In programming, the creation of  $deci[num\_seg]$  is not needed to sum up the converted numbers of 'element' bearing logic 0. Initially all elements are assigned 0 and creation of array  $deci[num\_seg]$  is started by running the decimal converted numbers only for elements where logic is 1 and the creation of array is performed pin wise instead of segment wise manner executing the following formula,

$$deci[ r ] = deci[ r ] + 2^{5-K}$$

Where,  $K$  represents pin numbers as shown in figure 3.10.

Six switching pulses to be generated have phase shifts from one another. The wave shapes of the switching pulses for each pin will be same with the fact that they starts from different initial position as,

$$init = 0.0 \quad \text{for } K= 5$$





OUTPUT PULSES								REPRESENTATION	
pin-9	pin-8	pin-7	pin-6	pin-5	pin-4	pin-3	pin-2	Byte	Hexadecimal
bit-7	bit-6	bit-5	bit-4	bit-3	bit-2	bit-1	bit-0	representation	conversion
					0°	t <sub>0</sub>	□	00000001	0x 01
						t <sub>1</sub>	□	00000000	0x 00
						t <sub>2</sub>	□	00000001	0x 01
						t <sub>3</sub>	□	00000000	0x 00
						t <sub>4</sub>	□	00000001	0x 01
						t <sub>5</sub>	□	00000000	0x 00
						t <sub>6</sub>	□	00000000	0x 00
						t <sub>7</sub>	□	00000001	0x 01
						t <sub>8</sub>	□	00000000	0x 00
					180°	t <sub>9</sub>	□	00000001	0x 01
						t <sub>0</sub>	□	00000010	0x 02
						t <sub>1</sub>	□	00000000	0x 00
						t <sub>2</sub>	□	00000010	0x 02
						t <sub>3</sub>	□	00000000	0x 00
						t <sub>4</sub>	□	00000010	0x 02
						t <sub>5</sub>	□	00000000	0x 00
						t <sub>6</sub>	□	00000000	0x 00
						t <sub>7</sub>	□	00000010	0x 02
						t <sub>8</sub>	□	00000000	0x 00
					360°	t <sub>9</sub>	□	00000010	0x 02

Figure 3.11 : Timing diagram of switching pulses showing the technique of their generation at the corresponding data pins, one for each bit in a byte to be at 0x378.

init =  $t_m/3$  for K= 4

init =  $2t_m/3$  for K= 3

init =  $t_m/2$  for K=2

init =  $5t_m/3$  for K=1

init =  $t_m/6$  for K=0

The flow chart for the generation of the composite byte is shown in figure 3.11 and this is used in the subfunction in the main program to generate three phase switching pulses.

### 3.2.2 On Line real time pulse generation.

Initially time span 'del' of each segment is defined by executing a dummy FORLOOP having 'YY' number of iterations. For on-line control, the program algorithm should inflict the parallel port of the computer to generate switching pulses without any interruption for changing modulation parameters. Provision is made to stop the generation only when 'q' is pressed on the key board. The flow chart of the main program for ON-LINE control is shown in figure 3.12 (a) and 3.12(b). The program algorithm starts with a defined initial set of parameters and its corresponding composite byte array `deci[num_seg]` executing subfunction `Combyte ( )`. The program checks whether any key is pressed using subfunction `Kbhit ( )`. If no Key is pressed the

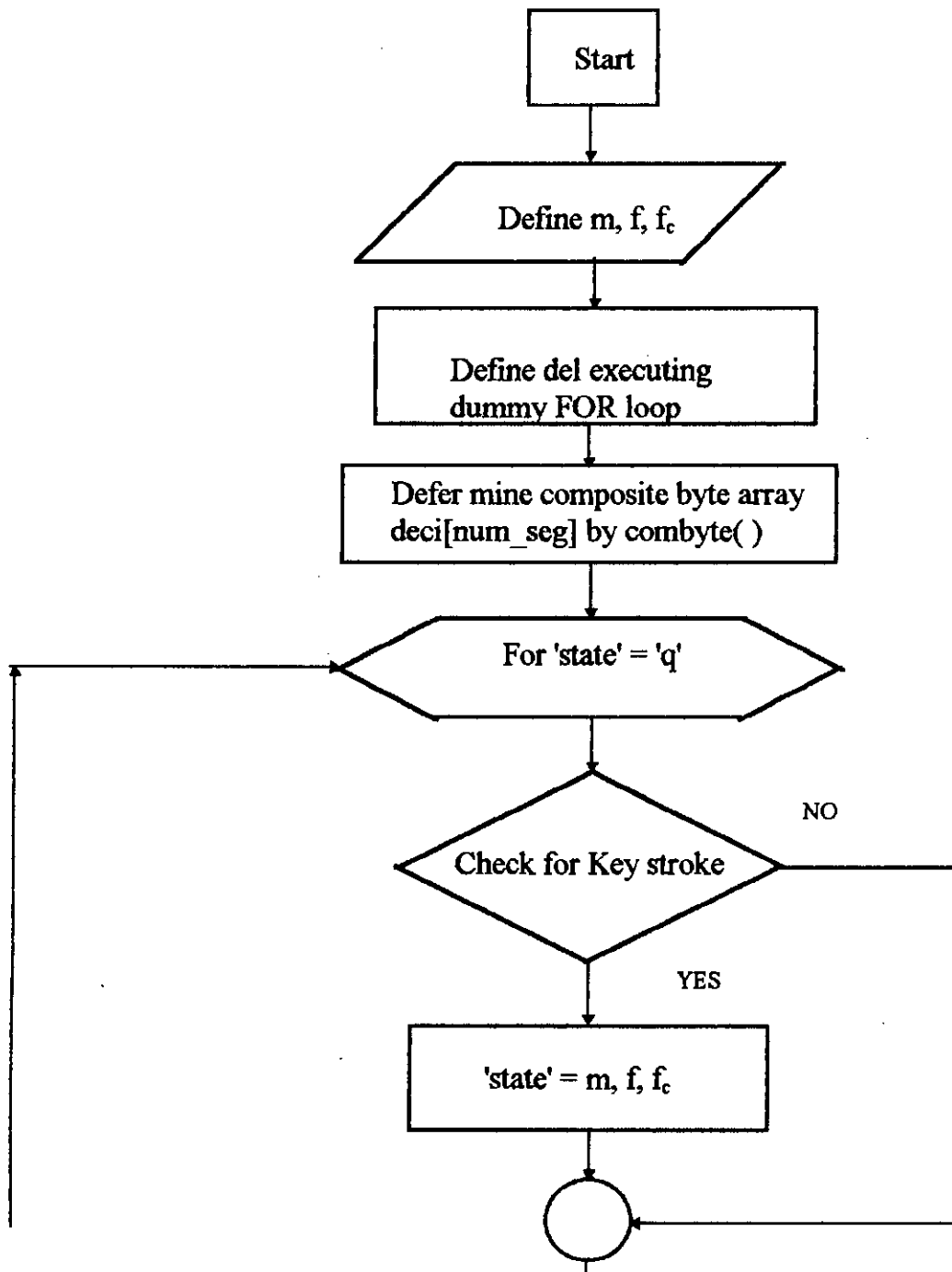


Figure 3. 12 (a) : Flow chart of the main program used for ON-Line Generation of PWM gating Pulse.

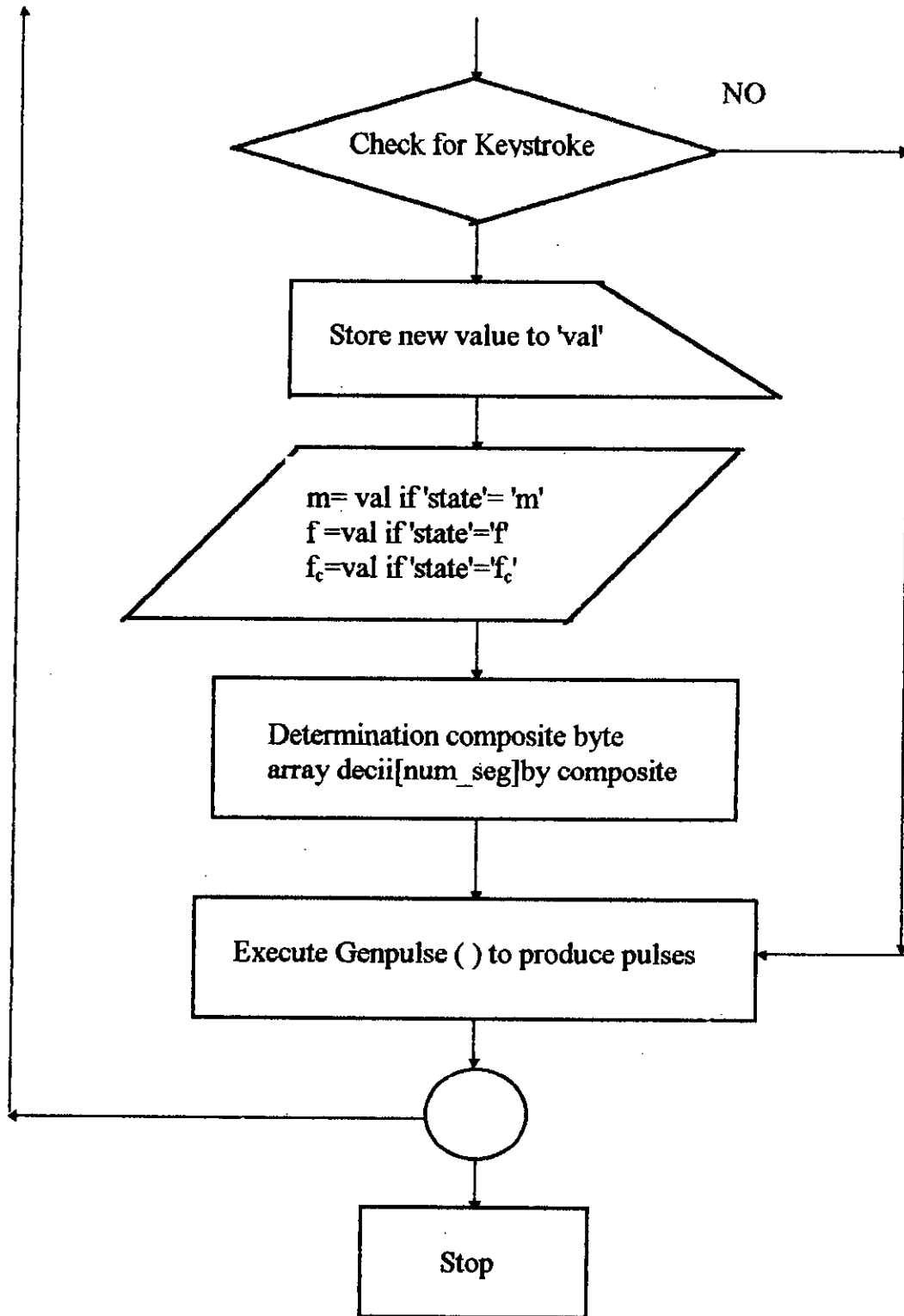


Figure 3. 12 (b) : Flow chart of the main program used for ON - LINE Generation of PWM gating Pulse.

program will execute Genpulse ( ) to produce switching pulses with initial parameters. If a key other than 'q' is pressed it will be stored as 'state' which will define a particular parameter that is to be changed. It will be 'f<sub>c</sub>', if carrier frequency has to be changed and 'm' if modulation index has to be changed. The new value is then assigned by key board input displayed on the monitor screen. This value is stored in a buffer 'val' . Only when the composite byte array deci[num\_seg] with new set of parameters is executed ( by subfunction combyte ( ) ) the program will execute the 'Genpulse( )' portion of the program to generate the new patterns of switching pulses at the parallel port of the computer.

### **3.2.3 Generation of pulses at the parallel port.**

To generate the required switching pulse pattern at the parallel port of the computer subfunction Genpulse(.) is used. Parallel port will generate pulses at its data pins as a composite byte when it is addressed as 0x378. This subfunction will sustain for each and every byte corresponding to the decimal numbers of the deci[num\_seg] for a time span of del sequentially. Once all the bytes of the array deci[num\_seg] are addressed, one cycle of the pulse patterns is completed. In this way the subfunction Genpulse(.) will be repeated until main program makes a 'quit' from the key board. The flow chart for the subfunction Genpulse(.) is given in figure 3.13.

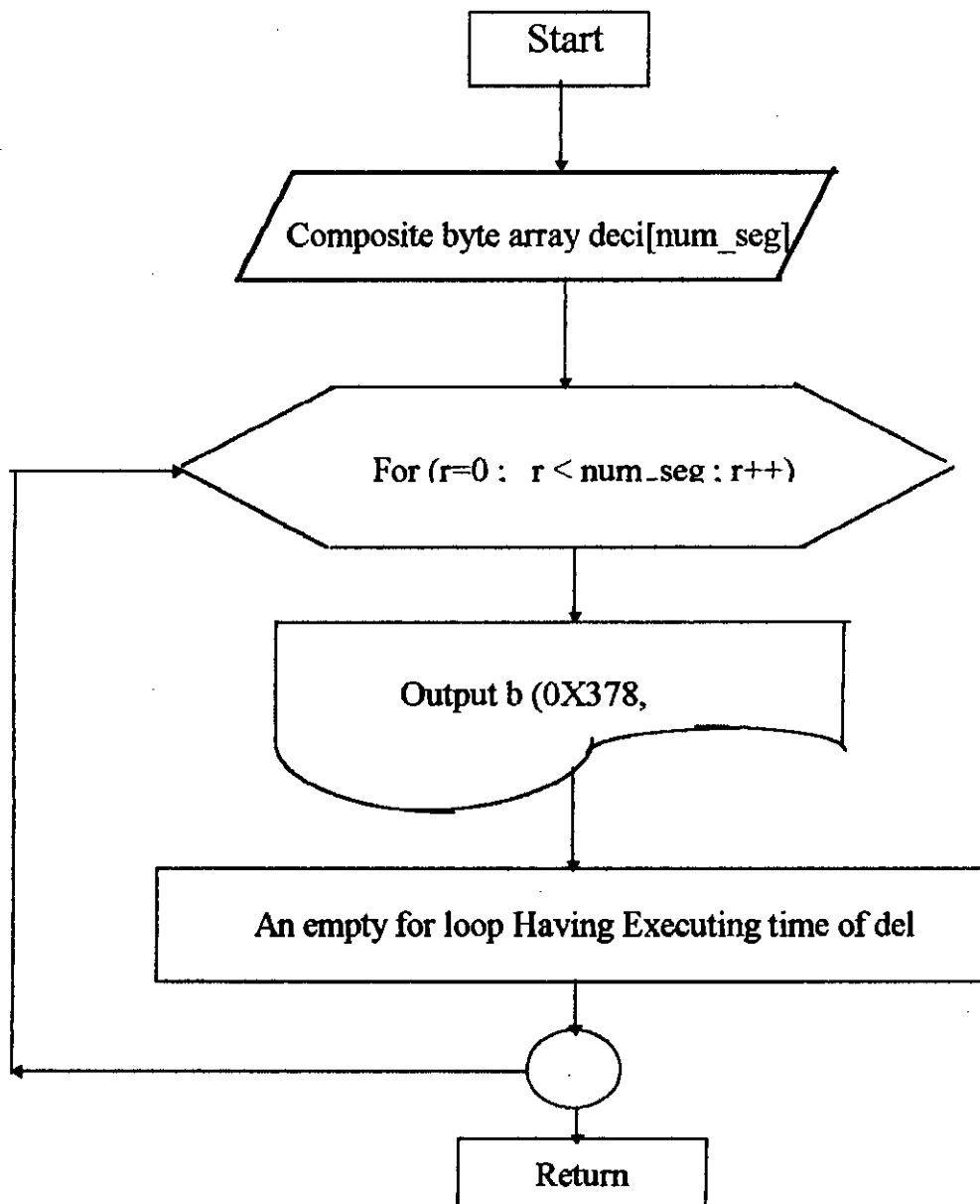


Figure 3.13 : Flow chart of the subfunction Genpulse ( ).

### 3.2.4 Synchronization of PWM wave with Line to Neutral voltage.

Proper gating of static switches of three phase voltage controllers and controlled rectifiers depends on the synchronization of gating pulses with the line to neutral voltage of the input to these converters. To synchronize the PWM waveforms generated by microcomputer with the line to neutral voltage of the input supply waveforms the interface circuit of figure 3.14 is used.

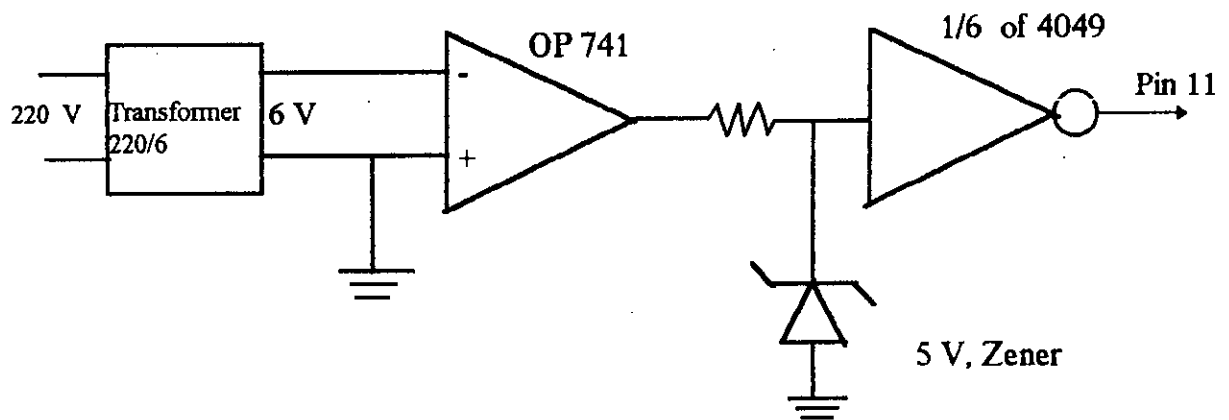


Figure 3.14 Interface Circuit for synchronized PWM pattern

A square wave synchronized with the sinusoidal reference is generated using a zero crossing detector circuit. The synchronized square wave is made TTL compatible and fed to one input pin (pin11) of the parallel port. The software program is so designed that it starts sending the PWM pattern to pins of parallel port at the positive zero

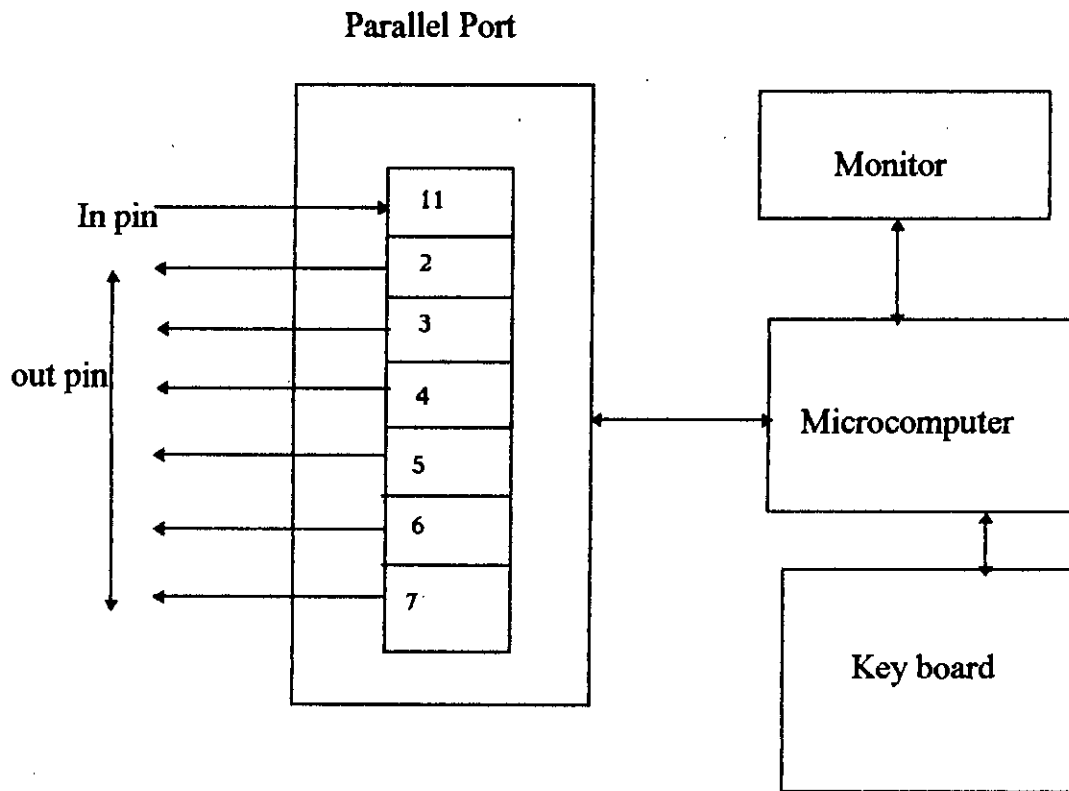


Figure 3.15 :Hardware schematic of implementation of synchronization of PWM waveforms with supply voltage.

crossing edge of the square wave (read from pin 11) . The software for PWM waveform generation is preceded by status reading of pin 11 of the parallel port. When the pin status is high it enters the PWM pattern calculation loop for one of the phases. Once the pattern for one of the phases is calculated and stored, the patterns for other two phases are generated by shifting the already calculated pattern by 120 degree and 240 degree. These patterns are stored and all three patterns and their inverted



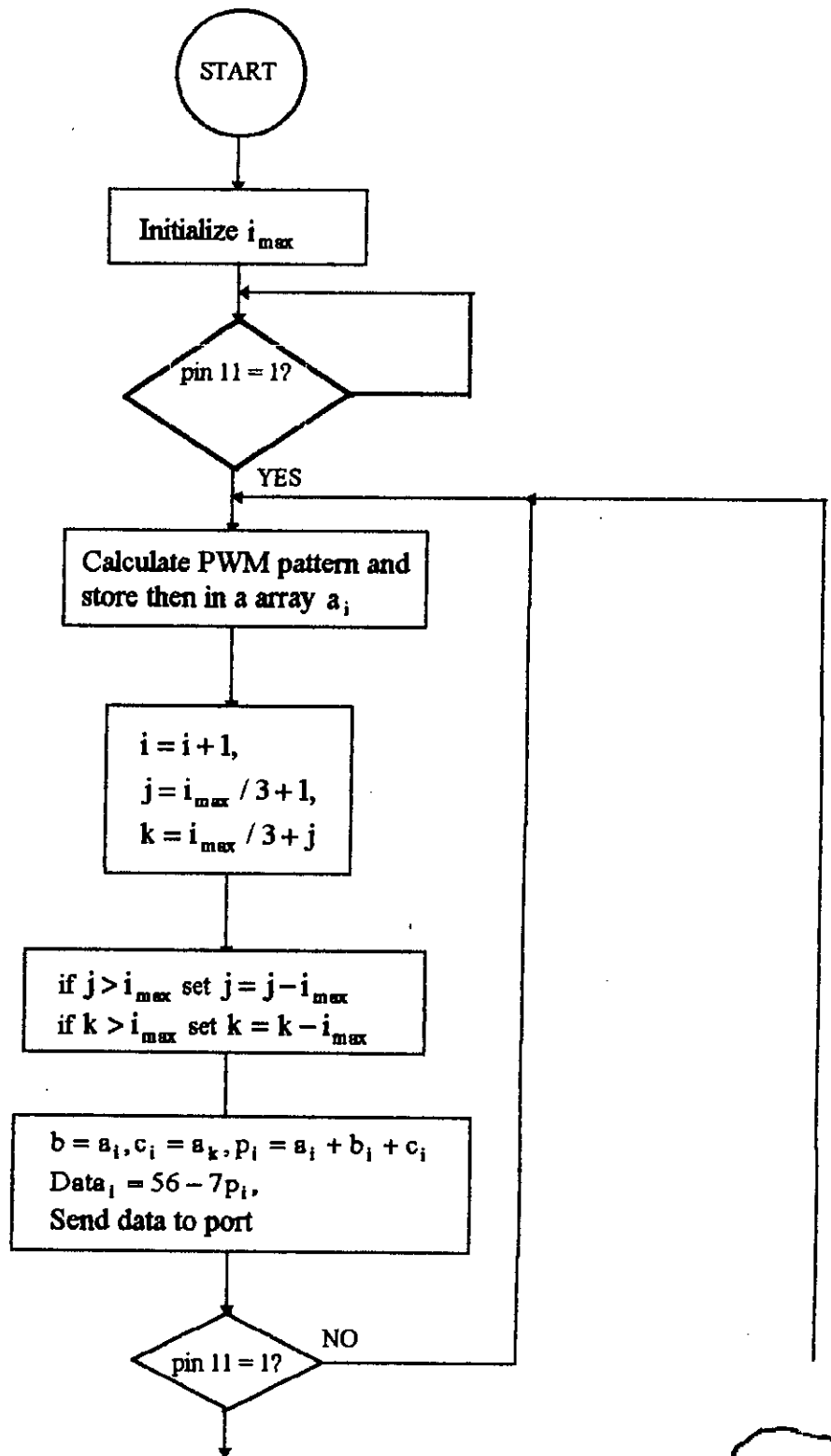


Figure 3.16 (a) : The flow chart of determination of 3 phase PWM waveform from single phase pattern synchronized with line to neutral voltage.

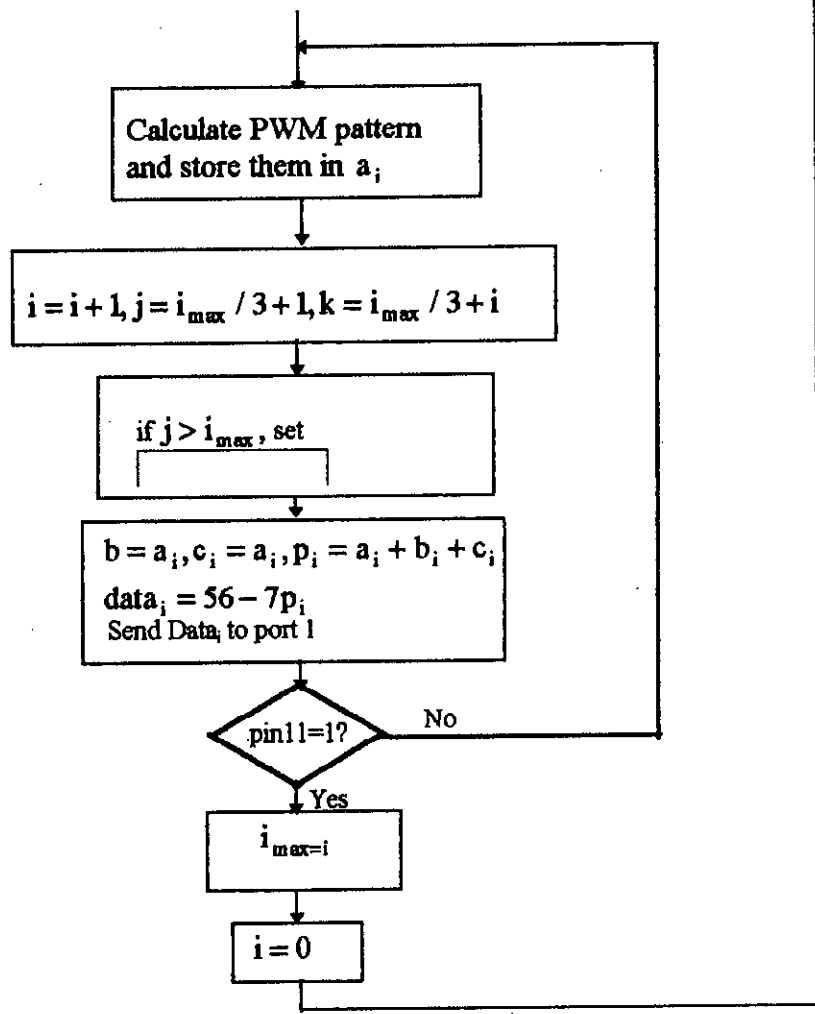


Fig. 3.16 (b) :The flow chart of determination of 3 phase PWM waveform from single phase pattern synchronized with line to neutral voltage.

patterns are made available to the 6 output pins of the parallel port. The PWM data are stopped at the positive edge of the square wave and a fresh cycle is repeated.

### **3.2.5 Computer generated PWM pulses.**

The waveshapes of six SPWM pulses available at the parallel port of an intel 80386 DX-2 microcomputer have been observed. The signals of figures 3.17 are of pin 2 and 7 having phase shift of 60 degree. The number of pulses thus generated have reasonable accuracy . Figures 3.20 to 3.23 are for different carrier frequency and figures 3.24 to 3.27 are for different modulation index of the single phase voltage controller. As expected changing modulation index to higher values produces pulse of wider width which will result voltage control in a voltage controller. Whereas, change in carrier frequency produces more pulses per modulating cycle indicating the shift of dominant harmonics to move at higher frequency of the spectra. The typical output waveform of the voltage controller switched by computer generated pulses are shown in figures 3.20 to 3.27 for single phase operation of the voltage controller. To interface the computer generated pulses with the voltage controllers power circuit, the following interface circuit is used.

### **3.3 Interface of microcomputer with three phase voltage controller & synchronization.**

The three phase voltage controller circuit designed for experimental test is shown in figure 3.18. The switching devices used in the voltage controller are power MOSFETs

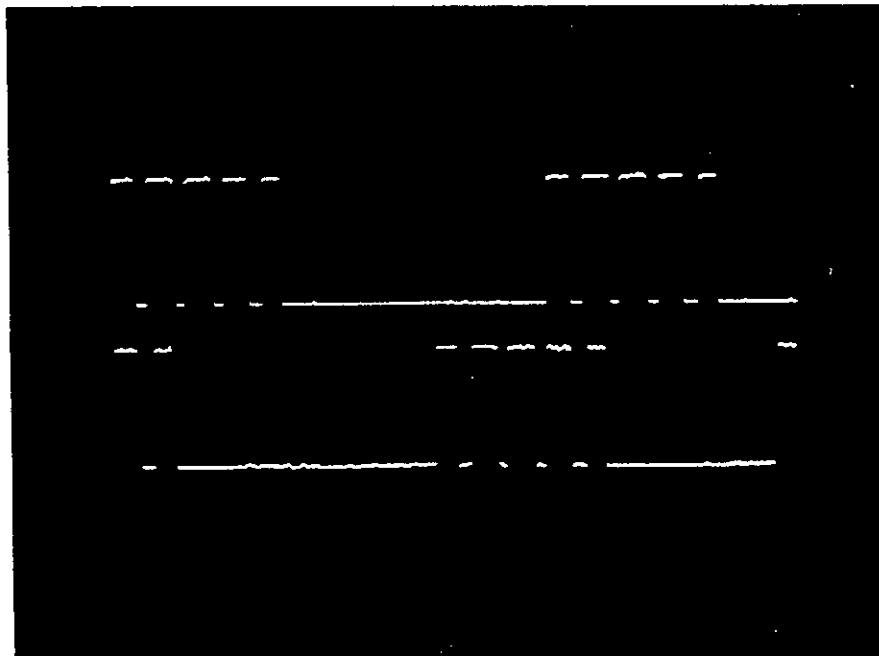


Figure 3.17 : Output pulses available at parallel port at 60 degree apart of pin nos. 2 & 7.



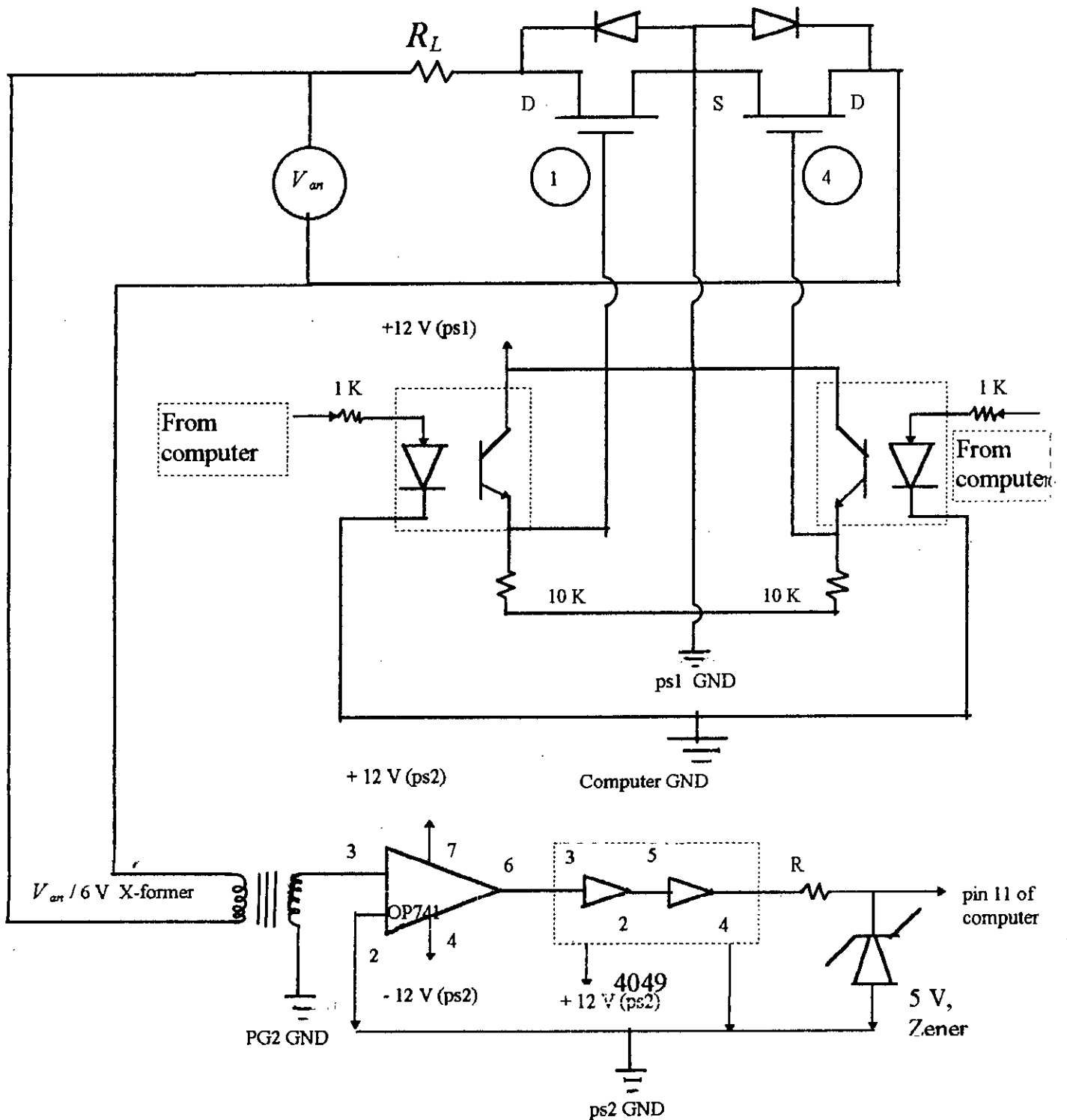


Figure 3.19 : Synchronizing with phase A

N.B : ps2 GND & computer GND is same, But ps1 GND is separate.

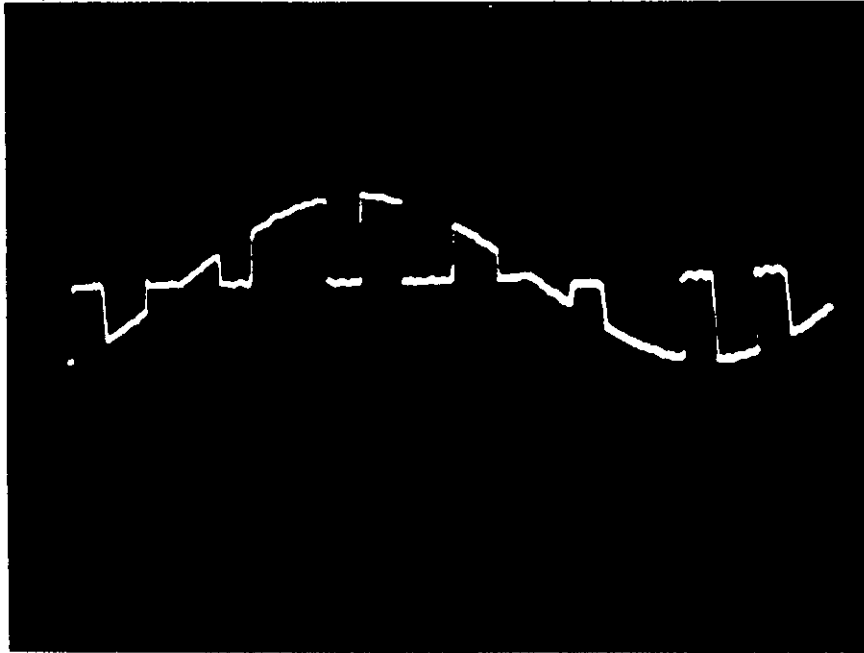


Figure 3.20: Output waveform of voltage controller at  $E_m = 0.1$ ,  $f_c = 450$  Hz,  
 $f_m = 50.0$  Hz.

Handwritten scribbles and marks in the bottom right corner of the page.

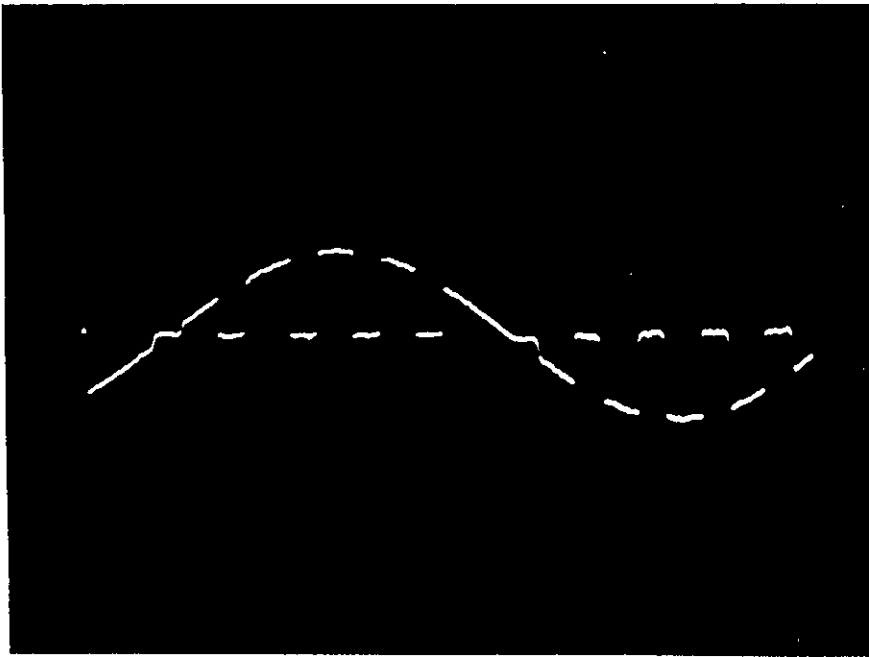


Figure 3.21: Output waveform of voltage controller at  $E_m = 0.1$ ,  $f_c = 550$  Hz,  
 $f_m = 50.0$  Hz.



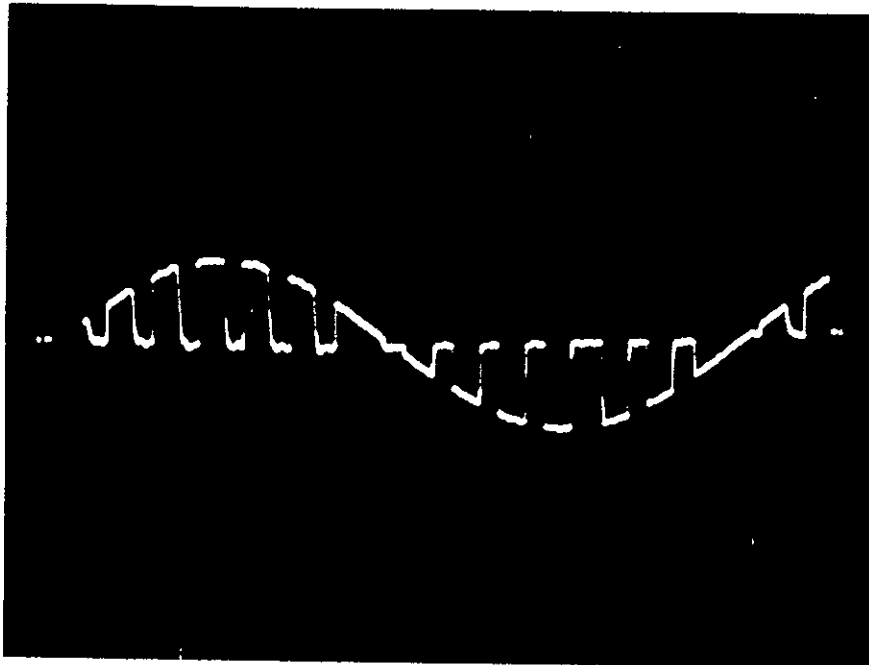


Figure 3.22: Output waveform of voltage controller at  $E_m = 0.1$ ,  $f_c = 750$  Hz,  
 $f_m = 50.0$  Hz.

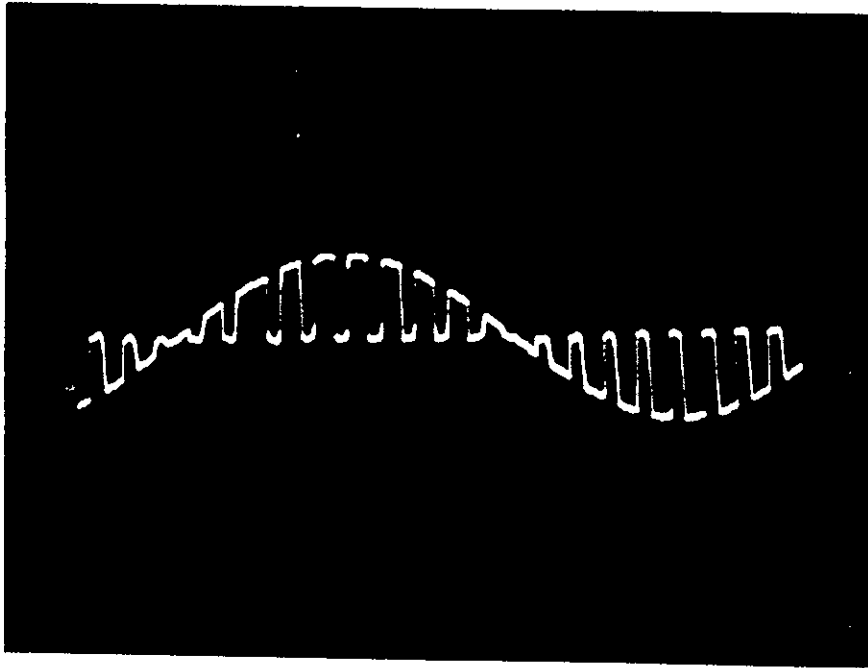


Figure 3.23: Output waveform of voltage controller at  $E_m = 0.1$ ,  $f_c = 1000$  Hz,  
 $f_m = 50.0$  Hz.

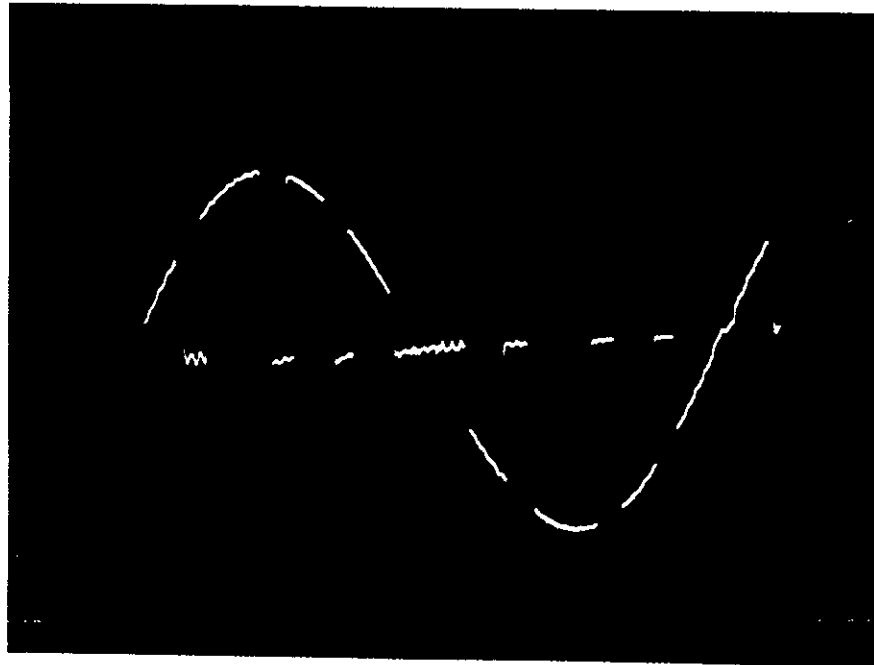


Figure 3.24: Output waveform of voltage controller at  $\alpha=0.25$ ,  $E_{\alpha} = 0.25$ ,  $f_s = 450$  Hz,  
 $f_m = 50.0$  Hz.

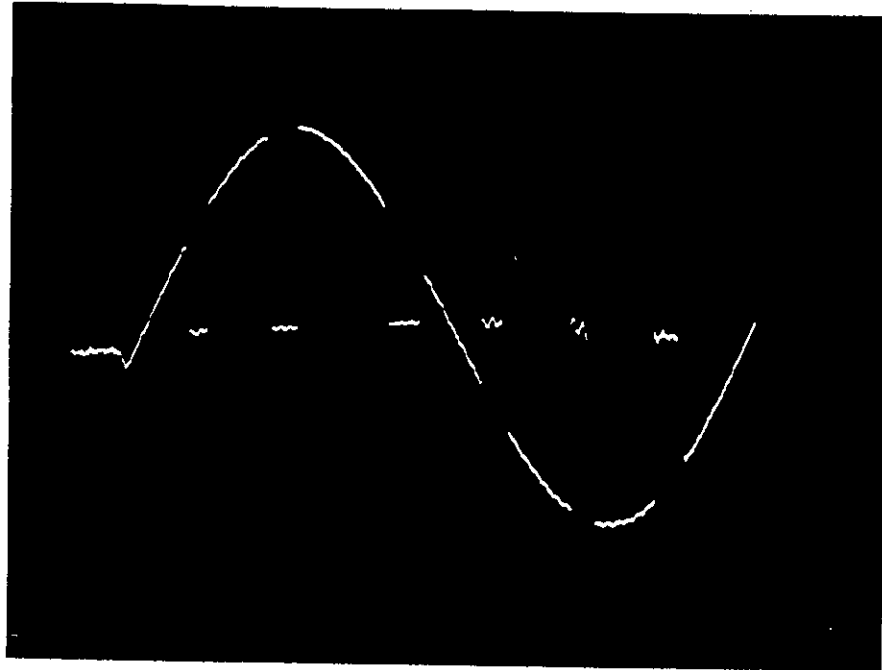


Figure 3.25: Output waveform of voltage controller at  $a=0.50$ ,  $E_{in} = 0.50$ ,  $f_c = 450$  Hz,  
 $f_m = 50.0$  Hz.

C.

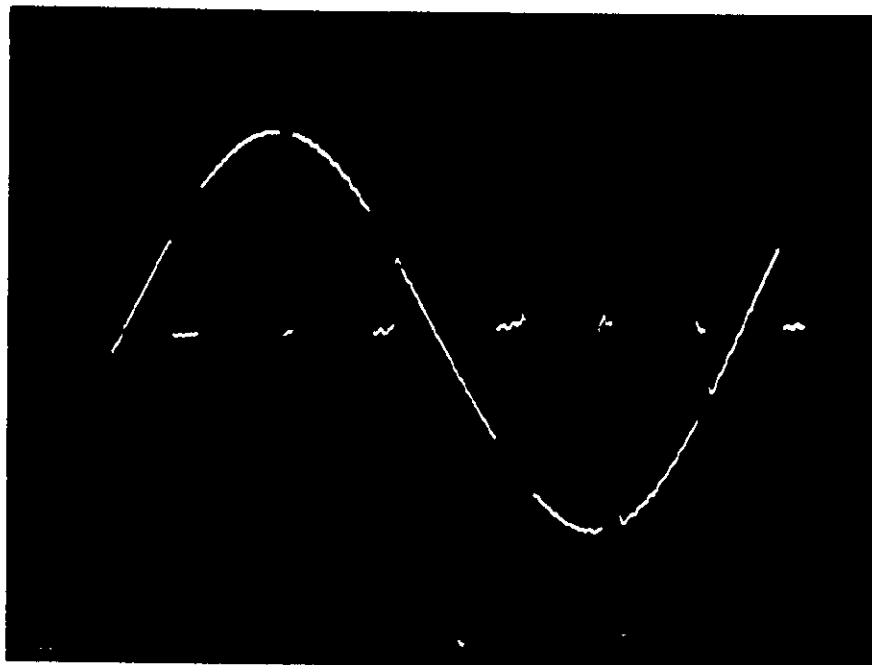


Figure 3.26: Output waveform of voltage controller at  $a=0.75$ ,  $E_{ra} = 0.75$ ,  $f_c = 450$  Hz,  $f_m = 50.0$  Hz.

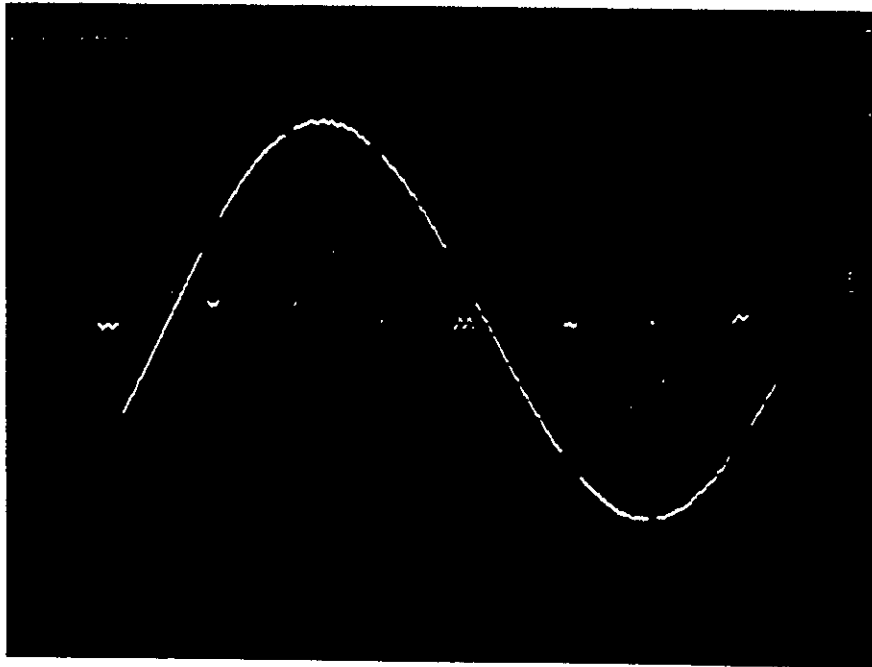


Figure 3.27: Output waveform of voltage controller at  $\alpha=0.90$ ,  $E_m = 0.90$ ,  $f_s = 450$  Hz,  $f_m = 50.0$  Hz.

with internally fabricated diodes across drain source terminals. As a result two MOSFETs connected in series with load serve as a bi-directional switch. Gates of these MOSFETs are to driven by PWM signals  $g_1$  to  $g_6$  produced by microcomputer. For the interface of microcomputer signals at the pin 2 - 7 of parallel port with gates of respective MOSFET of voltage controller, opto couplers with separate power source for the output transistors of opto coupler are used. The light emitting diodes of opto couplers are directly driven by computer generated signals through an input resistor of 1 Kilo Ohm for each signal.

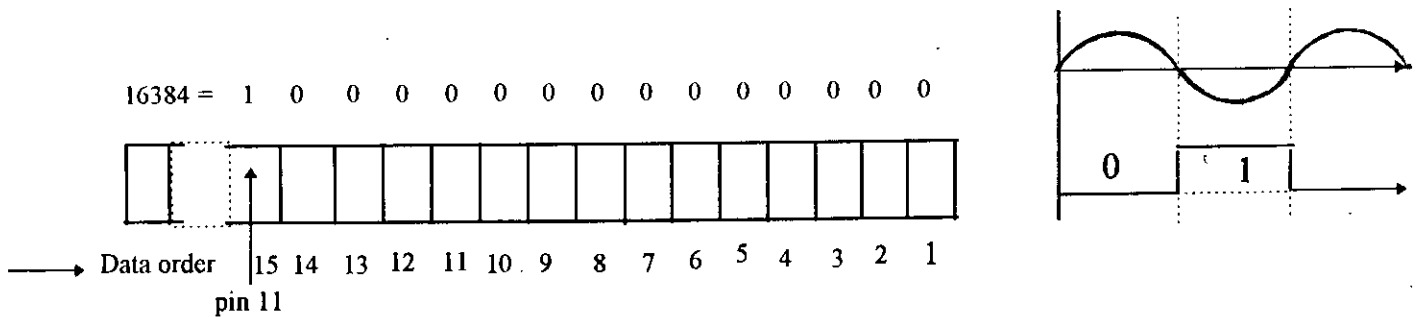
The output of the opto coupler is completely isolated from computer (as they are supplied by separate source). The outputs of opto couplers are connected to reference gate of MOSFETs of voltage controller circuit. Figure 3.18 shows the interface circuit with microcomputer with gates of voltage controller MOSFETs for phase Van. Figure 3.19. Also shows the synchronization pulse generation circuit necessary for synchronizing the PWM gate pulse with the supply voltages for proper operation of voltage controller. The synchronizing circuit is necessary in only one phase because synchronization of gate pulse of one phase with supply voltage will also ensure the synchronization of gate pulses for other two phases.

The synchronization pulse generation basically consist of a transformer connected to phase 'A' supply to provide a low voltage sine wave in phase with Van. The low voltage sine wave at the secondary of the 220/6 V transformers is the input to zero

crossing detector which produces a square wave in synchronism with Van. This square wave is passed through inverters and brought to 5 V level by zener diode circuit and then fed to pin 11 of the parallel port of the computer to edge trigger PWM gating signals by software routine as described in the following paragraph.

**Synchronization of gate pulse with Van supply :**

State of pin 11 controls the flow of data from parallel port. State '1' stops transmission and state '0' allows data transmission. In the program pin 11 is made high (state '1') causing stoppage of data transmission. This is done by assigning '1' the value of inport being shifted one bit right and then masked by  $2^{14} / 2^{14}$  to get the state '1' at the pin 11 of the parallel port. After bit wise masking, only pin 11 will be state '1' and rest will be '0'.



A "FORLOOP" logic is applied in the main program to read pin status of the pins. In the above configuration, it is evident that '0' state of square wave means '0' state of pin 11 and SPWM pulse will be transmitted and during '1' state no data will be transmitted. The PWM pulses produced by the main program stays on the pins as pin '11' remain in state '1'. But as the pin '11' becomes zero at every zero crossing of supply voltage, the pin eleven by wired 'OR' combination becomes zero which allow the PWM pulses to be transmitted starting at the begining of the positive zero crossing of sine wave.



## CHAPTER 4

### 4.0 Conclusion

Squirrel cage induction motors are the most used ac motors in industries today. They are simple in construction, cheap, reliable, and may be used in hostile environment requiring less maintenance and care. Introduction of power electronic control made possible the use of induction motors in variable speed drive applications and hence reducing the dependence of costly and difficult to maintain dc motors. Motors in most of the applications do not operate at constant loading during their entire period of operation. If load changes, the motors under rated voltage operation do not run at their maximum efficiency condition. Maximum efficiency of an induction motor occur near their rated load condition when operated by the rated voltage. At any other load, the maximum efficiency attainable also change. To maintain the operation of the motor at that maximum attainable efficiency usually variable frequency  $V/f$  control is employed using inverters or cycloconverters. However, inverter controls are very expensive and sophisticated normally used in many low cost applications. Since it is usually practiced that loading of motors are not to be exceeded beyond their rated load, a simple control strategy for lower than rated load operation of induction motor would have been very much appreciable.

In this thesis, a control strategy is proposed for variable load induction motor operation in which changing the voltage of the motor to obtain a certain  $V/I$  value interms of

motor parameters will keep the operation to its maximum attainable efficiency. The strategy was developed using simple argument that the slip of the motor can be found for its maximum attainable efficiency in terms of motor parameters. Substituting this efficiency value in motors impedance relationship give us a  $V/I$  ratio in terms of motor parameters. Which indicate that changing the voltage of a motor by appropriate voltage control will allow us to reach the desired  $V/I$  value which in the long run will ensure motor's maximum attainable efficiency at changed load. This simple control strategy can easily be implemented either by auto transformers or by static voltage controllers.

In this thesis the proposed control strategy is first verified by running a 3 phase induction motor at variable load supplied from a variable voltage from an auto transformer. It has been demonstrated that the arguments followed in the above mentioned control strategy holds good with very insignificant/acceptable deviation.

Rest of the thesis work is devoted in the development of a microcomputer based on line operation of a three phase MOSFET PWM voltage controller. The results of previous research works on switching point calculation and PWM pulse generation was extended to provide synchronized PWM gate pulses for the operation of a 3 phase PWM voltage controller. Successful microcomputer control of the static voltage controller has been shown in the thesis in the form of waveshapes of gate pulses and voltage controllers output waveform. The voltage control of the PWM voltage controller was achieved on line by the variation of modulation index of modulation

process. In implementing the control, simple techniques have been used allowing us to use the microcomputer without the need of extra AD/DA cards. The method used the parallel port of the computer as input/output port and rest of the job has been software controlled in C++ language.

In short, the main objectives achieved in this thesis are twofold. One is the development of suitable V/I control strategy for the maximum attainable efficiency operation of an induction motor under variable load condition. The second one is the development of a microcomputer controlled PWM voltage controller to implement the proposed control strategy.

#### **4.1 Recommendation of the future work.**

It is evident from the previous discussion that major goals towards the achievement of this research work has been fulfilled. Remaining part of the objective of the research is to integrate the proposed control scheme and the developed microcomputer controlled PWM voltage controller in a single package to run an induction motor in the field with variable load. The field tests will validate the importance and practicality of such control strategy. The integration part will require the development of proper voltage, current and load monitoring of the total scheme and their continuous monitoring by the computer. Major software and hardware development is necessary for this purpose which will eventually allow one to make the control automatic without human interaction. Such a control will be highly desirable in most of the unattended motors in operation.

## REFERENCES

- [1] I. J. Nagrath, D. P. Kothari, " Electric Machines", Tata McGrawHill publishing Company Limited, New Delhi, 1994.
- [2] L.W. Match : 'Electromagnetic and Electromechanical Machine' IEP Dun-Donnelley Harper & Row, 1977.
- [3] Institute of Electrical and Electronic Engineers : "Standard Test Procedure for Polyphase Induction Motors and Generators" No. 112-1984, IEEE, New York, 1984.
- [4] S. Ula and V. Bershinsky : 'Motor sizing for efficiency improvement', Industrial Electro-Technology conference, Texas A & M University - EDAC Centre, Houston, Texas, USA, March 1995.
- [5] S. F. Shams, A. H. Chowdhury, S. M. L. Kabir, M. A. Chowdhury " A New Method for Determining Efficiency Characteristics of Induction Motor ", Proceedings of IASTED on High Technology Power Industry, Banff, Alberta, Canada, pp. 188-121, June 1996,
- [6] S.B.Dewan, "Power Semiconductor Devices & Circuits"
- [7] M. H. Rasid, " Power Electronics : Circuits, Drives and Applications", Prentice, Hall of India, 1994.
- [8] B. K. Bose, " Adjustable speed ac drives", Proceedings of IEEE, Vol. 70, No. 2, February, 1982.
- [9] K. Thorborg and A. Nystorm, " Staircase PWM : An uncomplicated and efficient modulation technique for ac motor drives", IEEE transactions on power Electronics, Vol. PE 3, No. 4, 1988, pp. 391-398.
- [10] J.C. Salmon , S. Olsen and N. Durdle, " A three phase PWM strategy using a stepped reference waveform", IEEE transactions on Industry Applications, Vol. IA 27, No. 5, 1991, pp. 914-920.
- [11] K. Taniguchi and H. Trie, " Trapezoidal Modulating Signal for three phase PWM Inverter" , IEEE transactions on Industrial Electronics, Vol. IE 3, No. 2, 1986, pp. 193-200.

## REFERENCES

- [12] M. A. Rahman, J. E. Quaicoe and M. A. Choudhury, " Performance Analysis of Delta Modulated PWM Inverters", IEEE transactions on Ind. Applications, March/April 1981, pp. 199-204.
- [13] M. A. Rahman, A. R. D. Esmail and M. A. Chowdhury, " Analysis of Delta PWM static AC-DC Converters" IEEE transaction of power Electronics, Vol. No. 4, July 1995, pp. 494-503.
- [14] T. Kataoka, K. Mizumachi and S. Miyan, " A pulse width controlled AC-DC converter to improve power factor and waveforms of line current" IEEE transaction on Industrial Applications, Vol. IA-15, Nov./Dec., 1979, pp. 670-675.
- [15] P.C. Tang, S-S. Lu, and Y-C. Wu, " Microprocessor Based Converter Firing Circuit for Three Phase Full Wave Thyristor Dual Converter", IEEE Trans. Ind. Elec. Vol.IE-29, no.1, Feb. 1982, pp. 67-73.
- [16] W.L. Fredrich and K.S. Swenson, " Microprocessor Based Converter Firing Pulse Generator", conference record- IEEE-Industry Applications society annual meeting, 1982, pp. 439-445.
- [17] Ali Mirbod and Ahmed El-Amawy, "A Novel Microprocessor Based controller for a phase controlled rectifier connected to a weak AC System", conference record-IEEE - Industry Applications society annual meeting, 1985, pp. 1250-1258.
- [18] Eiichi Ohno, Mikio Ohta, Masao Yano, H. Naito, and Y. Yamamoto, " Microprocessor Applications for Thyristor Choppers and High Voltage Thyristor Switches", U. S. -JAPAN seminar conference record, 1982, 269-278.
- [19] P.M.S. Nambison, R. Mulchandani, and C.M. Bhatia, " Microprocessor Implementation of a four phase Thyristor Chopper Circuit", conference record IEEE Industry Applications Society Annual meeting , 1980, pp. 637-642.
- [20] G. Oliver, V.R. Stefanovic, and G.E. April, " Microprocessor Controller for a Thyristor Converter with an Improved power factor", IEEE Trans. on Industrial Electronics and Control Instrumentation, August 1981, pp. 188-194.

## REFERENCES

- [21] B.K. Bose, P.M. Szezesny, and R. L. Steigerwald, " Microprocessor Control of a Residential Photovoltaic Power Conditioning System", conference record-IEEE-Industry Applications society annual meeting, September/October 1984.
- [22] J.B. Casteel and R.G. Hoft, " Optimum PWM Waveforms of Microprocessor Controlled Inverter", 9th IEEE Power Electronics Specialists conference, 1978.
- [23] K.S. Rajashekera and J. Vithayathil, "Microprocessor Based Sinusoidal PWM Inverter by DMA Transfer", IEEE Trans. on Industrial Electronics, February 1982, pp. 46-51.
- [24] B.K. Bose and H.A. Sutherland, " A High Performance Pulse-Width Modulation For an Inverter-Fed Drive System Using a Microcomputer", IEEE Trans. Industrial Appl., vol. IA-19, No. 2, March-April, 1983, pp. 235-243.
- [25] Md. Basir Uddin, "Stability Analysis of PWM Inverter fed synchronous motor" Ph. D. Thesis, Department of Electrical & Electronic Engineering, BUET, Dhaka-1000, Bangladesh, 1995.
- [26] R. G. Hoft, R.W. McLaren, R.L. Pimmel and K.P.Gokhale, "The Impact of Microelectronics and Microprocessors on Power Electronics and Variable speed Drives", Int. power Elec. and variable speed Drives conf. Rec., London, 1984, pp. 191-198.
- [27] S.B. Dewan and A. Mirbod, " Microprocessor Based Optimum Control for four- Quadrant Chopper", IEEE Trans. on Ind. Appl., vol. IA-17, Jan./Feb., 1981, pp. 34-40.
- [28] S.R. Bowes, " New Sinusoidal Pulse Width Modulated Inverters", IEE Proc. vol. 122, pt. B, No. 11; 1975, pp. 1279-1285.
- [29] S.R. Bowes and M.J. Mount, " Microprocessor Control of PWM Inverters", IEE Proc. vol. 128, pt. B, No. 11, 1981, pp. 293-305.
- [30] S.R. Bowes and S.R. Clements, " Microprocessor Based PWM Inverters", IEE Proc. vol. 129, pt. B, No. 1, January /1982, pp. 1-17.
- [31] Hary Fairhead, The 386/486 PC, A power user's guide, 1994.

## REFERENCES

- [32] Intel IAPX 286, Hardware Reference Manual.
- [33] M.N. Anawar, "Implementation of Microcomputer Controlled Delta Modulated Inverter", M.Sc. Thesis, Department of EEE, BUET, Dhaka-1000, Bangladesh. December, 1995.

**APPENDIX -A : MOTOR TEST DATA**  
**Motor ratings : 175 W, 380 V, 0.53 A, 1315 RPM**

**DATA -1 : APPLIED LOAD : 0.16 N-M**

APPLIED VOLTAGE V (L-L)	LINE CURRENT I(PHASE)	INPUT POWER PER PHASE	RPM	SLIP	OUTPUT POWER THREE PHASE	MOTOR EFFICIENCY	V/I RATIO
405	0.340	30.65	1475	1.67	51.71	66.24	687.76
380	0.300	28.25	1460	2.67	51.46	60.72	731.33
360	0.280	26.40	1455	3.00	51.38	64.87	742.33
340	0.275	25.00	1445	3.67	51.21	68.28	713.84
320	0.260	23.85	1430	4.67	50.98	71.22	710.61
300	0.240	22.85	1420	5.33	50.79	74.10	721.71
280	0.230	22.10	1390	7.33	50.29	75.85	702.88
260	0.228	21.65	1340	10.67	49.45	76.14	658.40
240	0.240	21.45	1280	14.67	48.45	75.29	577.37
220	0.245	21.45	1250	16.67	47.94	74.51	516.45
200	0.245	21.80	1220	18.67	47.44	72.54	471.32
180	0.250	22.50	1200	20.00	47.11	69.79	415.70

**DATA -2 : APPLIED LOAD : 0.25 N-M**

APPLIED VOLTAGE V (L-L)	LINE CURRENT I(PHASE)	INPUT POWER PER PHASE	RPM	SLIP	OUTPUT POWER THREE PHASE	MOTOR EFFICIENCY	V/I RATIO
405	0.320	32.00	1450	3.33	64.96	67.87	730.73
380	0.300	31.25	1440	4.00	64.70	69.01	731.33
360	0.280	30.50	1430	4.67	64.44	70.42	742.33
340	0.270	30.00	1415	5.67	64.04	71.16	727.05
320	0.260	29.65	1400	6.67	63.65	71.56	710.61
300	0.260	29.30	1390	7.33	63.39	72.12	666.19
280	0.300	29.00	1360	9.33	62.60	71.96	538.88
260	0.305	29.00	1340	10.67	62.08	71.36	492.18
240	0.305	29.00	1310	12.67	61.30	70.45	454.32
220	0.310	29.00	1280	14.67	60.51	69.55	409.74



**APPENDIX -A : MOTOR TEST DATA**  
**Motor ratings : 175 W, 380 V, 0.53 A, 1315 RPM**

DATA -3 : APPLIED LOAD : 0.40 N-M

APPLIED VOLTAGE V (L-L)	LINE CURRENT (PHASE)	INPUT POWER PER PHASE	RPM	SLIP	OUTPUT POWER THREE PHASE	MOTOR EFFICIENCY	V/I RATIO
400	0.330	42.90	1410	6.00	86.06	66.87	699.84
380	0.320	41.70	1400	6.67	85.64	68.46	685.62
360	0.300	40.80	1400	6.67	85.64	69.97	692.84
340	0.300	40.30	1390	7.33	85.22	70.49	654.35
320	0.290	39.50	1360	9.33	83.97	70.86	637.09
300	0.290	39.50	1350	10.00	83.55	70.51	597.28
280	0.290	39.50	1320	12.00	82.29	69.44	557.46
260	0.300	39.80	1290	14.00	81.04	67.87	500.38
240	0.305	40.25	1240	17.33	78.94	65.38	454.32
220	0.325	40.00	1150	23.33	75.17	62.64	390.83

DATA -4 : APPLIED LOAD : 0.50 N-M

APPLIED VOLTAGE V (L-L)	LINE CURRENT (PHASE)	INPUT POWER PER PHASE	RPM	SLIP	OUTPUT POWER THREE PHASE	MOTOR EFFICIENCY	V/I RATIO
400	0.345	51.25	1400	6.67	100.30	65.24	669.41
380	0.330	50.25	1395	7.00	100.04	66.38	664.85
360	0.320	49.00	1380	8.00	99.28	67.52	649.54
340	0.310	48.10	1360	9.33	98.21	68.06	633.24
320	0.315	48.00	1345	10.33	97.42	67.66	586.53
300	0.315	48.00	1310	12.67	95.59	66.38	549.87
280	0.320	48.00	1280	14.67	94.02	65.29	505.20
260	0.340	48.00	1240	17.33	91.93	63.84	441.52

**APPENDIX -A : MOTOR TEST DATA**  
**Motor ratings : 175 W, 380 V, 0.53 A, 1315 RPM**

**DATA -5 : APPLIED LOAD : 0.60 N-M**

APPLIED VOLTAGE V (L-L)	LINE CURRENT I(PHASE)	INPUT POWER PER PHASE	RPM	SLIP	OUTPUT POWER THREE PHASE	MOTOR EFFICIENCY	VI RATIO
400	0.355	63.00	1380	8.00	113.71	71.51	650.55
380	0.350	62.00	1360	9.33	112.45	72.08	626.86
360	0.340	51.60	1350	10.00	111.82	72.38	611.33
340	0.340	61.00	1330	11.33	110.57	72.27	577.37
320	0.330	51.00	1310	12.67	109.31	71.44	559.87
300	0.340	50.00	1250	16.67	105.54	70.36	509.44
280	0.355	51.00	1230	18.00	104.28	68.16	455.39
260	0.370	51.00	1160	22.67	99.89	65.28	405.72
240	0.410	52.00	1080	28.00	94.86	60.81	337.97

**DATA -6 : APPLIED LOAD : 0.75 N-M**

APPLIED VOLTAGE V (L-L)	LINE CURRENT I(PHASE)	INPUT POWER PER PHASE	RPM	SLIP	OUTPUT POWER THREE PHASE	MOTOR EFFICIENCY	VI RATIO
400	0.380	62.00	1360	9.33	133.81	71.94	607.75
380	0.370	61.00	1350	10.00	133.03	72.69	692.97
360	0.365	60.50	1330	11.33	131.46	72.43	569.46
340	0.370	61.00	1300	13.33	129.10	70.55	530.55
320	0.390	61.50	1260	16.00	125.96	68.27	473.74
300	0.400	63.20	1230	18.00	123.60	65.19	433.03
280	0.430	63.20	1160	22.67	118.11	62.29	375.96

**APPENDIX -A : MOTOR TEST DATA**  
**Motor ratings : 175 W, 380 V, 0.53 A, 1315 RPM**

**DATA -7 : APPLIED LOAD : 0.90 N-M**

APPLIED VOLTAGE V (L-L)	LINE CURRENT I(PHASE)	INPUT POWER PER PHASE	RPM	SLIP	OUTPUT POWER THREE PHASE	MOTOR EFFICIENCY	V/I RATIO
400	0.420	72.00	1340	10.67	153.28	70.97	549.87
380	0.410	71.00	1310	12.67	150.46	70.64	535.12
360	0.410	71.00	1290	14.00	148.58	69.76	506.96
340	0.420	71.00	1250	16.87	144.81	67.99	467.39
320	0.440	71.10	1205	19.67	140.57	65.90	419.90
300	0.470	72.00	1140	24.00	134.44	62.24	368.53
280	0.510	73.55	1060	29.33	126.90	57.51	316.99

**DATA -8 : APPLIED LOAD : 1.0 N-M**

APPLIED VOLTAGE V (L-L)	LINE CURRENT I(PHASE)	INPUT POWER PER PHASE	RPM	SLIP	OUTPUT POWER THREE PHASE	MOTOR EFFICIENCY	V/I RATIO
400	0.440	80.00	1310	12.87	184.18	68.41	524.88
380	0.440	79.80	1285	13.67	162.61	67.92	498.64
360	0.450	79.80	1260	16.00	158.95	66.39	461.89
340	0.460	79.80	1210	19.33	153.71	64.21	426.75
320	0.490	81.00	1160	22.67	148.48	61.10	377.06

## Appendix-B

```
/**
// Program for on line control of voltage controller by SPWM
**/

#include <stdio.h>
#include <ctype.h>
#include <stdlib.h>
#include <iostream.h>
#include <dos.h>
#include <conio.h>
#include <math.h>
#include <fstream.h>
#include <tc\classlib\include\timer.h>
#include <tc\classlib\source\timer.cpp>

// This part identifies all the variable used in this program

double p, x ;
int n, N, i, ii, i1, i2, i3, i5, N1, j, k, r, l ;
int deci[3000], a, b, num_seg, bb, bbb;
float fc, Em, Ec, wm, fm, am, sp, tm, tt, del;
float t[50], theta[50], the[50], dev[50];
double Ftime=0.0;

int flag = 0;
char state = ' ', ch;
char val[100], z;
Timer Ftimer;
```

## Appendix-B

// This function calculates the timing instants and generates deci[num\_seg]

void SPGDA (void)

```
{
    puts ("running ...");
    N1=0;
    Ec=1.0;
    wm=2.0*M_PI*fm;
    tm=1.0/fm;
    num_seg=tm/del;

    printf ("\segment=%d\n",num_seg);
    printf ("\del=%f\n",del);
    N=fc/fm;
    am=Em/Ec;
    for(i=1 ;; i++)
    {
        theta[i]=((2.0*i-1.0)*M_PI)/N;
        dev[i]=(M_PI/N)*(1+am*sin(theta[i]))/(2.0*M_PI*fm);
        the[i]=theta[i]/(2.0*M_PI*fm);
        i3=2*i;
        i2=2*i-1;
        for(i1=i2; i1<=i3; i1++)
        {
            x=-1.0;
            p=pow(x,i1);
            t[i1]=(the[i]+p*dev[i]/2.0);
            if(t[i1]>=M_PI/wm)break;
        }
        N1=i1;
        if(t[i1]>=M_PI/wm)break;
    }
}
```

## Appendix-B

```
//This portion generates deci[num_seg] array
for(r=0; r<num_seg;r++) deci[r]=0;
for(k=0; k<6; k++)
{
    if(k==0)    sp =0.0;
    else if(k= =1) sp =tm/6.0;
    else if(k= =2) sp =tm/3.0;
    else if(k= =3) sp =tm/2.0;
    else if(k= =4) sp =2.0*tm/3.0;
    else if(k= =5) sp =5.0*tm/6.0;

    for(ii =1; ii < N1; ii = ii+2)
        {for (tt=t[ii]; tt<=t[ii+1]; tt=(tt+del))
            {r=(int) ((tt+sp)/del);
                if(r>(num_seg))
                    r=(r-(num_seg));
                deci[r]=deci[r]+(int) (pow(2.0,(float)(k))) ;
            }
        }
    }
}
```

// This function generates the required pulses

```
void SPWM(void)
{
    union REGS regs;
    do {
        regs.h.ah=2;
        regs.x.dx=0;
        int86 (0X17, &regs, &regs);
    }while ((regs.h..ah & 0x80) == 0);
}
```

## Appendix-B

```
for (r=0; r<num_seg; r++)
{
    outportb (0x378, deci[r];
    a=1;
    do{
        b= 2*3;
        bb = b*2;
        bbb = bb*2;
    }while (++a<=15);
    }
}
```

//This is the main program

```
void main (void)
{
    Em=0.1;
    fc=550;
    fm=50.0;
    Ftimer.reset ();
    Ftimer.start ();
    a=1;
    do{
        b=2*3;
        bb=b*2;
        bbb=bb*2;
    } while(++a<=10);
    Ftimer.stop();
    del=Ftimer.time();

    SPGDA ();
    for(;state !='q';)
    {
        if(!flag&&kbhit())
```

## Appendix-B

```
{state = getch( );
  printf("\n I am ready to take new [%c] ..\n\n", state);
  flag=1;
  z=0;
}

if (flag&&kbhit( ) )
{ch=getche( );
if (isdigit(ch) || ch = '.')
{val[z++]=ch;}

else {val[z]=0;
switch(state){
case 'f' : sscanf (val, "%f", &fm); break;
case 'e' : sscanf (val, "%f", &Em); break;
case 'c' : sscanf (val, "%f", &fc); break;
}
SPGDA( );
flag=0;
}
}

l=inportb(0x378);
l=l>>1;
l=(l&16384)/16384;
for(;;)
{
if (l == 0)break;
}
SPWM( );
}
}
```

